Distributed Radio Resource Management in LTE-Advanced Networks with Type 1 Relay Nodes

Chen Sun
BEng, MEng

A Dissertation submitted in fulfilment of the requirements for the award of Doctor of Philosophy (Ph.D.)

Dublin City University

School of Electronic Engineering
Supervisor: Dr. Xiaojun Wang
July 2014

Declaration

I hereby certify that this material, which I now submit for assessment on the programme of study leading to the award of Ph.D is entirely my own work, that I have exercised reasonable care to ensure that the work is original, and does not to the best of my knowledge breach any law of copyright, and has not been taken from the work of others save and to the extent that such work has been cited and acknowledged within the text of my work.

Signed:_____

Candidate ID No:_____

Date:_____

To my lovely wife and to my adorable son.

Acknowledgements

This dissertation is the result of a four and half years research project at the School of Electronic Engineering, Dublin City University, Ireland, under the supervision and guidance of Dr. Xiaojun Wang. This research project is co-financed by Dublin City University and Chinese Scholarship Council.

First and foremost, I want to thank my dear parents. Your endless love support me in these 4 years. You gave me your encouragement and expectation to help me continue and complete the research project. Your attitude towards work, people, and life always inspired me so much. You are great parents I love you all!

An extra special acknowledgement goes to my dear wife, Ms. Lina Duan. We have been together for eight years and have been married for four years. In these years, you are always supporting my decision and encouraging me to complete what I should do. Four-year long-distance marriage made us stronger than ever. I do believe that we can handle every difficulty in our future life. More importantly, I would like to thank you for giving birth to my son. He is now my everything. I love you so much.

I would like to greatly appreciate the significant help from my supervisor, Dr. Xiaojun Wang. I am and will always be very glad to be your student. Without you, it would not have been possible to complete this doctoral thesis or even start this PhD study. Every moment I was facing difficulties in academic and living, your help and suggestions would always be the key factor of overcoming the difficulties. Also, I would like to acknowledge the great help from Prof. Weidong Wang from Beijing University of Posts and Telecommunications, China. I appreciate your constructive feedback.

I would to give big thanks to Dr. Gaofeng Cui, Dr. Zhiguo Qu and Dr. Olga Ormond. After every discussion between you and me, many excellent ideas and feedback would be obtained. My heartfelt thanks are

given to my lovely colleagues, Xiaofei Wang, Yachao Zhou, Feng Guo, Ming Zhao, Khalid Javeed, Brendan Cronin. It was and is a wonderful time working with you.

Special thanks to my old friends, Haoxuan Li, Zhenhui Yuan, Lily He, Longhao Zou, Xing Zheng, Jie Jin, Yongli Tang, Siyuan Sun, Yan Liu. Thank you for the constructive feedback. I enjoy every moment we sharing food and happiness together. I am so proud of being your friend.

I would like to extend a very special thank to the technical staff of the School of Electronic Engineering, Dublin City University for their valuable support.

Last but not the least, I gratefully acknowledge Dr. Chris Phillips, Dr. Gabriel-Miro Muntean and Prof. Paul Whelan for organizing the PhD defense and giving me constructive feedback.

List of Publications

1. **Chen Sun**, Xiaojun Wang, Xiaofei Wang, Weidong Wang, Gaofeng Cui, "A Novel Route Selection Strategy in Decode-and- Forward Relay Enhanced LTE-A Network", *2011 IET International Conference on Communication Technology and Application (IET ICCTA2011)*, Beijing, China, 14-16 Oct 2011.

2. **Chen Sun**, Weidong Wang, Gaofeng Cui, Xiaojun. Wang, "Service-aware bidirectional throughput optimisation route selection strategy in LTE-Advanced networks", *IET Networks*, Jan 2014, online published, DOI:10.1049/iet-net.2012.0191.

3. **Chen Sun**, Weidong Wang, Yinghai Zhang, Xiaojun Wang, "Distributed 2-hop proportional fair resource allocation in LTE-Advanced networks", *Wireless Communications and Mobile Computing*, AUG 2014, online published, DOI: 10.1002/wcm.2517

Contents

Distributed Radio Resource Management in LTE-Advanced Networks with Type 1 Relay Nodes

Chen Sun
BEng, MEng

Abstract

Long Term Evolution (LTE)-Advanced is proposed as a candidate of the 4th generation (4G) mobile telecommunication systems. As an evolved version of LTE, LTE-Advanced is also based on Orthogonal Frequency Division Multiplexing (OFDM) and in addition, it adopts some emerging technologies, such as relaying. Type I relay nodes, defined in LTE-Advanced standards, can control their cells with their own reference signals and have Radio Resource Management (RRM) functionalities.

The rationale of RRM is to decide which resources are allocated to which users for optimising performance metrics, such as throughput, fairness, power consumption and Quality of Service (QoS). The RRM techniques in LTE-Advanced networks, including route selection, resource partitioning and resource scheduling, are facing new challenges brought by Type 1 relay nodes and increasingly becoming research focuses in recent years. The research work presented in this thesis has made the following contributions.

A service-aware adaptive bidirectional optimisation route selection strategy is proposed to consider both uplink optimisation and downlink optimisation according to service type. The load between different serving nodes, including eNBs and relay nodes, are rebalanced under the fixed resource partitioning. The simulation results show that larger uplink throughputs and bidirectional throughputs can be achieved, compared with existing route selection strategies.

A distributed two-hop proportional fair resource allocation scheme is proposed in order to provide better two-hop end-to-end proportional fairness for all the User Equipments (UEs), especially for the relay UEs. The resource partitioning is based on the cases of none Frequency Reuse (FR) pattern, full FR pattern and partial FR patterns. The resource scheduling in access links and backhaul links are considered jointly.

A proportional fair joint route selection and resource partitioning algorithm is proposed to obtain an improved solution to the two-hop Adaptive Partial Frequency Reusing (APFR) problem with one relay node per cell. In addition, two special situations of APFR, full FR and no FR, are utilised to narrow the iterative search range of the proposed algorithm and reduce its complexity.

List of Figures

List of Tables

List of Abbreviations

2G the 2nd Generation

3G the 3rd Generation

3GPP the 3rd Generation Partnership Project

4G the 4th Generation

ABO Adaptive Bidirectional Optimisation

AF Amplify-and-Forward

AMBR Aggregate Maximum Bit Rate

AMC Adaptive Modulation and Coding

APFR Adaptive Partial Frequency Reusing

ARP Adaptive Resource Partitioning

ARP Allocation Retention Priority

ARQ Automatic Repeat Request

BS Base Station

BSC Base Station Controller

C-DFA Cell-colouring based Distributed Frequency Allocation

CDF Cumulative Distribution Function

CDMA Code Division Multiple Access

CDMA Code Division Multiple Access

CoMP Coordinated Multi-Point

CP Cyclic Prefix

CQI Channel Quality Indicator

CRS Common Reference Signal

CRS Conventional Resource Scheduling

CSI Channel State Information

DAA Dynamic Allocation Algorithm

DDFFA Dynamic Fractional Frequency Allocation

DF Decode-and-Forward

DFT Discrete Fourier Transform

DL Downlink

DTHPF Distributed Two-Hop Proportional Fair

DwPTS Downlink Pilot Timeslot

E-UTRAN Evolved Universal Terrestrial Radio Access Network

EDGE Enhanced Data rates for GSM Evolution

eNB evolved Node B

EPC Evolved Packet Core

EPS Evolved Packet System

ETSI the European Telecommunications Standards Institute

Fair-RU Fair-Resource-Unit

Fair-TP Fair-Throughput

FDD Frequency Division Duplex

FDM Frequency-Division Multiplexing

FFR Full Frequency Reusing

FFT Fast Fourier Transformation

FR Frequency Reuse

FR Full Reuse

GBR Guaranteed Bit Rate

GGSN Gateway GPRS Support Node

GP Guard Period

GPF Generalised Proportional Fairness

GPRS General Packet Radio Service

GSM Global System for Mobile communications

HARQ Hybrid Automatic Repeat Request

HSDPA High Speed Downlink Packet Access

HSUPA High Speed Uplink Packet Access

ICG Interference Coordination Game

ICI Inter-Cell Interference

ICIC Inter-Cell Interference Coordination

ID Identifier

iFFT inverse Fast Fourier Transformation

IICS Integrated Interference Coordination Scheme

IMT International Mobile Telecommunications

IP Internet-Protocol

ISD Inter-Site Distance

ITU International Telecommunication Union

JRSRP Joint Route Selection and Resource Partitioning

KKT Karush-Kuhn-Tucker

LB-RS Load Balancing Relay Selection

LoBO Load-Balancing Opportunistic

LTE Long Term Evolution

MAC Medium Access Channel

MBSFN Multimedia Broadcast multicast service Single Frequency Network

MCS Modulation and Coding Scheme

MIMO Multi Input Multi Output

MME Mobility Management Entity

MS Mobile Station

MSC Mobile Switching Center

NAS Non-Access Stratum

NFR None Frequency Reusing

OFDM Orthogonal Frequency Division Multiplexing

OFDMA Orthogonal Frequency Division Multiple Access

OR Orthogonal Reuse

OTH Orthogonal Two-Hop

P-GW Packet Data Network Gateway

PAG Power Allocation Game

PAPR Peak-to-Average Power Ratio

PCA Pre-Configuration Algorithm

PDCCH Physical Downlink Control Channel

PDCP Packet Data Convergence Protocol

PDN Packet Data Network

PDN-GW Packet Data Network Gateway

PDSCH Physical Downlink Shared Channel

PF Proportional Fair

PFR Partial Frequency Reusing

PHY Physical Layer

PR Partial Reuse

PRB Physical Resource Block

PSTN Public Switched Telephone Network

QAM Quadrature Amplitude Modulation

QCI QoS Class Identifier

QoS Quality of Service

QPSK Quadrature Phase Shift Keying

RAC Radio Admission Control

RAG Resource Allocation Gap

RB Radio Bearer

RBAG Resource Block Assignment Game

RE Range Expansion

RLC Radio Link Control

RN Relay Node

RNC Radio Network Controller

RND RN Distance

RR Round-Robin

RRC Radio Resource Control

RRM Radio Resource Management

RSP Received Signal Power

S-GW Serving Gateway

SC-FDMA Single Carrier Frequency Division Multiple Access

SGSN Serving GPRS Support Node

SINR Signal to Interference plus Noise Ratio

SMS Short Messaging Service

SSAA Semi-Static Allocation Algorithm

STH Simultaneous Two-Hop

TD-SCDMA Time Division-Synchronous CDMA

TDD Time Division Duplex

TDM Time Division Multiplex

TDMA Time-Division Multiple-Access

TTI Transmission Time Interval

UE User Equipment

UL Uplink

UpPTS Uplink Pilot Timeslot

UTRAN UMTS Terrestrial Radio Access Network

WCDMA Wideband CDMA

WiMAX Worldwide Interoperability for Microwave Access

Chapter 1

Introduction

1.1 Research Motivation

A mobile cellular telecommunication network is a wireless network providing mobile services over land areas called cells. In each cell, mobile phones or devices are served by at least one fixed transceiver called a base station. The two decades since the early 1990s have witnessed tremendous development of mobile telecommunications from the 2nd Generation (2G) mobile networks to the 4th Generation (4G) mobile networks. The mobile telecommunication networks of new generations should supply more and more users with ubiquitous services with high quality. In order to satisfy this requirement, radio resources in different domains, such as time and frequency, are controlled by Radio Resource Management (RRM) functionalities. In different generation mobile networks, the RRM faces new-coming challenges and need innovation.

Global System for Mobile communications (GSM) is usually recognised as the most successful 2G standard series developed by the European Telecommunications Standards Institute (ETSI). On July 1, 1991, the world's first GSM call was made in a city park in Helsinki, Finland, built by Telenokia and Siemens and operated by Radiolinja [1]. The GSM, a digital, circuit-switched network, was expanded to General Packet Radio Service (GPRS)[2] and Enhanced Data rates for GSM Evolution (EDGE)[3] in ways of packet switching and faster data rates, up to 473.6 kbit/s in theory. Frequency-Division Multiplexing (FDM) and Time-Division Multiple-Access (TDMA) [4] are used to allocate different time slots in multiple frequency bands to different users. Therefore, the main RRM issues, such as channel allocation, power

control and handover techniques, are studied to exploit multi-user diversity, reduce co-channel interference and manage user movement.

The 3rd Generation (3G) mobile telecommunication technologies are the standards that fulfil the International Mobile Telecommunications-2000 (IMT-2000) specifications by the International Telecommunication Union (ITU). Apart from voice telephony and the Short Messaging Service (SMS) supported in 2G networks, more applications are offered, such as mobile Internet access, fixed wireless Internet access, video calls and mobile TV. Code Division Multiple Access (CDMA) technology is used in three major 3G standards: Wideband CDMA (WCDMA) in Europe [5], CDMA 2000 in the US [6] and Time Division-Synchronous CDMA (TD-SCDMA) in China [7]. The High Speed Downlink Packet Access (HSDPA) and High Speed Uplink Packet Access (HSUPA), which are evolved from the 3G networks, can now support up to 14.4 Mbits/s data rates in the downlink and 5.76 Mbits/s data rates in the uplink respectively. The inter-code interference feature of CDMA introduces more challenges to the 3G networks, and more RRM techniques, such as admission control, soft handover, load balancing and congestion control [8], are studied.

Facing the challenges from Worldwide Interoperability for Microwave Access (WiMAX), the 3rd Generation Partnership Project (3GPP) organisation started the Long Term Evolution (LTE) project [9] to support packet switching with an all-Internet-Protocol (IP) network and achieve the peak data rate up to 100 Mbits/s in the downlink and 50 Mbits/s in the uplink. In many countries and regions, LTE has been deployed widely as a natural evolution of GSM and UMTS networks and can be considered as a revolution in technique and performance. Orthogonal Frequency Division Multiple Access (OFDMA) is used in the downlink and Single Carrier Frequency Division Multiple Access (SC-FDMA) is adopted in the uplink. The new RRM problems existing in the LTE networks include the Inter-Cell Interference Coordination (ICIC) for improving cell-edge performance [10]and the resource scheduling for utilising the multi-channel diversity [11].

Nonetheless, the LTE is not a real 4G network as in the commercial advertisements, because it does not fulfil the requirements of the 4G specifications, IMT Advanced [12], defined by ITU. Hence in September 2009, the 3GPP partners made a formal submission to the ITU to propose LTE Release 10 and beyond (LTE-Advanced) to be evaluated as a candidate of IMT-Advanced [13]. Therefore, the requirements of LTE-Advanced are naturally decided to achieve or even enhance IMT-Advanced requirements. Peak data rates of up to 1 Gbits/s in the downlink and 500 Mbits/s in the uplink, and scalable bandwidth up to 100 MHz are expected.

Lower user and control plane latencies, larger VoIP capacity and better cell-edge performance are also anticipated. These requirements will enable LTE-Advanced to address increasing user requirements. Accordingly, the main issue in LTE-Advanced is to develop new technologies allowing LTE-Advanced to meet the proposed targets. Spectrum aggregation, relaying and Coordinated Multi-Point (CoMP) transmission and reception are proposed as promising technologies in LTE Release 10 [14, 15]. Other important requirements of LTE-Advanced also include backward compatibility and spectrum flexibility [16]. Hence, LTE-Advanced should be considered as an evolution rather than a revolution from LTE with better system performance, different system structure and lower cost.

Relaying is one of the promising technologies in LTE-Advanced to expand coverage and enhance capacity. As Type 1 and Type 2 in-band half-duplex Relay Nodes (RNs) have been defined in LTE-Advanced standards [14], in-band relaying brings new challenges to the RRM. Thus, there is a need for some new RRM techniques in relay enhanced LTE-Advanced networks.

1.2 Problem Statement

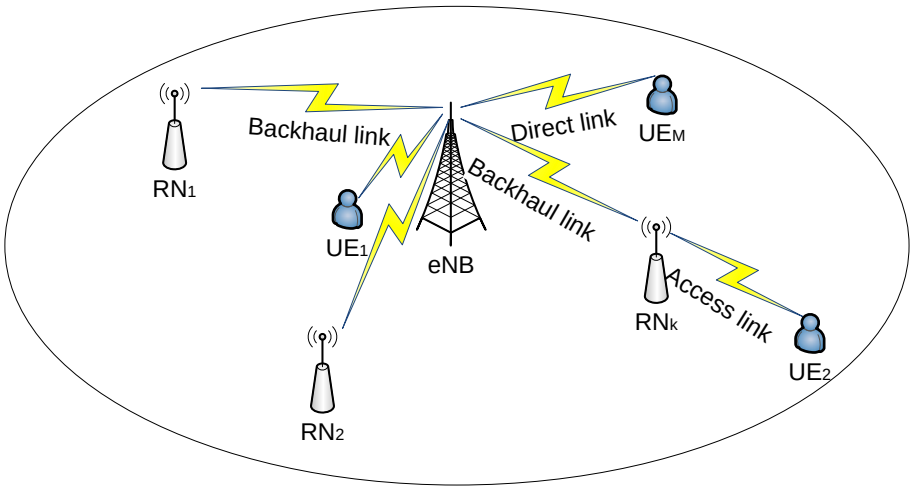

Figure 1.1: A LTE-Advanced cell with RN deployment

In a LTE-Advanced cell shown in Fig. 1.1, one or multiple RNs are deployed in the cell-edge area. They are connected to an evolved Node B (eNB) through wireless backhaul links. Thus, a cell-edge User Equipment (UE) can choose these RNs in order to obtain potential extra performance gain by utilising two-hop transmission. There are three types of links in the cell, i.e. eNB-RN links, RN-UE links and

eNB-UE links, which are named as backhaul links, access links and direct links respectively.

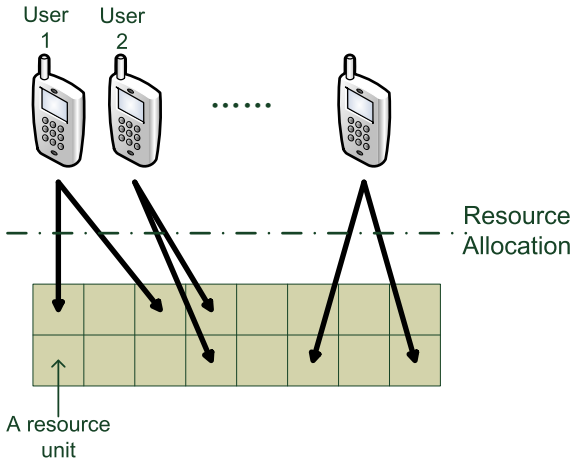

Figure 1.2: Resource allocation in single-hop networks

In single-hop networks, such as LTE networks without relays, the cells are selected by the UEs based on the received signal power, and the resources in each cell are allocated to the UEs in different manners to satisfy performance goals, as shown in Fig. 1.2. However, in the LTE-Advanced networks with RNs, Type 1 in-band half-duplexing RNs are defined, which makes the resource allocation process of UEs more complicated. As illustrated in Fig. 1.3, RRM in the LTE-Advanced networks with Type 1 in-band half-duplexing RNs decomposes the resource allocation of UEs into three phases, including route selection, resource partitioning and resource scheduling. Route selection is used to decide the serving nodes for the UEs, either eNBs or RNs. Hence, the UEs are divided into direct UEs and relay UEs connecting to eNBs and RNs respectively. Resource partitioning divides a whole time-frequency block into different resource segments for different links. Resource scheduling allocates the resource segments of different links to their subscribed UEs.

These three phases of RRM can be executed in centralised manner or distributed manner. When centralised RRM is applied, route selection, resource partitioning and resource scheduling are determined together at the eNB of each cell. When the decision is made, the Channel State Information (CSI) of access links ought to be collected and fed back by the RNs. The frequent CSI exchange will cost a large amount of signal load and is not time-efficient. Making decision for three phases together will lead to high-complexity algorithms in the eNB. In addition, frequent changes of route selection and resource partitioning bring challenges to signalling

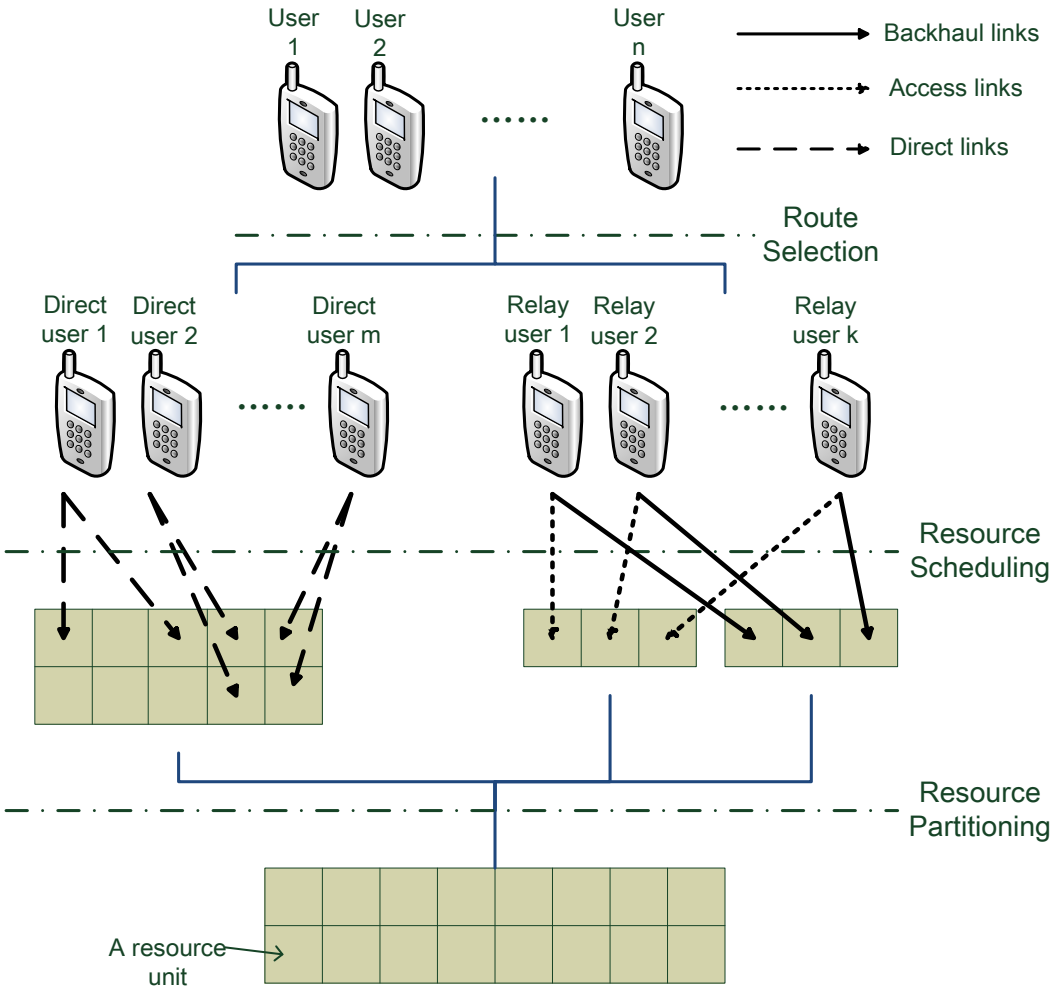

Figure 1.3: RRM in the LTE-Advanced networks with Type 1 in-band half-duplexing RNs

protocols. Since the Type 1 RNs appear as low-power serving nodes to the users and are allowed to execute some RRM functionalities, a distributed RRM architecture is feasible in the LTE-Advanced networks in order to reduce CSI exchanges and the complexity of RRM. Therefore, the distributed RRM architecture is considered in this thesis, in which the resource scheduling of relay UEs is executed at their RNs.

Although there are plenty of research works on RRM in the LTE networks, the two-hop in-band transmission still brings new challenges to distributed RRM techniques. Route selection divides the UEs into direct UEs and relay UEs; resource partitioning divides the whole resources into the resources for direct links, access links and backhaul links respectively; resource scheduling divides the resource allocation of relay UEs into resource scheduling of access links and backhaul links

separately. Through these procedures, the balance between some elements of RRM may be distorted. Therefore, the principles of designing distributed RRM techniques in this thesis is "rebalancing".

The first and the foremost target of rebalancing are performance metrics. Proportional fairness is considered as the common metric in this thesis, because it can achieve an effective balance between increasing throughput and guaranteeing fairness [17]. The proportional fairness in single-hop networks can be easily ensured, however guaranteeing two-hop end-to-end proportional fairness should be considered more carefully.

The problems and challenges in route selection, resource partitioning and resource scheduling are describe as follows:

Route Selection

A important challenge in the route selection is caused by the low transmitting power of RNs, which is called uplink/downlink gain imbalance. For the UEs in the traditional single-hop LTE networks, the serving nodes are chosen according to the largest received signal power. In the two-hop LTE-Advance networks, at least one transmission route among single-hop direct links and two-hop links should be chosen. Note that in this thesis only one route can be selected for each UE, and hence cooperative relaying is not considered. Due to a large degree of difference between the transmitting power of eNBs and RNs [14], the UEs in a certain area of a cell will receive higher downlink signal power with larger path loss from the eNB and lower downlink signal power with less path loss from the RN. For these UEs, the downlink performance can be improved by the eNB. However, better uplink quality can be provided by the RN because the RN receives larger signal power with less path loss than the eNB from the UE. The performance gains provided by the RN in the uplink and downlink are different. The traditional cell selection strategies neglect the uplink/downlink gain imbalance because of the homogeneous transmitting characteristics. Some route selection strategies aim at downlink optimisation, which prefer to connect the UEs to the eNB for better downlink performance without optimal uplink performance. Using some route selection strategies for the purpose of uplink optimisation, the UEs are prone to access the RNs for better uplink performance and their downlink gain will be decreased. Thus, a new balance between uplink optimisation and downlink optimisation should be achieved, either fixed for simplicity and compatibility, or adaptive to the different data rate requirements in the uplink

and the downlink of different asymmetric UEs.

Resource Partitioning

Another research topic of interest is that assembling different types of links in a whole spectrum brings challenges to resource partitioning. In order to support in-band relaying and avoid serious interference at RNs, all subframes in a radio frame are grouped into backhaul subframes and access subframes. In the backhaul subframes, the backhaul links and the direct links share the resources. In the access subframes, the direct and access links can share or reuse the resources in the access subframes. Additionally, due to the limited buffer size of a RN, the aggregate throughputs of its access links should approach the throughput of its backhaul link, called a two-hop match. Through the above steps, the whole resources in the cell are partitioned between these three types of links. A resources partitioning scheme can be fixed or adaptive.

The challenge to the fixed resource partitioning is load imbalance. Because of the randomness of UE location and smaller coverage of the RNs than that of the eNBs, the numbers of UEs associating with the eNB and the RNs may change dramatically from serving node to serving node. Thus, assigning the same amount of resources to different serving nodes can cause load imbalance. Moreover, due to limited buffering in the RNs, the aggregated throughput of access links should be equal to the throughput of the corresponding backhaul link, which can be called a "two-hop match". The unmatched two-hop will lead to resource waste either in the access links or in the backhaul links, which can be considered as another form of load imbalance. A load balancing mechanism is a requirement for fair resource distribution and reducing resource waste. The benefit of fixed resource partitioning is that an inter-cell interference coordination scheme can be applied.

The advantage of using adaptive resource partitioning is that every UE can choose a transmission channel with the best condition and without load balancing. However, in-band two-hop relaying brings two more challenges to designing adaptive resource partitioning schemes. First, both the access links and the backhaul links of two-hop transmission should occupy a different number of resources to transmit the same amount of data, and these two links should satisfy the two-hop match. Second, the requirements of in-band half-duplex relaying result in the whole resources being partitioned into three parts, each part for one type of link. For instance, a radio frame is partitioned into backhaul subframes for backhaul links and access subframes

for access links and direct links, and then the access subframes are orthogonally shared, partially reused or fully reused by access links and direct links. Sharing, fixed or adaptive two-hop reusing between access links and direct links may need different resource partitioning methods. Adaptive partial reusing can achieve a balance between increasing reused resource number and reducing interference caused by frequency reusing. Besides, orthogonal sharing and full reusing can be considered as two special cases of adaptive partial reusing.

Resource Scheduling

Last but not the least, resource scheduling is also one of the challenges to distributed RRM. For the relay UEs, both the resources for the access links and the resources for the backhaul links should be scheduled between them. For the purpose of optimising two-hop end-to-end performance and satisfying the two-hop match, the resource scheduling in the access links and the resource scheduling in the backhaul links need a careful rebalancing in a two-hop resource scheduling algorithm. Different from the conventional scheduling algorithm in the single-hop cellular networks, the two-hop resource scheduling algorithms may consider the channel condition of access links and backhaul links simultaneously and may be different with different resource partitioning results.

1.3 Thesis Contributions

The research work presented in this thesis made the following contributions to the RRM in relay enhanced LTE-Advanced networks:

- proposed a service-aware Adaptive Bidirectional Optimisation (ABO) route selection strategy, which
  - optimises both downlink performance and uplink performance. The bidirectional throughput is maximised, which is the sum of the throughputs of uplink and downlink. A balance between uplink optimisation and downlink optimisation is achieved.
  - achieves load balance between different serving nodes. Load balancing is integrated into the proposed route selection strategy with fixed resource partitioning. Load imbalance is a natural consequence of random

UE distribution and fixed resource partitioning, which will cause some performance loss.

  - introduces service types into the proposed route selection algorithm. The UEs with different service types have different requirements in the downlink and the uplink. The bidirectional throughput is optimised adaptively for the UEs according to the service type.
  - provides larger uplink throughput without significant downlink throughput loss shown in performance evaluation. In particular, the UEs with large uplink requirement can obtain larger uplink throughput to improve their quality of service.

- proposed a Distributed Two-Hop Proportional Fair (DTHPF) resource allocation algorithm, which

  - provides better two-hop end-to-end proportional fairness for the relay UEs. The data transmitted in the backhaul links should be retransmitted in the access links. The two-hop end-to-end throughput is no more than the throughput in the backhaul links and the aggregated throughput in the access links. Due to various channel conditions in the access links and unique channel condition in the corresponding backhaul link, two-hop end-to-end proportional fairness for the relay UEs cannot be represented by the single-hop proportional fairness.
  - formulates the proportional fair resource allocation problem as a Generalised Proportional Fairness (GPF) problem. The GPF problem is further decomposed into two sub-problems, a resource partitioning sub-problem and a resource scheduling sub-problem, which are related to each other. The proportional fair based adaptive resource partitioning has been well studied in order to obtain an improved resource partitioning results. Hence, the relationship between the resource numbers of access links and backhaul links is made clear.
  - considers different two-hop transmission protocols with different frequency reusing patterns between access links and direct links. Simultaneous two-hop transmission protocol with full frequency reusing and fixed partial frequency reusing, and orthogonal two-hop transmission protocol draw different resource number constraints between access links and backhaul links.
  - utilises the Lagrange multiplier method to determine an improved result for resource scheduling in two hops simultaneously.

- provides better proportional fairness and larger 5% worst throughputs with different RN numbers per cell.

- proposed a proportional fair joint route selection and resource partitioning algorithm, which:

  - formulates the two-hop adaptive partial frequency reusing problem between the access links and the direct links as a GPF problem. Proportional fairness is considered as the metric of performance, which is an effective compromise between throughput and fairness. Given that the route selection has been determined, the two-hop adaptive partial frequency reusing problem is transformed into a proportional fair based resource partitioning problem. The scenario with one relay node per sector is considered.

  - proposes a proportional fair resource partitioning algorithm in order to obtain a near-optimal solution to the two-hop adaptive partial frequency reusing problem.

  - utilises two special situations, full frequency reusing and no frequency reusing, to narrow the iterative search range of the proposed resource partitioning algorithm and reduce its complexity. In these two special situations, there are many effective algorithms to acquire their near-optimal resource partitioning results.

  - proposes a proportional fair route selection algorithm in the determined cell. Based on the assumed resource partitioning results, the proposed route selection algorithm estimates the achievable data rates when choosing single-hop link and two-hop links.

  - has evaluated the performance of the proposed joint proportional fair resource partitioning and route selection scheme. Compared with traditional resource partitioning and route selection schemes, it can achieve larger throughput and better fairness, and thus larger proportional fairness.

1.4 Thesis Outline

This thesis includes 6 chapters and 1 appendix. The first chapter is the introduction and the last chapter concludes the thesis. In the first chapter, the motivation of the

research in this thesis is introduced, the problem existing in the scope of the thesis is analysed and stated, and then the main contributions of this thesis are detailed. A brief description of the following chapters is given below:

- *Chapter 2* introduces the necessary technical background of the research work in this thesis.
- *Chapter 3* proposes a service-aware Adaptive Bidirectional Optimisation (ABO) route selection strategy. The current related research and the system models are also introduced. Benchmarking the performance of the proposed ABO strategy is also presented.
- *Chapter 4* proposes a Distributed Two-Hop Proportional Fair (DTHPF) resource allocation algorithm. The current related research, the system models, the problem formulation and the problem relaxation are included. The performance of the proposed DTHPF algorithm is evaluated and compared with conventional proportional fair resource allocation algorithms.
- *Chapter 5* proposes a proportional fair joint route selection and resource partitioning algorithm for the Adaptive Partial Frequency Reusing (APFR) problem. The current related research is reviewed and the system models are described. A proportional fair joint route selection and resource partitioning algorithm is proposed. The effectiveness of the proposed algorithms is evaluated through performance simulations.
- *Chapter 6* concludes the thesis and indicates some potential future research directions.

Chapter 2

Technical Background

2.1 Introduction

This chapter presents the background technologies related to the research in this thesis. First, the network structures and the multiple access techniques of GSM, UMTS and LTE are described briefly. As important background techniques of RRM, the radio transmission techniques, the resource grid, the system structure and the RRM functions in LTE networks are depicted. Then, LTE-Advanced with relaying technology are introduced briefly, as the evolution of LTE. Finally, the classification of relay nodes and the principles of two-hop transmission are presented.

2.2 Evolution of 3GPP Mobile Networks

2.2.1 Global System for Mobile (GSM) Communication

The GSM is the most successful mobile cellular network standard until now. It has given guidelines for the following mobile network generations. As shown in Fig. 2.1, the GSM radio network consists of several cells. Each cell controlled by a Base Station (BS) is a geographical representation of the coverage area within which the BS can send and receive data. Cells are commonly illustrated by hexagonal shapes for simplicity. In each cell, a number of Mobile Stations (MSs), representing the users, are served. The wireless link from the BS to the MS is named as Downlink (DL) and the other direction is named as Uplink (UL). Several BSs are controlled by the Base Station Controller (BSC) for RRM. The BSC is connected to the GSM core network,

including a Mobile Switching Center (MSC) and some databases. The MSC handles some RRM functions and deliver the data to the external networks. The databases are responsible for operation functionalities, such as mobility management, user information storing, service controlling functions and billing. The external networks include Public Switched Telephone Network (PSTN) or other GSM networks. The details of the GSM is given in [4].

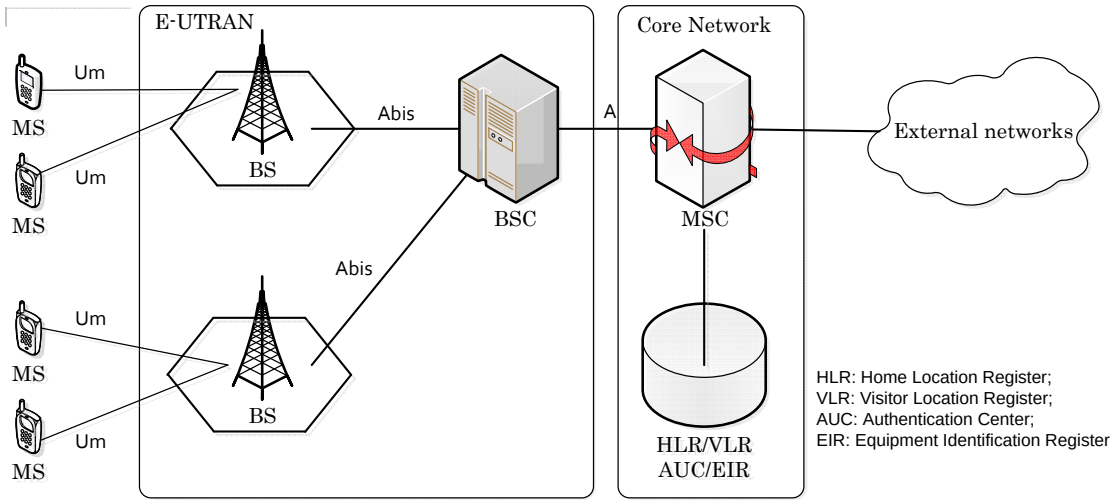

Figure 2.1: GSM network architecture

The GSM uses Time Division Multiple Access (TDMA) based on Frequency Division Multiplexing (FDM) as the multiple access scheme. The FDM in the GSM divides the whole spectrum into several carrier frequency bands with the width of 200 kHz. A frame in each carrier frequency band is then divided into 8 time slots using TDMA. Each time slot can be used by a MS for transmission. In the GSM, Frequency Division Duplex (FDD) is used to separate the downlink frequency band from the uplink. A guard frequency band is needed between a downlink frequency band and a uplink frequency band.

2.2.2 Universal Mobile Telecommunication System (UMTS)

The UMTS network is structured similarly to GSM with several modifications, which is shown in Fig. 2.2. The radio access network in UMTS, called UMTS Terrestrial Radio Access Network (UTRAN), consists of Radio Network Controller (RNC) and several NodeBs (which represent the UMTS base stations). The UMTS core network supports both circuit switching and packet switching. The circuit switching is used to carry voice services, whereas packet switching is used for data services, like web

browsing and file downloads/uploads. The MSC is essentially the same as that in GSM. The Gateway MSC is its interface to the PSTN. Serving GPRS Support Node (SGSN) and Gateway GPRS Support Node (GGSN) are used to support data switching services and provide interfaces to the external packet switched networks. More technical knowledges can be found in [5] and [1].

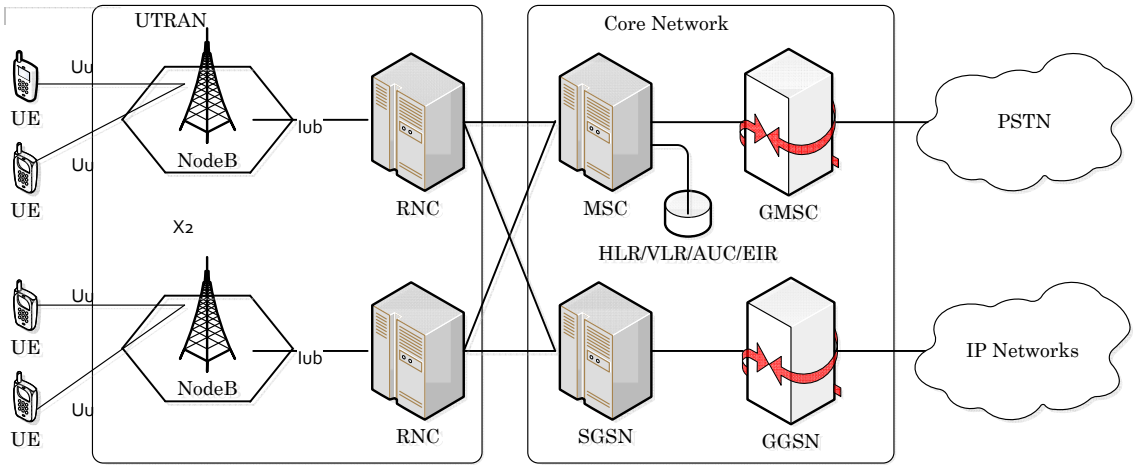

Figure 2.2: UMTS network architecture

The UMTS adopts Code Division Multiple Access (CDMA) as the channel access method. The CDMA is a multiple access technique, where several users can send their data simultaneously through a single channel. Each user is assigned a code to achieve high spectral efficiency without undue interference.

In 3GPP standard release 5 and release 6, High Speed Downlink Packet Access (HSDPA) and High Speed Uplink Packet Access (HSUPA) were proposed to increase system capacity and reduce system latency. The goal of HSDPA was to enhance the downlink data rates of the UMTS standard up to 14 Mbps. Several new functions, such as Adaptive Modulation and Coding (AMC) and Hybrid Automatic Repeat Request (HARQ), are introduced. The AMC supports the adaptive modulation and coding schemes of each user transmission adjusted depending on the channel conditions. The HARQ performs retransmissions of the erroneous packets between the NodeB and the UE instead of waiting for higher layer retransmissions, which results in latency reduction.

2.2.3 Long Term Evolution (LTE)

The LTE project was Initiated in 2004. In December 2008, 3GPP standard Release 8 was frozen, which has been the basis for the first wave of LTE equipment. Now, the LTE (both radio and core network evolution) is on the market. The study of the LTE focused on developing an Evolved Universal Terrestrial Radio Access Network (E-UTRAN) architecture and adapting better radio multiple access technologies. Orthogonal Frequency Division Multiplexing (OFDM)-based multiple access schemes, Orthogonal Frequency Division Multiple Access (OFDMA) in the downlink and Single Carrier Frequency Division Multiple Access (SC-FDMA) in the uplink, are adopted. The main targets and requirements of LTE are described in [18], including

- Scalable bandwidth 1.25, 1.6, 2.5, 5, 10, 15 and 20 MHz
- Significantly increased peak data rate, up to 100 Mbps in the downlink and 50 Mbps in the uplink
- Shorter latency, less than 100 ms from an idle state to an active state in control-plane and less than 5 ms in user-plane
- Supporting All-IP architecture

2.3 LTE Physical Layer

2.3.1 Transmission Scheme

In the LTE E-UTRAN, the multiple access schemes are based on OFDM. OFDMA scheme is used in the downlink and SC-FDMA scheme is used in the uplink. The reason why OFDMA is applied in the LTE downlink is its robust features against frequency selective channels. In order to provide lower peak-to-average ratio between the transmitted signals, SC-FDMA is used in the uplink transmission, which is beneficial for saving batter life of mobile devices.

OFDM

OFDM is actually a frequency division multiplexing scheme used as a digital multi-carrier modulation method [19]. The long history of the OFDM technique has witnessed its growing popularity in wireless and wired networking. Due to recent

enhancements in digital processing technology, OFDM has been accepted for wireless high-speed communications in many standards.

The principle of OFDM is to divide a high-rate serial data stream into a set of low-rate parallel data streams, each of which is modulated on a sub-carrier [20]. Therefore, the bandwidth of sub-carriers is smaller than the coherence bandwidth of multipath fading, and hence each sub-carrier can experience flat fading with simple equalisation. As it is shown in Figure 2.3 from [20], these sub-carriers are computed by an inverse Fast Fourier Transformation (iFFT) to generate the baseband OFDM signal. When the signal is received by the receiver, the parallel data streams can be obtained by a forward FFT and a symbol detector. Through the iFFT and FFT, the sub-carriers overlap with each other and guarantee the orthogonality. High spectral efficiency can be obtained, because the interference between the sub-carriers is eliminated through the orthogonality. In order to ensure the orthogonality of the sub-carriers in the mobile wireless environment, a Cyclic Prefix (CP) is employed before each OFDM symbol.

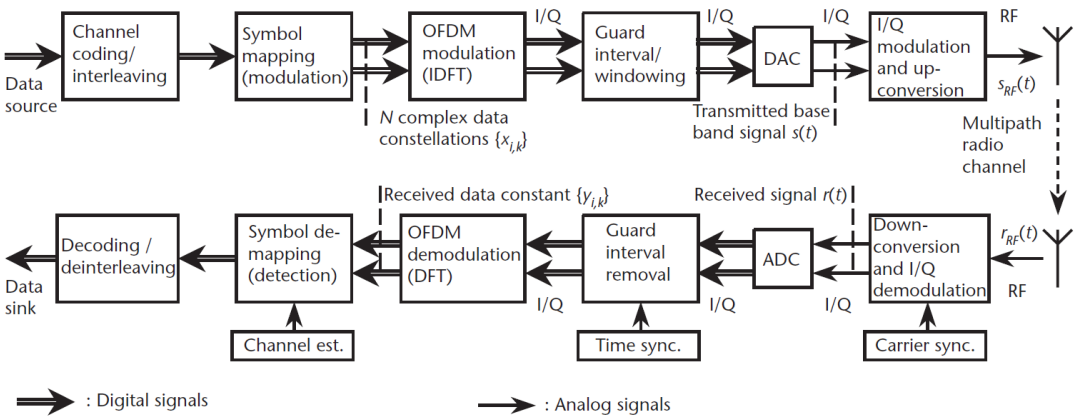

Figure 2.3: A Simple point-to-point transmission using OFDM [20]

The basic OFDM parameters include sub-carrier spacing, number of sub-carriers and CP length. The LTE uses a basic sub-carrier spacing of 15 kHz. The number of sub carriers depends on the transmission bandwidth. As an example, 600 sub-carriers are considered over a 10 MHz system bandwidth.

OFDMA

The Orthogonal Frequency Division Multiple Access (OFDMA) scheme is achieved by assigning different sub-carriers to different users. Thus, the interference in OFDMA systems is mainly generated between the users in different cells reusing the same sub-carriers. The mitigation of Inter-Cell Interference (ICI) is a hot research issue of RRM in LTE and LTE-Advanced. Differentiated QoS levels are supported by scheduling the sub-carriers between the users.

One of the major drawbacks of OFDMA is the high Peak-to-Average Power Ratio (PAPR) of the transmitted signals [21]. The signals with a high PAPR require highly linear power amplifiers, which bring a heavy burden to portable wireless devices with low power efficiency. Meanwhile, another problem of OFDMA in the uplink transmission is the inevitable frequency offset of the reference signals. This frequency offset will destroy the orthogonality of uplink transmissions, and thus introduce inter-channel interference.

SC-FDMA

Single Carrier Frequency Division Multiple Access (SC-FDMA) is introduced in LTE as an uplink multiple access scheme due to its distinguishing feature of lower PAPR. The SC-FDMA transmitters use different orthogonal sub-carriers to transmit symbols, which are first preprocessed by a Discrete Fourier Transform (DFT) block. Therefore, the SC-FDMA sub-carriers are transmitted sequentially rather than in parallel, resulting in lower PAPR of the signals. Besides, it also has a low sensitivity to carrier frequency offset. However, the main drawbacks of SC-FDMA are lower performance than OFDMA and complex signal processing at the BS side.

2.3.2 Resource Grid

The transmitted signal in each time slot consists of $N_{RB}^{UL} \times N_{sc}^{RB}$ sub-carriers and N_{symb}^{UL} SC-FDMA symbols in the uplink, and $N_{RB}^{DL} \times N_{sc}^{RB}$ sub-carriers and N_{symb}^{DL} OFDM symbols in the downlink. N_{RB}^{UL} and N_{RB}^{DL} represent the numbers of resource blocks in the uplink and in the downlink respectively. In each resource block, there are N_{sc}^{RB} sub-carriers. N_{symb}^{UL} and N_{symb}^{DL} denote the numbers of SC-FDMA symbols in the uplink and OFDM symbols in the downlink separately. Uplink resource gird and downlink resource grid are illustrated in Fig. 2.4, which is redrawn from [22].

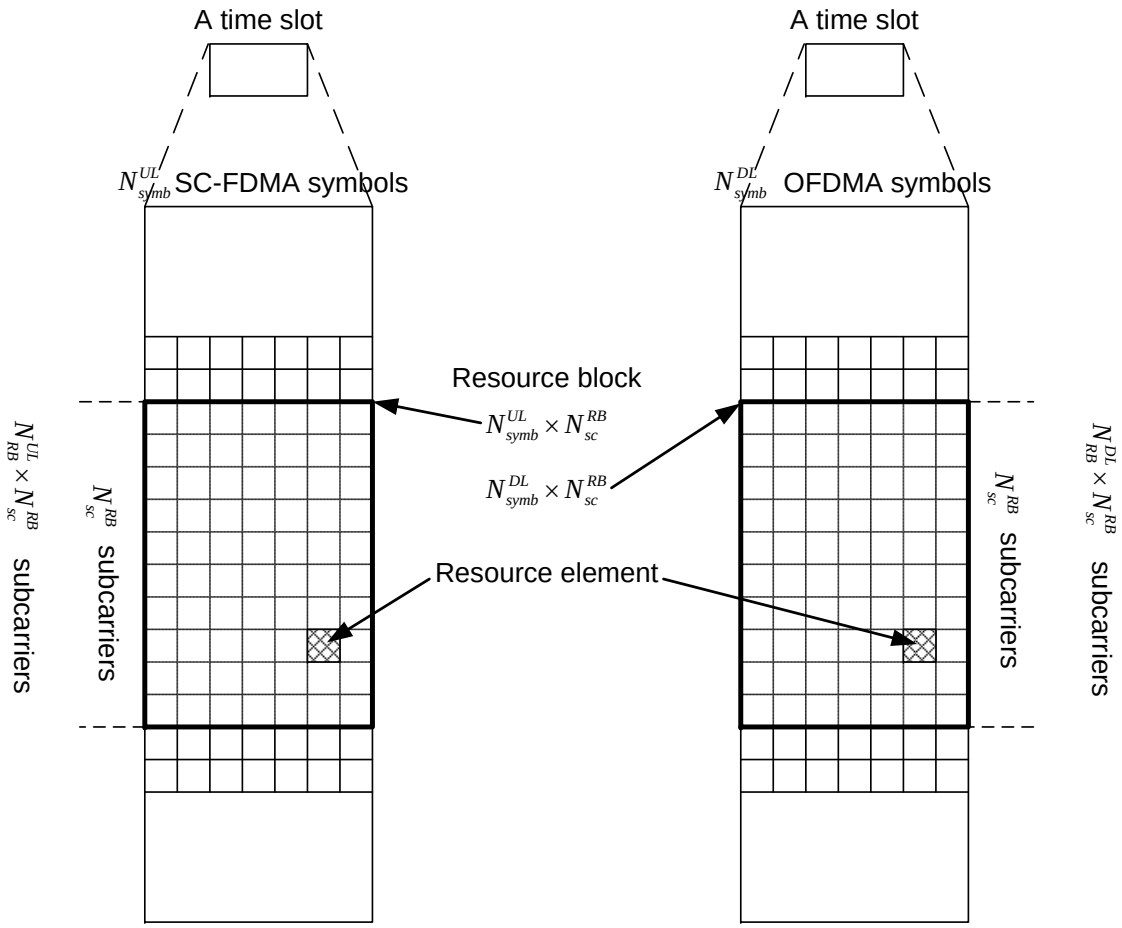

Figure 2.4: Resource grid in the uplink and the downlink [22]

Table 2.1: Resource block parameters [22]

Configuration	N_{sc}^{RB}	N_{symb}^{UL}	N_{symb}^{DL}
Normal cyclic prefix	12	7	7
Extended cyclic prefix (Δf =15kHz)	12	6	6
Extended cyclic prefix (Δf =7.5kHz)	24	/	3

Each element in the resource grid is called a resource element. A Physical Resource Block (PRB) in the uplink is defined as N_{symb}^{UL} consecutive SC-FDMA symbols in the time domain and N_{sc}^{RB} consecutive sub-carriers in the frequency domain. Similarly, a PRB in the downlink is defined as N_{symb}^{DL} consecutive OFDM symbols in the time domain and N_{sc}^{RB} consecutive sub-carriers in the frequency domain. N_{symb}^{UL}, N_{symb}^{DL} and N_{sc}^{RB} in different configurations are given in Table 2.1.

2.3.3 Frame Structure

To support transmission in paired and unpaired spectrum, two duplex modes are defined in the LTE standards [22], i.e. Type 1 Frequency Division Duplex (FDD) supporting full duplex and half duplex operation, and Type 2 Time Division Duplex (TDD).

Frame structure Type 1 is illustrated in Figure 2.5. Each 10 ms radio frame is divided into ten equally sized sub-frames. Each sub-frame consists of two equally sized time slots. There are 10 sub-frames available for downlink transmission and 10 sub-frames available for uplink transmissions in each 10 ms radio frame. Uplink and downlink transmissions are separated by the guard frequency band in the frequency domain.

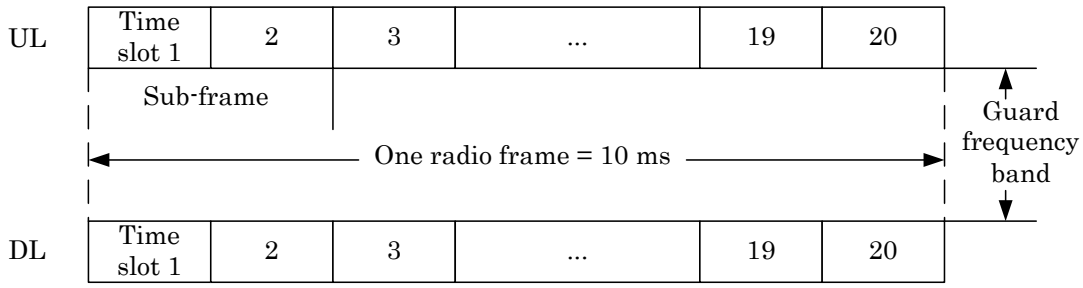

Figure 2.5: Frame structure type 1 [22]

Frame structure Type 2 is illustrated in Figure 2.6. Each 10 ms radio frame

consists of two half-frames of 5 ms each. Each half-frame consists of eight time slots of length 0.5 ms and three special fields: Downlink Pilot Timeslot (DwPTS), Guard Period (GP) and Uplink Pilot Timeslot (UpPTS). The length of DwPTS and UpPTS is configurable subject to the total length of DwPTS, GP and UpPTS being equal to 1ms. Both 5ms and 10ms switch-point periodicity are supported. Subframe 2 in all configurations and subframe 7 in the configuration with 5ms switch-point periodicity consist of DwPTS, GP and UpPTS. Subframe 6 in the configuration with 10 ms switch-point periodicity consists of DwPTS only. All other subframes consist of two equally sized time slots. GP is reserved for the downlink to uplink transition. Other subframes/fields are assigned for either downlink or uplink transmission. Uplink and downlink transmissions are separated in the time domain.

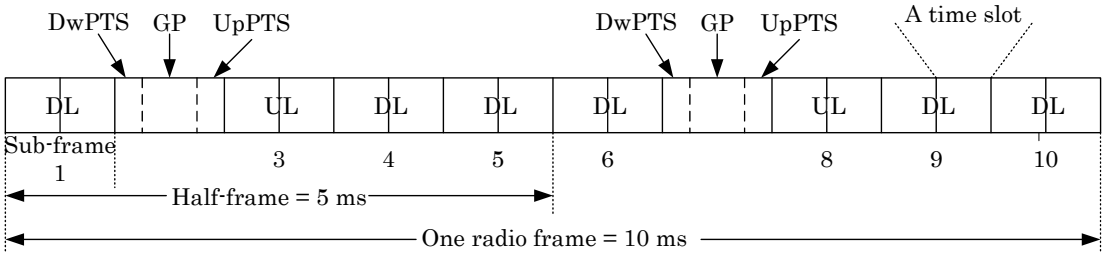

Figure 2.6: Frame structure type 2 [22]

2.4 LTE System Structure

2.4.1 Network Architecture

The LTE network is designed to provide the packet switched services with IP connectivity between the Packet Data Network (PDN) and the UEs. The LTE network are composed of Evolved Packet Core (EPC) as a core network and E-UTRAN as a radio access network. The EPC and the E-UTRAN together constitute the Evolved Packet System (EPS). Figure 2.7 shows the LTE EPS architecture.

EPC

The EPC is responsible for supporting the users and establishing their bearers of packet-based services. In the EPC, there are three main entities:

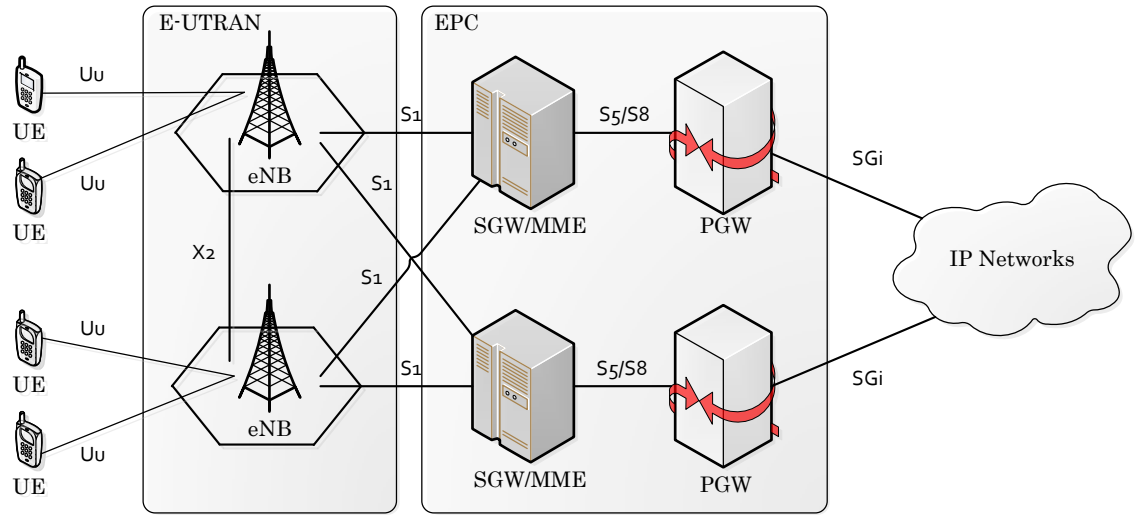

Figure 2.7: LTE EPS architecture

- Mobility Management Entity (MME), which enables the transfer of subscription and authentication data for authenticating/authorizing user access;
- Serving Gateway (S-GW), which is the main gateway for the user traffic from the eNBs, and the local mobility anchor point for inter-eNB handover as well as the mobility anchoring for inter-3GPP handover;
- Packet Data Network Gateway (PDN-GW or P-GW), acting as the user connectivity point for the user traffic to the Internet, which is responsible for assigning the users IP addresses as well as classifying the user traffic into different QoS classes.

The detailed functions of above three entities are given in [23].

E-UTRAN

The LTE E-UTRAN consists of eNBs, providing the E-UTRAN user plane and control plane protocol terminations towards UE. The eNBs are interconnected with each other by means of the X2 interface. Using the S1 interface, the eNBs are also connected to the Evolved Packet Core (EPC), more specifically to the MME through the S1-MME and to the S-GW through the S1-U. The S1 interface supports a many-to-many relation between MMEs/Serving Gateways and eNBs [24]. For more details of the E-UTRAN, please refer to [23].

In Figure 2.7, Uu is the interface where the UE is connected to the E-UTRAN;

S5/S8 is the interface between S-GW and P-GW; and SGi is used to access the external IP networks.

2.4.2 Radio Protocol Architecture

Through the user plane and control plane protocol stacks shown in Figure 2.8, the eNB performs the physical procedures for transmission and reception, and hosts the RRM functions, such as admission control, link connection control, link adaptation and dynamic resource allocation (scheduling). Note that there are protocols between the UE and the core network, which are transparent to the radio layers and generally referred to as Non-Access Stratum (NAS) signalling.

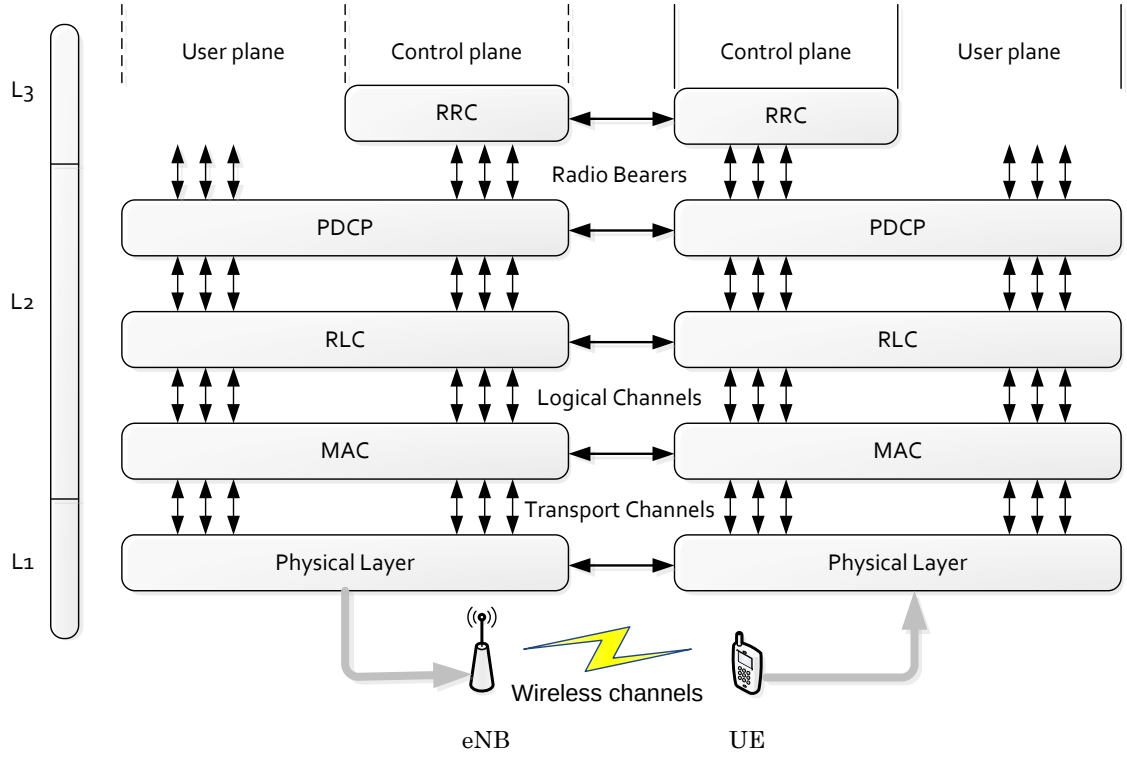

Figure 2.8: LTE Radio Protocol Architecture

The LTE radio interface protocols include:

- Radio Resource Control (RRC): is responsible for the admission control functions, such as handover and cell selection/reselection decisions, and the transfer of UE context from serving eNodeB to target eNodeB during handover. In addition, it controls the periodicity of the Channel Quality Indicator (CQI) and

is also responsible for the setup and maintenance of the radio bearers [25].

- Packet Data Convergence Protocol (PDCP): is responsible for compressing the IP header for better efficiency over the radio interface. This layer also performs additional functionalities, e.g., ciphering and integrity protection. A detailed description of the PDCP functionality can be found in [26].

- Radio Link Control (RLC): is responsible for the segmentation and concatenation of the PDCP packets. It also performs retransmissions and guarantees in-sequence delivery of the packets to the higher layers. The RLC also performs error corrections using the well-known Automatic Repeat Request (ARQ) method. A detailed description of the PDCP functionality can be found in [27].

- Medium Access Channel (MAC): is responsible for scheduling PRBs between different UEs in both uplink and downlink. Together with the scheduling functionality, the MAC layer controls the uplink and downlink physical layer retransmission to correct errors through the Hybrid Automatic Repeat Request (HARQ) mechanism. In addition, it also performs transport block format selection as part of the link adaptation functionality [28].

- Physical Layer (PHY): is responsible for radio related issues: e.g., modulation/demodulation, coding/decoding, Multi Input Multi Output (MIMO) techniques.

The physical layer carries the transport channels provided by the MAC layer. The MAC layer offers the logical channels to the RLC layer. Above the RLC layer, there is the PDCP layer. Layer 2 provides upward radio bearers. Signalling Radio Bearers carry the RRC signalling messages. Correspondingly the user plane Radio Bearers (RBs) carry the user data.

2.5 LTE Radio Resource Management

The RRM algorithms in this thesis are related to various functionalities from Layer 1 to Layer 3 as illustrated in Figure 2.9 redrawn from [29]. The RRM functions at Layer 3, such as QoS management and admission control, are mainly executed during the setup of new data flows. The RRM algorithms at Layer 1 and Layer 2, such as Hybrid Automatic Repeat Request (HARQ) management, dynamic packet

scheduling and link adaptation, are highly dynamic functions with new actions conducted every Transmission Time Interval (TTI) of 1 ms. The Channel Quality Indicator (CQI) management at Layer 1 processes the received CQI reports for the downlink and Sounding Reference Signals (SRSs) for the uplink from active users in the cell. Each received CQI report and SRS can help the eNB to make scheduling decisions and achieve link adaptation in the downlink and the uplink.

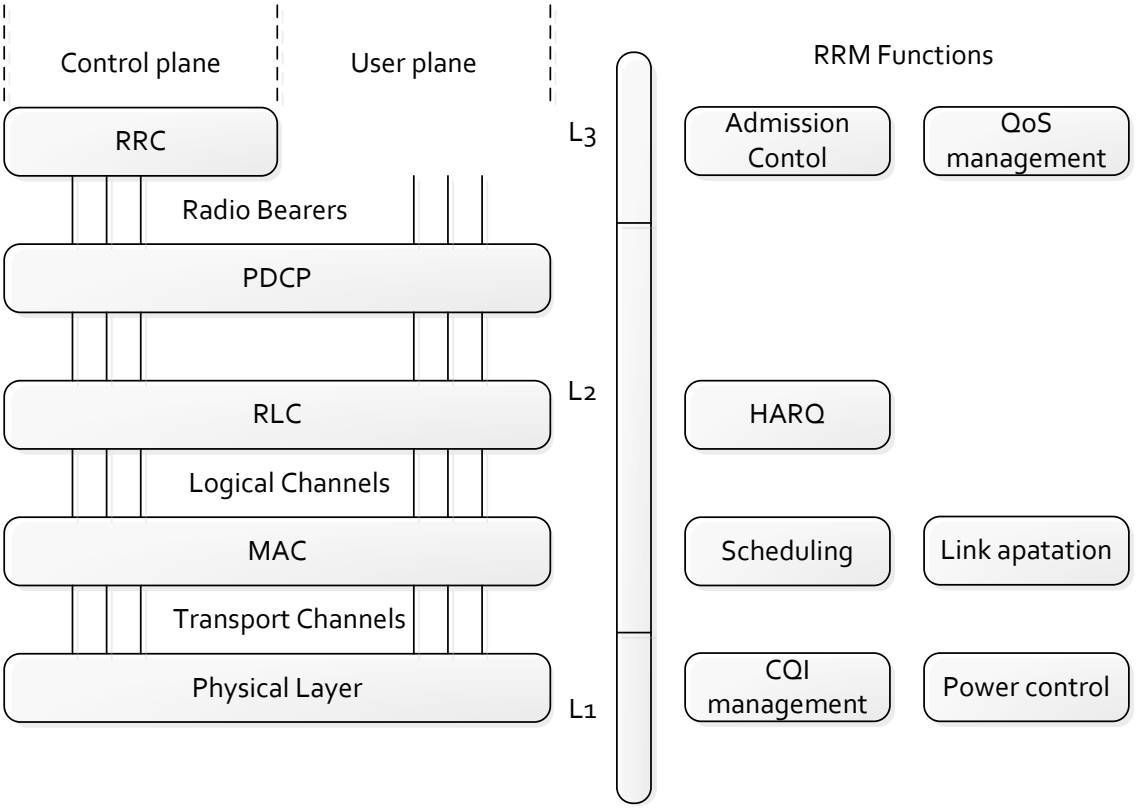

Figure 2.9: The mapping of related RRM function to the LTE radio protocol layers [29]

2.5.1 Radio Admission Control

The Radio Admission Control (RAC) function decides whether the requests of new UEs in a cell are granted or rejected. The RAC usually considers the channel conditions and QoS requirements of the UEs as well as the load situation of the cell. A new request can only be granted if it is estimated that the QoS requirements of the new UE are satisfied, while the service to the existing active UEs in the cell with the same or higher priority is still acceptable. In the LTE, the QoS is applied on radio bearer between the RRC layers of UEs, eNBs and PGW. Each LTE UE is

associated with a set of QoS parameters, including:

- Allocation Retention Priority (ARP): ARP decides whether a UE is accepted or rejected considering limited resources. Higher ARP gives larger opportunities of admission to the UEs.
- Guaranteed Bit Rate (GBR): GBR presents the expected Layer 3 data rate, which is independent in the uplink and downlink. Note that for non-GBR UEs, an Aggregate Maximum Bit Rate (AMBR) is specified instead of GBR.
- QoS Class Identifier (QCI): The QCI is a reference to a more detailed set of QoS attributes. The QCI includes parameters like the Layer 2 packet delay budget, packet loss rate and scheduling priority, as shown in Table 2.2.

Table 2.2: QCI parameters [18]

QCI	Priority	L2 packet delay budget	L2 packet loss rate	Example services
1 (GBR)	2	100 ms	10^{-2}	Conversational voice
2 (GBR)	4	150 ms	10^{-3}	Conversational video
3 (GBR)	5	300 ms	10^{-6}	Buffered streaming
4 (GBR)	3	100 ms	10^{-3}	Real-time gaming
5 (non-GBR)	1	100 ms	10^{-6}	IMS signaling
6 (non-GBR)	7	100 ms	10^{-3}	Live streaming
7 (non-GBR)	6	300 ms	10^{-6}	Video (Buffered Streaming), TCP-based (e.g., web browsing, ftp, p2p file sharing, etc.)
8 (non-GBR)	8	300 ms	10^{-6}	Voice, Video (Live Streaming), Interactive Gaming
9 (non-GBR)	9	300 ms	10^{-6}	Video (Buffered Streaming), TCP-based (e.g., web browsing, ftp, p2p file sharing, etc.)

2.5.2 Packet Scheduling

The scheduling algorithm in Layer 2 performs scheduling decisions every TTI by allocating Physical Resource Blocks (PRBs) to the UEs. The overall packet scheduling goal is to maximize the cell capacity, while guaranteeing the minimum QoS requirements of GBR UEs and the fairness between the non-GBR UEs. In this thesis, two

scheduling algorithms, Round-Robin (RR) and Proportional Fair (PF), are considered.

As the Round-Robin (RR) algorithm is used, the PRBs are assigned to the UEs in equal portions and in circular order. There is no priority for the UEs, and there is no need to acquire the channel condition information of the UEs. Therefore, the RR algorithm is simple and easy to implement. In some cases, the RR algorithm can be extended to the weighted RR algorithm [30], which is considered in Chapter 3.

The Proportional Fair (PF) scheduling algorithm is aimed at achieving an effective compromise between throughput and fairness. This algorithm is performed by giving each UE a priority that is proportional to its instantaneous data rate, and inversely proportional to its past average data rate. According to [17, 31], the resources can be fairly allocated to the UEs, and a scheduling gain compared with the RR algorithm can be obtained.

In these two scheduling algorithms, each UE can get equal portion of Physical Resource Blocks (PRBs), which is important to the fairness between the UEs. Each allocated PRB should select an appropriate Modulation and Coding Scheme (MCS) according to the channel condition. This is called Adaptive Modulation and Coding (AMC) scheme used for link adaptation. The PRB allocation information and the selected MCS are acknowledged by the scheduled UEs through the control channels.

2.5.3 Link Adaptation

Link adaptation is used to determine the data rate carried in each sub-carrier based on the MCS. AMC is adopted by the link adaptation in the LTE. AMC primarily makes its decisions according to the CQI feedback from the UEs. LTE supports fast adaptive link adaptation performed on a millisecond basis. The mapping from the CQI to the MCS is illustrated in Table 2.3.

2.5.4 Power Control

In LTE, slow power control is used for the uplink transmission, and there is no power control in the downlink transmission [32].

The main purpose of the power control in the LTE uplink is to reduce the energy

Table 2.3: CQI table [18]

CQI index	**modulation**	**code rate x 1024**	**efficiency**
0	out of range		
1	QPSK	78	0.1523
2	QPSK	120	0.2344
3	QPSK	193	0.377
4	QPSK	308	0.6016
5	QPSK	449	0.877
6	QPSK	602	1.1758
7	16QAM	378	1.4766
8	16QAM	490	1.9141
9	16QAM	616	2.4063
10	64QAM	466	2.7305
11	64QAM	567	3.3223
12	64QAM	666	3.9023
13	64QAM	772	4.5234
14	64QAM	873	5.1152
15	64QAM	948	5.5547

consumption of mobile devices and avoid unbalanced uplink coverage of the eNBs. A closed loop fractional uplink power control method is applied in LTE. In order to maximise the desired received power while limiting the generated interference, the transmitting power of UE is based on fractional path loss (PL) compensation, which is defined in [32]:

$$P = \min\{\ P_{max}, P_0 + 10\log_{10}(N) + \alpha PL\} \tag{2.1}$$

where P_{max} is the maximum transmitting power of a UE, α and P_0 are the path loss compensation factor and a parameter to ensure the minimum received signal power level, and N is the number of uplink PRBs allocated to the UE.

In the LTE downlink, the total transmitting power of eNBs will not change according to the channel conditions. Nonetheless, the eNBs can decide the energy distributed on each sub-carrier, which is called power allocation. The power in some sub-carriers can also be eliminated or reduced to achieve Inter-Cell Interference Coordination (ICIC) [33].

2.6 LTE-Advanced

Nonetheless, the LTE is not a real 4G network as in the commercial advertisements, because it does not fulfil the requirements of the 4G specifications, International Mobile Telecommunication (IMT) Advanced [12], defined by the ITU. In addition, cell-edge performance of the LTE should also be improved. Hence in September 2009, the 3GPP Partners made a formal submission to the ITU to propose LTE Release 10 and beyond (LTE-Advanced) be evaluated as a candidate of IMT-Advanced [13]. The requirements of LTE-Advanced are naturally decided to achieve or even enhance IMT-Advanced requirements. Peak data rates of up to 1 Gbits/s in the downlink and 500 Mbits/s in the uplink, and scalable bandwidth up to 100 MHz are expected. Lower user and control plane latencies, larger VoIP capacity and better cell-edge performance are also anticipated. These requirements will enable LTE-Advanced to address increasing user requirements. Accordingly, the main issue in LTE-Advanced is to develop new technologies allowing LTE-Advanced to meet the proposed targets. Several techniques have been proposed and confirmed in Release 10 [14, 15], including spectrum aggregation, relaying and Coordinated Multi-Point (CoMP) transmission and reception. Other important requirements of LTE-Advanced also include backward compatibility and spectrum flexibility [16].

Hence, LTE-Advanced should be considered as an evolution rather than a revolution from LTE with better system performance, different structure and less cost. Relaying technology is expected to promote the cell-edge performance. Thus, the LTE-Advanced networks with relays is the research area of concern in this thesis.

2.6.1 Network Architecture with Relay

As the cell edge performance becomes more critical to LTE-Advanced networks, relaying technology is proposed to alleviate the performance degradation at the cell edge. The cell-edge performance degradation is caused by low signal strength and high interference levels. The idea of relaying is not new, which has been applied in microwave communication and Ad hoc networks. Nonetheless, the use of relaying in LTE-Advanced is different from those in other networks. LTE-Advanced uses a fixed relay infrastructure without a wired backhaul connection, and the messages between the eNB and UEs go through no more than two hops.

The relay node (RN) is connected to a donor cell of a donor eNB via the wireless Un interface, and the UE connects to the RN via the Uu interface [24], which is shown in Fig. 2.10 . The link between the eNB and the RN is usually called the backhaul link, and the link between the RN and the UE is the access link. The link between the eNB and the UE is commonly named the direct link.

2.6.2 Types of Relay Nodes

Relay nodes (RNs) in LTE-Advanced have several different classifications according to different criteria.

Amplify-and-Forward v.s. Decode-and-Forward RNs

In the Amplify-and-Forward (AF) relaying scheme, the transmitted data is received and amplified by the RNs. There are less computation and delay with this scheme. However, the interference and the thermal noise at the RNs are also amplified.

In the Decode-and-Forward (DF) relaying scheme, the RNs decode the received signal from the eNB and transmit the encoded data to the destination UEs in the downlink. Better channel conditions of the two-hop transmission can be obtained.

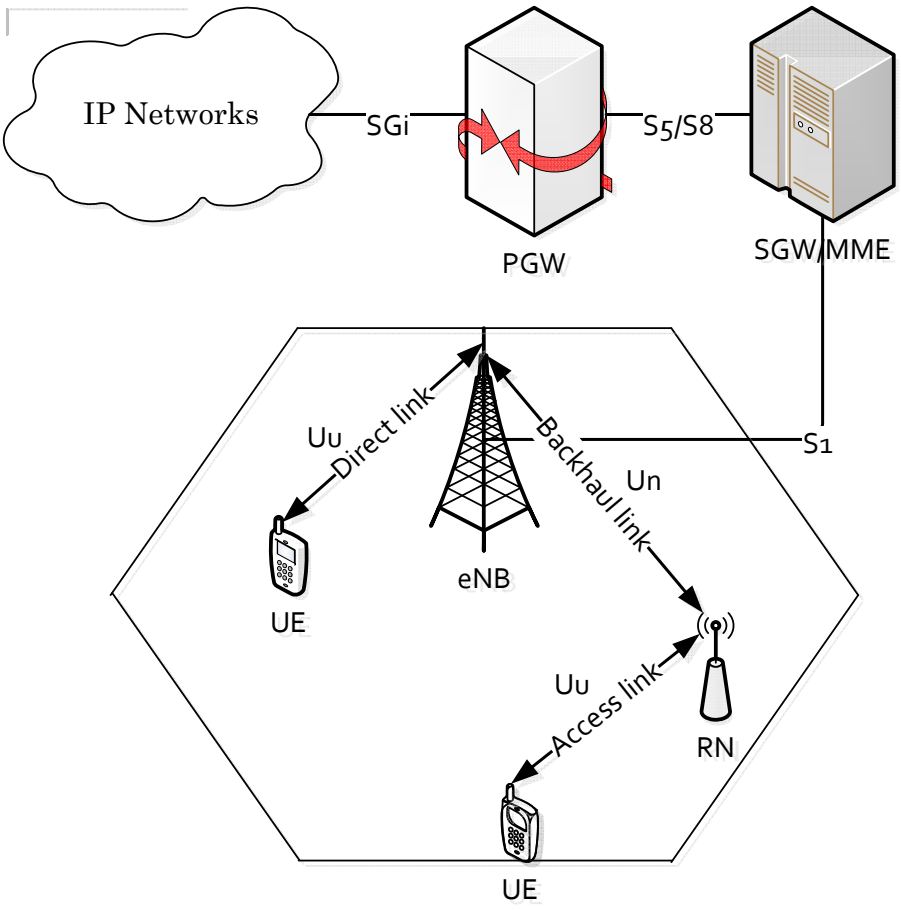

Figure 2.10: Simplified LTE-Advanced network architecture with relay node

Since the RN buffer is finite, all the data received from the eNB should be transmitted to the UEs to avoid resource waste.

L1, L2 and L3 RNs

From the perspective of the protocol architecture of relaying, L1, L2 and L3 RNs are specified in [34]. The L1 RN just amplifies the signal from eNB/UE and forwards it to the UE/eNB. The L2 RN performs the scheduling function. The resource allocation between the UE and the L2 RN is performed in coordination with eNB and the other L2 RNs, taking inter-cell interference and load conditions into consideration. The L3 RN has partial or full functions of RRC resided in eNB. The latency due to the handover and fast data routing can be reduced. The L3 measurements may be utilised for handover decisions in the RNs.

In-band v.s. Out-band RNs

With respect to the usage of spectrum, the operation of RNs can be classified into in-band and out-band. The eNB-RN links of the out-band RNs are not allowed to operate on the same carrier frequency band as RN-UE links; the in-band RNs can operate the eNB-RN links and the RN-UE links on the same carrier frequency band, which can reduce the complexity of frequency band planning. In addition, for both in-band and out-band relaying, it is possible to operate the eNB-RN link on the same carrier frequency band as eNB-to-UE links.

Transparent v.s. Non-transparent RNs

In relation to the information for UEs, RNs can be classified into transparent and non-transparent, according to whether the UEs are aware of their associating RN or not. The transparent RNs will not extend the coverage, but is beneficial for cooperative communication. The non-transparent RNs have cell IDs and can provide some RRM functions.

Type 1 and Type 2 RNs

In the LTE-Advanced standards [14], Type 1 and Type 2 RNs are defined with the following characteristics:

- A basic Type 1 RN is an in-band relay node with the following characteristics:
  - It controls a cell, and appears to a UE as a separate cell different from the donor cell;
  - The cells controlled by the RNs shall have their own physical cell Identifier (ID), defined in LTE Rel-8, and the RNs shall transmit their own synchronization channels, reference symbols and so on;
  - In the context of single-cell operation, scheduling and HARQ functions can be conducted by the RN. The control channels also exist at the RNs;
  - It shall appear as a special UE to the eNB.
- Type 1a and Type 1b RNs are characterised by the same set of features as the basic Type 1 RN described above, except that the Type 1a RN operates out-band and the Type 1b RN operates in-band with adequate antenna isolation. A basic Type 1 RN is expected to have little or no impact on LTE Release-8 specifications.
- A Type 2 relay node is an in-band relay node with the following characteristics:
  - It does not have a separate Physical Cell ID and thus would not create any new cells;
  - It is transparent to Rel-8 UEs; a Rel-8 UE is not aware of the presence of a Type 2 relay node;
  - It can transmit Physical Downlink Shared Channel (PDSCH) as the data channel;
  - At least, it does not transmit Common Reference Signal (CRS) and Physical Downlink Control Channel (PDCCH) for control functionalities.

Depending on different types of RNs, a RN may be part of the donor cell or controls a cell of its own. In the case that the RN is part of the donor cell, it does not have a cell identity of its own, but still has a relay ID. Most of RRM functions are executed by the eNB of the donor cell, and few parts of the RRM functions may be located in the RN. In the case that a RN is in control of a cell of its own, a unique physical layer cell ID is provided in its cell. The same RRM mechanisms as the eNB are available at the RNs. There is no significant difference between accessing cells controlled by a RN and connecting cells controlled by a normal eNB from the perspective of the RRM of a UE. The cells controlled by the RNs should support also LTE Rel-8 UEs.

Among the above types of relay nodes in LTE-Advanced, basic Type 1 decode-and-forward in-band non-transparent half-duplex fixed RNs are considered as the research objective in this thesis.

2.6.3 Resource Partitioning for Relay Backhauling

Due to the transmitter of RN causing interference to its own receiver, simultaneous eNB-to-RN and RN-to-UE transmissions on the same time-frequency resource units may not be feasible, unless sufficient isolation of the outgoing and incoming signals is provided. Similarly, at the RN, it may not be possible to receive UE transmissions simultaneously with the RN transmitting to the eNB.

In order to accommodate Type 1 RNs, [4] defines a general principle for resource partitioning at the RN as follows:

- eNB→RN and RN→UE links are time division multiplexed in a single carrier frequency (only one is active at any time)
- RN→eNB and UE→RN links are time division multiplexed in a single carrier frequency (only one is active at any time)

The backhaul links, i.e. eNB→RN and RN→eNB transmissions, are done in the downlink frequency band and the uplink frequency band respectively in the FDD mode. In the TDD frames, the backhaul links are in the downlink subframes of the eNB and the uplink subframes of the RN separately.

Considering backward compatibility with 3GPP Rel-8 LTE, the RN is not permitted to transmit to UEs when it is supposed to receive data from the donor eNB, i.e. to create gaps in the RN-to-UE transmission. In these gaps, the UEs associating with the RN are not supposed to expect any transmission from the RN. These gaps can be created by configuring Multimedia Broadcast multicast service Single Frequency Network (MBSFN) subframes as exemplified in Fig. 2.11. RN-to-eNB transmissions can be facilitated by not allowing any UE-to-RN transmissions in some subframes.

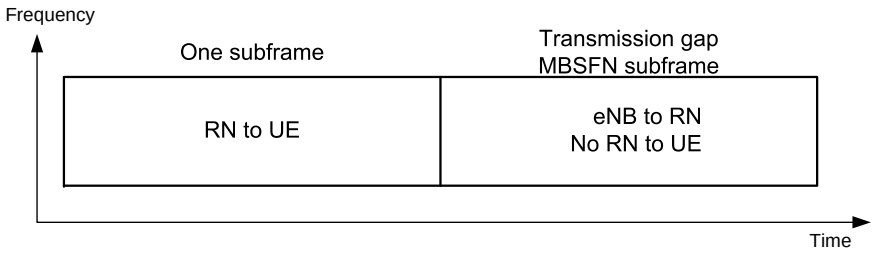

Figure 2.11: Example of RN-to-UE transmission in one normal subframe and eNB-to-RN transmission in a MBSFN subframe [24]

2.7 Conclusion

In this chapter, some related technologies are introduced in order to help readers understand the proposed RRM algorithms in this thesis. First, GSM, UMTS and LTE networks are introduced briefly. Next, the network structures and the multiple access techniques of GSM and UMTS are given. The network structure and the multiple access technique of LTE are included in the individual sections. After the description of radio transmission techniques, frame structures and resource grids, the minimum resource unit for RRM, PRB, is introduced. LTE system and protocol structures provide a framework for the RRM functions, which are also described in this chapter. The changes in the networks architecture of LTE-Advanced are given in the last section, as well as the types of relay nodes and the principles for the two-hop transmission.

Chapter 3

Service-Aware Adaptive Bidirectional Optimisation Route Selection

3.1 Introduction

Due to a great degree of difference between the transmitting power of an eNB and a RN, uplink performance and downlink performance sometimes cannot be optimised simultaneously. As an important aspect of RRM, the conventional route selection strategies optimise either downlink performance only or uplink performance only. However, the UEs launching different types of services have different requirements in the uplink and the downlink. By being aware of service type, an Adaptive Bidirectional Optimisation (ABO) route selection strategy is proposed in this chapter to optimise uplink performance and downlink performance adaptively and dynamically. The objective of the proposed ABO strategy is to maximise the UE bidirectional throughput, which is the sum throughput of uplink and downlink. Moreover, load balancing is considered in the formulation of the proposed strategy to be adapted to different fixed resource partitioning schemes. Through system-level simulation, it can be seen that the proposed strategy is better than the benchmark strategies in different frame configurations.

In this chapter, the related work to this study is reviewed first. After presenting the system models and assumptions, the problem of bidirectional optimisation route selection is formulated and analysed. Then, the proposed ABO route selection

strategy is described together with a complexity analysis. Finally, the simulation results demonstrate the performance advantages of the proposed ABO route selection strategy.

3.2 Related work

[35] proposes a distributed Load Balancing Relay Selection (LB-RS) scheme for relay enhanced OFDMA networks. By considering the current CSI and the relay user number, the proposed LB-RS scheme adopts the ratio of the current data rate to the user number plus 1 as the selection criterion.

In [36], the two-hop achievable efficiency is considered as the harmonic mean of the separate efficiency of backhaul links and access links. Besides, an utility function based on the demand of the relay users and the efficiency of the relay nodes is taken into account. Although this research is based on the MIMO channel and multiple relay cooperative transmission, it can be extended to the non-cooperative scenario. By using the proposed utility function in the relay selection strategy, both the QoS requirement and the effects of the relay nodes are considered.

In [37], the relay selection algorithm allows users to select a relay node with less load and larger instantaneous data rate. Less load of the relay node expects less handover and delay. The load factor of the relay node is defined as the available resource number divided by the subscribed relay users. The two-hop data rate is the harmonic mean of the data rates of backhaul and access links respectively. The load factor and the two-hop data rate are combined by two normalised weights.

In [38], an admission control algorithm with dynamic resource sharing in the backhaul subframes is proposed. The users are connected to the serving nodes with largest received signal power. When the new traffic is launched, the required PRB number for the guaranteed data rate is estimated. If the available resources of the connected serving node is not enough to satisfy the PRB requirement of the new traffic, the traffic is denied.

Due to different transmitting power between relay nodes and eNBs, the relay nodes can provide wider coverage of uplink performance gain and smaller downlink gain coverage. In order to balance the uplink/downlink gain, a cell selection method called 'Range Expand' is investigated in [39] and [40]. In [39], the results show that with larger range extension offset, the downlink performance is degrading and

the uplink performance is improving; when the range extension offset is 6 dB, the bidirectional performance is optimised. With full frequency reuse and ideal backhaul link, [40] presents that 5-tile worst throughput can be increased in downlink with the bias of up to 4 dB and in uplink with the bias of up to 12 dB. The 5-tile worst throughput indicates the 5th percentile of the ascending throughputs. The method of 'Range Expansion' is proposed to the 3GPP[41, 42]. In this method, a 9 dB bias is added to the received signal power level from the Relay Nodes, which is considered as the route selection metric. Hence, the coverage of RNs can be expanded. In [43, 44], the inter-cell interference coordination schemes are proposed for the 'Range Expansion' route selection strategy in order to obtain better performance.

In [45], a weighted energy consumption per bit is used as the selection criteria, which considers data rate requirement in both downlink and uplink. However, the throughputs in the uplink and downlink under different load conditions are not considered.

Two route selection strategies based on Signal to Interference plus Noise Ratio (SINR) are proposed in [46]. In the first strategy, all the relay nodes and the donor eNB in the same sector are reusing the resources in the access subframes. In the second strategy, the resources in the access subframes are partitioned for the direct links and access links according to the ratio of direct users and relay users. Only the relay nodes are reusing the resources.

The traffic throughput balance between direct users and relay users is considered in [47]. In the proposed route selection strategy, the average throughputs of the direct and relay users are calculated respectively, and then either the direct users with the minimum SINR in the direct link or the relay users with the minimum SINR in the access link is changed to be relay users and direct users in order to approach the critical point of throughput balancing.

In [48], the spectral efficiency of a two-hop link is analysed for DF half duplex relaying. Assuming that all the relay nodes are reusing the same resources, the two-hop spectral efficiency is the harmonic mean of the backhaul spectral efficiency and the reuse factor times of average access spectral efficiency. It is also pointed out in this paper that with the increasing reuse factor, the two-hop spectral efficiency will not increase linearly since the inter-relay interference is rising.

[49] provides an early research on route selection and interference coordination. An interference coordination based fractal frequency reuse scheme is proposed. In any macro cell, all the relays cannot reuse the resources of the donor eNB, however

they reuse the resources from another cells and receive less intra-cell interference. In addition, a SINR-based route selection strategy is proposed. However, the reuse factor 4 decreases the area spectral efficiency and peak data rate because the whole frequency bandwidth within a cell is reduced to 1/4 of the reuse factor 1. The frequency reuse factor K indicates the number of cells which cannot use the same frequencies.

In [50], a power-based route selection strategy is proposed to achieve a better trade-off between power consumption and data rate in the uplink. A multi-objective optimisation problem is formulated, which maximises a utility by considering the power consumption as a price for the data rate. As the solution of the optimisation problem, the optimal power and utilities can be derived for all the links. Three power-based route selection algorithms are presented, including power consumption minimisation algorithm, utility maximisation algorithm and the ratio of utility and power maximisation algorithm. Simulation results show significant better performance than the SINR based routing algorithm with the modified open loop fractional power control.

In [51], the authors investigated the impact of various relaying node selection strategies on the system coverage in a fully loaded cellular system. The results show that coverage is sensitive to the relaying node selection strategy. Moreover, the degree of improvement depends on the density and maximum transmit power level of potential relaying nodes.

[52] investigates three route selection strategies in relay enhanced LTE-Advanced networks. Two traditional strategies, downlink received signal power based and downlink minimum SINR based, are compared with the proposed two-hop spectral efficiency based strategy. In the effective spectral efficiency based strategy, the spectral efficiencies of access links and backhaul links are estimated through Shannon formula. Since the data rates of access links and the corresponding backhaul link should be identical to avoid resource waste, the effective two-hop spectral efficiency is derived. Note that the numbers of resources assigned to access links and backhaul links should be adaptive.

In [53], different resource management policies for relay enhanced networks are considered. The authors propose a route selection strategy similar to [52]. However, different frequency reuse patterns of multiple relay nodes are considered in the proposed route selection strategy. The more times the same frequency is reused, the higher the spectral efficiency of access links the users would experience.

[54] focuses on the route selection problem in relay enhanced OFDMA networks with adaptive resource partitioning and none frequency reuse in access subframes, where the traditional proportional fair scheduling algorithm is independently executed at the eNB and relay nodes. The generalised proportional fairness problem is formulated and solved through the Lagrange multiplier algorithm. Hence, the possible data rates of different connections for a user can be estimated and the GPF objective function is derived. A greedy route selection algorithm is proposed to maximise the improvement of the GPF objective function.

[55] proposed a QoS-guaranteed route selection strategy in relay enhanced OFDMA networks. The minimum resource number to fulfil the guaranteed data rate and the bit error rate is calculated. And the objective of the algorithm is to maximise the number of users having the minimum resource number. However, the subframe division is not considered and only rate-constrained services are considered.

[56], the authors firstly design an adaptive resource partitioning scheme with the upper bound of each resource segment in order to improve resource utility and reduce inter-cell interference. Secondly, under constraints brought by the proposed resource partitioning scheme, a utility-based heuristic routing mechanism was developed, which can be used to maximize the cell aggregate utility. The users are initiated with the relay nodes and the eNB by comparing the spectral efficiencies of access links and direct links. Then, the sub-optimal system aggregate utility and the constraint condition are satisfied by changing some relay users to be direct users one by one.

The route selection strategies based on downlink optimisation are proposed in [35, 36, 37, 38, 46, 47, 48, 49, 51, 52, 53, 54, 55, 56]. In these research, the route selection strategies do not consider the uplink performance. The researchers in [50] focus on uplink performance and power consumption without considering downlink performance. Uplink and downlink performance in terms of data rate and energy consumption is studied in [45]. However, the performance of different service types is not considered and the energy consumption in uplink and downlink cannot be compared due to different sources of electrical supply. The 'Range Expansion' based route selection strategies are proposed in [39, 40, 41, 42, 43, 44], which sacrifice downlink performance for uplink performance. In addition, load balancing is not considered in these strategies. Although the load balancing mechanism is considered in many researches [35, 37, 47], the load balancing between direct links and two-hop links is not considered and is not incorporated into the proposed strategies. If uplink performance and downlink performance cannot be considered simultaneously,

the services with larger uplink requirement cannot be supported. If load balancing is incorporated in the route selection strategies, the performance improvement in different frame configurations cannot be guaranteed.

3.3 System model

3.3.1 Cell Structure

As a LTE-Advanced macro cell structure, illustrated in Fig.3.1, an eNB is located in the centre of a macro cell. K RNs are deployed at the cell edge with the same distance from the eNB. All the RNs can be numbered from 1 to K to generate a set of serving nodes $\{\mathcal{K}\}$, and the eNB can be added into $\{\mathcal{K}\}$ as serving node 0. M UEs may connect with any serving node.

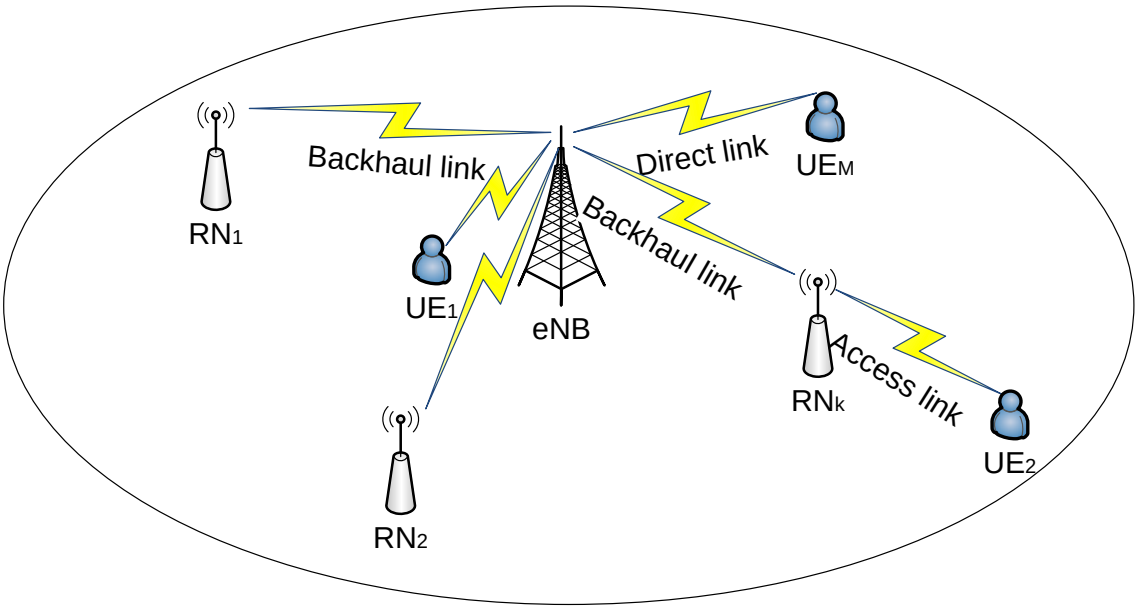

Figure 3.1: Illustration of a LTE-Advanced macro cell

There are three types of links, i.e. eNB-RN links, RN-UE links and eNB-UE links, which are named as backhaul links, access links and direct links respectively. In order to avoid significant interference at RNs, backhaul links should use resources isolated from access links [14]. The data rate in each backhaul link is assumed to be equal to the sum of the data rates in the corresponding access links.

3.3.2 Radio Transmission Model

In LTE-Advanced uplink and downlink, different time slots and different amount of resources are assigned to different links according to different frame configurations. In these frame configurations, the direct links and the access links are reusing all the resources assigned to them. For the multi-cell scenario, the cells adjacent to each other are using the same carrier frequency band since the inter-cell interference can be alleviated by employing RNs.

Physical resource block (PRB) is a basic OFDM resource allocation unit, which comprises of a constant number of subcarriers and OFDM symbols [22]. All the serving nodes and the UEs are assumed to allocate the same power over every occupied PRB, and the sum of the transmitting power in all occupied PRBs should not exceed the maximum power. In addition, fractional uplink power control is applied in UEs. In order to maximise the desired received power while limiting the generated interference, the transmitting power of a UE is based on fractional path loss (PL) compensation, which is defined in [32]:

$$P = \min\{\ P_{max}, P_0 + 10\log_{10}(N) + \alpha PL\} \tag{3.1}$$

where P_{max} is the maximum transmitting power of a UE, α and P_0 are the path loss compensation factor and a parameter to ensure the minimum received signal power level, and N is the number of uplink PRBs allocated to that UE.

In order to estimate the achievable data rate, we consider a long term Signal to Interference plus Noise Ratio (SINR) which is a average value of past instantaneous SINRs obtained through channel measurements. Hence, the long term SINR is updated in periodically with a reasonable moving filter to alleviate the effect of fast fading. The durations are different considering different UE movement speeds. A transmission between UE m and serving node k has different SINR values in different assigned PRBs.

To simplify the analysis, three service types with different uplink and downlink requirements, i.e. Q^{UL} and Q^{DL}, are defined in this study, including uplink-biased service, downlink-biased service and symmetric service. One UE can only launch one type of service at one time. Q^{UL} and Q^{DL} are defined as the maximum PRB numbers which can be scheduled to the services in the uplink and the downlink respectively. They prevent the data rates of the UEs in the top channel from exceeding the Maximum Bite Rate (MBR) under the constraint of fair allocation. These two

parameters and the MBR can be determined from the QoS class identifier (QCI) which is assigned to each transport layer bearer by the network [57]. The QCI is used as a reference to the eNB parameters (e.g., scheduling weights, admission thresholds, queue management thresholds, etc.), which can be preconfigured by operators.

3.3.3 Scheduling Algorithms

Round-Robin (RR) scheduling is considered in this research to guarantee the allocation fairness between UEs, which is usually considered as a benchmark scheduling scheme. Being executed in the direct links and the access links independently, Round-Robin scheduling assigns an equal portion of PRBs to each UE until the maximum uplink and downlink PRB requirements, i.e. Q^{UL} and Q^{DL}, are satisfied. When the Round-Robin scheduling scheme is applied, UE m is, statistically speaking, allocated to all PRBs randomly. Thus, its data rate per PRB can be estimated to be the average data rate of all PRBs. Through Shannon's formula, the achievable data rate per PRB in the transmission of the $m \leftrightarrow k$ link can be calculated as

$$\sigma_{m,k} = B\overline{\log_2(1+\gamma_{m,k,i})}, \forall i \in all\ PRBs \tag{3.2}$$

where B is the bandwidth of a PRB and $\gamma_{m,k,i}$ is the large scale SINR on PRB i in the $m \leftrightarrow k$ link.

Proportional-fair (PF) scheduling is also considered in this research to exploit the channel variation and guarantee the allocation fairness between UEs. In the direct links and the access links, the PF scheduling assigns each PRB to the UE m^* with the largest ratio of the current data rate $r_{m,k,i}$ to the history data rate $\bar{R}_m$

$$m^* = \arg\max \frac{r_{m,k,i}}{\bar{R}_m} \tag{3.3}$$

When Proportional-fair scheduling is utilised, the achievable data rate per PRB can be simplified into a UE number related scheduling gain G multiplying the data rate per PRB achieved by the Round-Robin scheduling [31, 58]. The achievable data rate per PRB in the transmission of the $m \leftrightarrow k$ link under Proportional-fair scheduling can be calculated as

$$\sigma_{m,k} = G(k) \times B\overline{\log_2(1+\gamma_{m,k,i})}, \forall i \in all\ PRBs \tag{3.4}$$

The scheduling gain $G(k)$ is different for different serving node k according to the

numbers of UEs being scheduled, which can be derived by off-line simulation.

3.4 Problem Formulation and Analysis

With the objective of maximising the bidirectional throughput of the UEs, the route selection problem is formulated as

$$\begin{aligned} \max R_m &= \max(R_m^{UL} + R_m^{DL}) \\ &= \max \sum_{k \in \mathcal{K}} \rho_{m,k}(\beta_{m,k}^{UL}\sigma_{m,k}^{UL} + \beta_{m,k}^{DL}\sigma_{m,k}^{DL}) \end{aligned} \tag{3.5}$$

subject to

$$\sum_{m \in M} \rho_{m,k}\beta_{m,k}^{UL} \leq BW_k^{UL}, \forall k \in \mathcal{K} \tag{3.6}$$

$$\sum_{m \in M} \rho_{m,k}\beta_{m,k}^{DL} \leq BW_k^{DL}, \forall k \in \mathcal{K} \tag{3.7}$$

$$\sum_{k \in \mathcal{K}}^{k \neq 0} \sum_{m \in M} \frac{\rho_{m,k}\beta_{m,k}^{UL}\sigma_{m,k}^{UL}}{\sigma_{k,0}^{UL}} \leq BW_{\mathcal{K},0}^{UL} \tag{3.8}$$

$$\sum_{k \in \mathcal{K}}^{k \neq 0} \sum_{m \in M} \frac{\rho_{m,k}\beta_{m,k}^{DL}\sigma_{m,k}^{DL}}{\sigma_{k,0}^{DL}} \leq BW_{\mathcal{K},0}^{DL} \tag{3.9}$$

In the utility function (3.5), R_m is the bidirectional data rate achieved by UE m, R_m^{UL} and R_m^{DL} represent its uplink and downlink data rate respectively. When UE m is connected to serving node k, the uplink data rate and the downlink data rate are determined by the achievable numbers of the occupied PRBs, denoted as $\beta_{m,k}^{UL}$ and $\beta_{m,k}^{DL}$, and the achievable data rates per PRB in these links, i.e. $\sigma_{m,k}^{UL}$ and $\sigma_{m,k}^{DL}$, which are derived from equations (3.2) and (3.4). In addition, $\rho_{m,k}$ is a connection index.

$$\rho_{m,k} = \begin{cases} 1 & \text{when UE } m \text{ is connected to node } k \\ 0 & \text{otherwise} \end{cases}$$

$$\sum_{k \in \mathcal{K}} \rho_{m,k} = 1 \tag{3.10}$$

In the constraints (3.6) and (3.7), if UE m is not associating with serving node k, $\beta_{m,k}^{UL}$ and $\beta_{m,k}^{DL}$ will be 0. BW_k^{UL} and BW_k^{DL} are the maximum uplink and downlink PRB numbers in serving node k respectively according to the frame configurations

defined in Section 4. As shown in the expressions (3.8) and (3.9), the achievable data rates in the access links are also constrained by the total PRB numbers assigned to the backhaul links. $BW_{\mathcal{K},0}^{UL}$ and $BW_{\mathcal{K},0}^{DL}$ are the total uplink and downlink PRB numbers respectively assigned to the backhaul links. $\sigma_{k,0}^{UL}$ and $\sigma_{k,0}^{DL}$ indicate the data rates per PRB in these backhaul links.

Using fair-based resource scheduling algorithms, e.g. Round-Robin and Proportional-fair, the PRBs can be assigned to each UE in equal portions. Thus, under the constraints (3.6)-(3.9), $\beta_{m,k}^{UL}$ and $\beta_{m,k}^{DL}$ can be calculated as follows:

- for a direct link between UE m and the macro eNB

$$\beta_{m,0}^{UL} = \min(Q_m^{UL}, \lfloor Q_m^{UL} \frac{BW_0^{UL}}{\sum_{m \in M} \rho_{m,0} Q_m^{UL}} \rfloor) \tag{3.11}$$

$$\beta_{m,0}^{DL} = \min(Q_m^{DL}, \lfloor Q_m^{DL} \frac{BW_0^{DL}}{\sum_{m \in M} \rho_{m,0} Q_m^{DL}} \rfloor) \tag{3.12}$$

- for a relay link via a RN, serving node k, where $k \in \mathcal{K}$ and $k \neq 0$

$$\begin{aligned} \beta_{m,k}^{UL} = \min(Q_m^{UL}, \lfloor Q_m^{UL} \frac{BW_k^{UL}}{\sum_{m \in M} \rho_{m,k} Q_m^{UL}} \rfloor, \\ \lfloor Q_m^{UL} \frac{BW_{\mathcal{K},0}^{UL}}{\sum_{k \in \mathcal{K}}^{k \neq 0} \sum_{m \in M} \rho_{m,k} Q_m^{UL} \sigma_{m,k}^{UL} / \sigma_{k,0}^{UL}} \rfloor) \end{aligned} \tag{3.13}$$

$$\begin{aligned} \beta_{m,k}^{DL} = \min(Q_m^{DL}, \lfloor Q_m^{DL} \frac{BW_k^{DL}}{\sum_{m \in M} \rho_{m,k} Q_m^{DL}} \rfloor, \\ \lfloor Q_m^{DL} \frac{BW_{\mathcal{K},0}^{DL}}{\sum_{k \in \mathcal{K}}^{k \neq 0} \sum_{m \in M} \rho_{m,k} Q_m^{DL} \sigma_{m,k}^{DL} / \sigma_{k,0}^{DL}} \rfloor) \end{aligned} \tag{3.14}$$

Load balancing in conventional cellular networks usually refers to distributing traffic load among base stations, while maintaining QoS for users. In relay-enhanced networks, load balancing is usually defined as an integral part of RRM schemes, which is aimed at evenly distributing traffic load among all serving nodes in a macro cell. However, there is no literature on load balancing mechanism considering both uplink and downlink so far. Thus, a new load balancing mechanism is necessary for the ABO route selection strategy.

According to Round-Robin and Proportional-fair scheduling algorithms and the assumed resource allocation rules, traffic load in a link is defined as the ratio of the

total PRB requirements to the maximum PRB number assigned to this link. The traffic load of the direct links and the access links are expressed as:

$$CL_{m,k}^{UL} = \frac{\sum_{m \in M} \rho_{m,k} Q_m^{UL}}{BW_k^{UL}}, \forall k \in \mathcal{K} \tag{3.15}$$

$$CL_{m,k}^{DL} = \frac{\sum_{m \in M} \rho_{m,k} Q_m^{DL}}{BW_k^{DL}}, \forall k \in \mathcal{K} \tag{3.16}$$

and the traffic load of the backhaul links are presented as

$$CL_{\mathcal{K},0}^{UL} = \sum_{k \in \mathcal{K}}^{k \neq 0} \sum_{m \in M} \frac{\rho_{m,k} Q_m^{UL} \sigma_{m,k}^{UL}}{BW_{\mathcal{K},0}^{UL} \sigma_{k,0}^{UL}}, \forall k \in \mathcal{K}, k \neq 0 \tag{3.17}$$

$$CL_{\mathcal{K},0}^{DL} = \sum_{k \in \mathcal{K}}^{k \neq 0} \sum_{m \in M} \frac{\rho_{m,k} Q_m^{DL} \sigma_{m,k}^{DL}}{BW_{\mathcal{K},0}^{DL} \sigma_{k,0}^{DL}}, \forall k \in \mathcal{K}, k \neq 0 \tag{3.18}$$

By substituting (3.15)-(3.18) into (3.11)-(3.14), the achievable PRB numbers of all UEs can be expressed as:

- for a direct link between UE m and the macro eNB

$$\beta_{m,0}^{UL} = \lfloor \frac{Q_m^{UL}}{\max(1, CL_{m,0}^{UL})} \rfloor \tag{3.19}$$

$$\beta_{m,0}^{DL} = \lfloor \frac{Q_m^{DL}}{\max(1, CL_{m,0}^{DL})} \rfloor \tag{3.20}$$

- for a relay link via a RN, serving node k, where $k \in \mathcal{K}$ and $k \neq 0$

$$\beta_{m,k}^{UL} = \lfloor \frac{Q_m^{UL}}{\max(1, CL_{m,k}^{UL}) \max(1, CL_{\mathcal{K},0}^{UL})} \rfloor \tag{3.21}$$

$$\beta_{m,k}^{DL} = \lfloor \frac{Q_m^{DL}}{\max(1, CL_{m,k}^{DL}) \max(1, CL_{\mathcal{K},0}^{DL})} \rfloor \tag{3.22}$$

3.5 Algorithm Description

To implement the adaptive bidirectional optimisation (ABO) route selection strategy with load balancing proposed in this chapter, several channel parameters are necessary: the data rates per PRB in each uplink and each downlink, i.e. $\sigma_{m,k}^{UL}$ and

$\sigma_{m,k}^{DL}$, which can be derived from the channel measurement process, and the resource requirements of different types of services, i.e. Q_m^{UL} and Q_m^{DL}.

In the multi-cell environment, the available serving nodes $\{\mathcal{K}_m\}$ comprise a macro eNB from which the largest signal power is received, and the nearest K RNs. By computing the achievable PRBs from (3.19)-(3.22) , the demand metric of UE m on serving node k is given as

$$D_{m,k} = \beta_{m,k}^{UL}\sigma_{m,k}^{UL} + \beta_{m,k}^{DL}\sigma_{m,k}^{DL}, when\ k \in \mathcal{K}_m \tag{3.23}$$

When UE m is connected to serving node k which has the largest demand metric $D_{m,k}$, the bidirectional throughput of UE m can be achieved according to the utility function (3.5).

The route selection processes of all the UEs are executed in a one-by-one manner. When UE m needs to select a new route to launch a service, the detailed execution of the ABO strategy is described in Algorithm 1. The ABO strategy is deployed at the

Algorithm 1 The ABO algorithm

Input: $\sigma_{m,k}^{UL}$, $\sigma_{m,k}^{DL}$, Q_m^{UL}, Q_m^{DL}

for $k = 0 : |\mathcal{K}_m|$ **do**
  if k is a macro eNB **then**
    $CL_{m,0}^{UL}$, $CL_{m,0}^{DL} \leftarrow$ the new traffic loads considering UE m through the calculation in (3.15) and (3.16)
    $\beta_{m,0}^{UL}$, $\beta_{m,0}^{DL} \leftarrow$ the calculation according to (3.19) and (3.20)
  else
    $CL_{m,k}^{UL}$, $CL_{m,k}^{DL} \leftarrow$ the new access traffic loads considering UE m through (3.15) and (3.16)
    $CL_{\mathcal{K},0}^{UL}$, $CL_{\mathcal{K},0}^{DL} \leftarrow$ the new backhaul traffic loads considering UE m through (3.17) and (3.18)
    $\beta_{m,k}^{UL}$, $\beta_{m,k}^{DL} \leftarrow$ the calculation according to (3.21) and (3.22)
  end if
  Obtain $D_{m,k}$, according to (3.23)
end for
$k \leftarrow \arg\max D_{m,k}, \forall k \in \mathcal{K}_m$
return k
Connect UE m and serving node k

eNB of each cell. The SINRs of direct UEs are measured by the eNB, and the SINRs of relay UEs are measured by the RNs. The RNs calculate the $CL_{m,k}^{UL}$ and $CL_{m,k}^{DL}$ instead of the feedback of the channel conditions of relay UEs. Then, $\beta_{m,k}^{UL}$ and $\beta_{m,k}^{DL}$ can be obtained. The measurement of SINR is carried out every radio frame and the long term SINR is also updated in the same period, which are the same in the

existing strategies and the proposed strategy. Compared with the existing simple route selection strategies, the frequency of SINR measurement and the messaging between the RNs and the eNB are the same. The calculation complexity at the RNs increases, which is within the capability of Type 1 RNs.

3.6 Complexity Analysis

In a N-cell network with K RNs per cell and overall M UEs, the calculation of all demand metrics requires revisiting the information of UEs M times, and the determination of the largest demand metric needs $N(K+1)$ basic operations. Hence, The execution of the proposed strategy has a computation complexity of $O(NK + M)$. Compared with the existing simple route selection strategies with the complexity of $O(NK)$, such as Received Signal Power based strategy, the proposed ABO strategy should acknowledge all the UEs in the network and hence increase the complexity. However, it is quite acceptable for the practical LTE systems with the active number of UEs not more than 120 per cell.

3.7 Performance Evaluation

3.7.1 Simulation Parameters

Based on the LTE self-evaluation methodology [14], a static system-level Matlab simulation platform is developed to evaluate system performance using the ABO strategy and the benchmark strategies, the Received Signal Power based (RSP) strategy and the "Range Expansion" (RE) strategy. This simulation platform is extended from a open source product, Vienna LTE simulators [59], of Vienna University of Technology, Austria. In order to evaluate the proposed strategy, the two-hop links are added based on the single-hop LTE simulators. Some simple scenarios, such as single direct UE and single relay UE at fixed positions, have been tested to validate the simulation platform.

A seven-cell LTE-Advanced network is generated where inter-cell distance is 500 meters and 6 RNs per cell are deployed at the same distance of 2/3 of the cell radius from the eNB. A unique number of UEs are randomly dropped in each macro cell. A 20 MHz frequency band at 2 GHz is utilised and 100 PRBs in a time slot

can be used for data transmission, whilst a 10 MHz frequency band with 50 PRBs per time slot is also considered for some performance measurements. The "Typical Urban Macro-cell" deployment model from 3GPP TR 36.814 [14] is employed using lognormal shadowing with different standard deviations, 6 dB between eNB and relay, 8 dB between eNB and macro UE and 10 dB between relay and relay UE. The Rayleigh fast fading model is utilised to create frequency and time selective channels. The maximum transmitting power of eNB, RN and UE is set to be 46 dBm, 30 dBm, and 23 dBm respectively. 15 dBi omni antenna is equipped in eNB, and 5 dBi omni antenna is installed in RN, when no gain antenna is integrated in UE. The minimum power of -56 dBm and the path loss compensation factor of 0.6 are configured in fractional uplink power control of UEs. In addition, QPSK, 16QAM and 64QAM modulation schemes are supported.The Manhattan mobility model is considered, where the probability of going straight is 0.5 and taking a left or right is 0.25 each. The maximum UE speed v_m is assumed as 60 km/h. The coherence time T_C caused by Doppler frequency shift can be calculated according to [60]

$$T_C = \sqrt{\frac{9v_C^2}{16\pi v_m^2 f_c^2}} \approx 11.4ms \tag{3.24}$$

where v_C is the speed of radio wave and f_c is the carrier frequency, which is 2 GHz. Since the duration of a radio frame in LTE-Advanced is 10ms, the long term average SINR is designed to be updated every radio frame using the exponential moving average method [61]. The length of the moving average filter is set up as 100 according to [62].

Time division duplexing (TDD) LTE-Advanced is discussed in the simulations. In a TDD LTE-Advanced radio frame, different time slots are assigned to different links in different frame configurations, and different amount of resources are assigned to each type of link. Two different frame configurations, Variant A and Variant B, are considered. Inherited from the frame structure type 2 defined in [22], two frame configurations are shown in Fig.3.2. In these two configurations, the direct links and the access links share the same resources in some subframes, and the direct links and the backhaul links can only use isolated resources in other subframes. In Variant A, the direct links and the access links share subframe 2 in the uplink and subframe 0, 3 and 4 in the downlink. In subframe 5, 7, 8 and 9, one time slot is assigned to the direct links and the other one is orthogonally allocated to the backhaul links according to their date rates in order to avoid serious interference between these two types of links. In Variant B, all of subframe 7, 8, and 9 are occupied by the backhaul links. Besides, the access link share subframe 0, 2, 3 and

4 with the direct links. In Variant B, the resource ratio of the backhaul links to the direct links is 1:1, while the ratio is 1:2 in Variant A. The frame configuration Variant A represents the scenario that there are fewer resources for relay UEs, and the Variant B represents the scenario that there are more resources for relay UEs. Two frame configurations are possible in practical networks, and the effectiveness of the ABO strategy and the benchmarking strategies should be evaluated in these two fixed frame configurations. The performance differences caused by load balancing mechanisms in these strategies are tested through the simulation in these frame configurations.

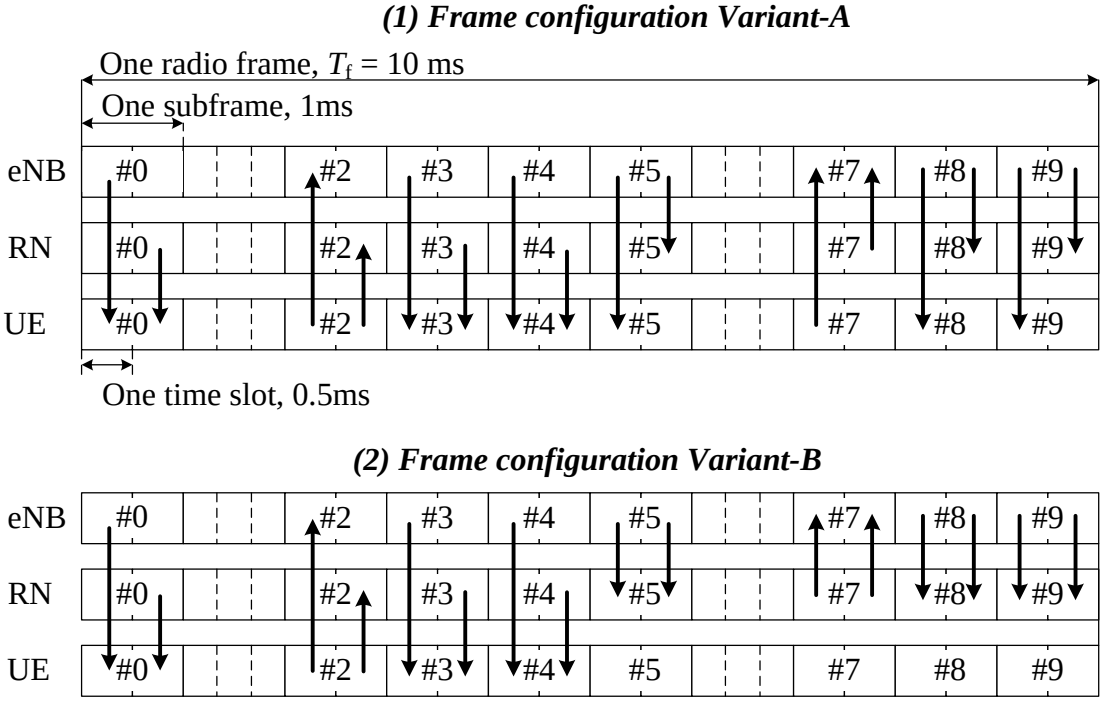

Figure 3.2: Frame configuration, Variant-A and Variant-B

As shown in Table 3.1, three service types are assumed with different Q^{UL} and Q^{DL}, which are assigned to different proportions of services. As a result, the ratio of the total uplink PRB requirements to the total downlink PRB requirements should match the ratio of uplink PRBs and downlink PRBs in a radio frame.

Table 3.1: Traffic Model

Service Type	Q^{UL}	Q^{DL}	Proportion
Uplink-biased	20	2	1/9
Symmetric	2	2	1/3
Downlink-biased	2	20	5/9

The proposed ABO strategy is compared with two benchmark schemes:

- The traditional received signal power based (RSP) strategy: This strategy is also commonly used in LTE network without relaying. Each UE is associated with the serving node from which UE receive the strongest signal power.
- The "Range Expansion" (RE) strategy [41, 42, 43, 44]: For each UE, the serving node is selected based on the largest received signal power plus a selection bias. The selection bias is set to be 9 dB in this work. Besides, the direct links and the access links are fully reusing the entire frequency band.

3.7.2 Results and Discussions

Through simulations, the ABO strategy is compared with the benchmark strategies in terms of cell throughput and UE throughput. Both Round-Robin (RR) scheduling and Proportional fair (PF) scheduling are implemented. The effects of these strategies with different UE numbers per cell and different frame configurations are studied. Besides, the uplink throughputs of uplink-biased UEs and the relation between UE throughput and UE distance from the cell centre are also analysed.

3.7.2.1 Cell throughput

From Fig.3.3 to Fig.3.6, it can be observed that the mean cell throughputs increase along with the growing UE number per cell because the cell loads are increased with more allocated PRBs. However, they are not strictly in a direct proportion due to the decreasing mean UE throughput, which can be found in Fig.3.7 and Fig.3.8. Since the cell loads are increased, the interference between different links will also increase to lower the mean UE throughput.

In Fig.3.3, the average uplink throughputs in each cell using the route selection strategies in Variant A versus UE numbers per cell are illustrated. When the RR scheduling algorithm and the PF scheduling algorithm are utilised, the ABO strategy can obtain larger uplink throughput than the benchmarking RSP and RE route selection strategies with any UE numbers per cell. The RSP strategy is slightly more effective than the RE strategy in Variant A except when 100 UEs are located in a cell and RR scheduling is utilised. By using the PF scheduling algorithm, the RSP strategy has similar effectiveness with the ABO strategy when the UE number per cell is not very large, and has better performance than the RE strategy.

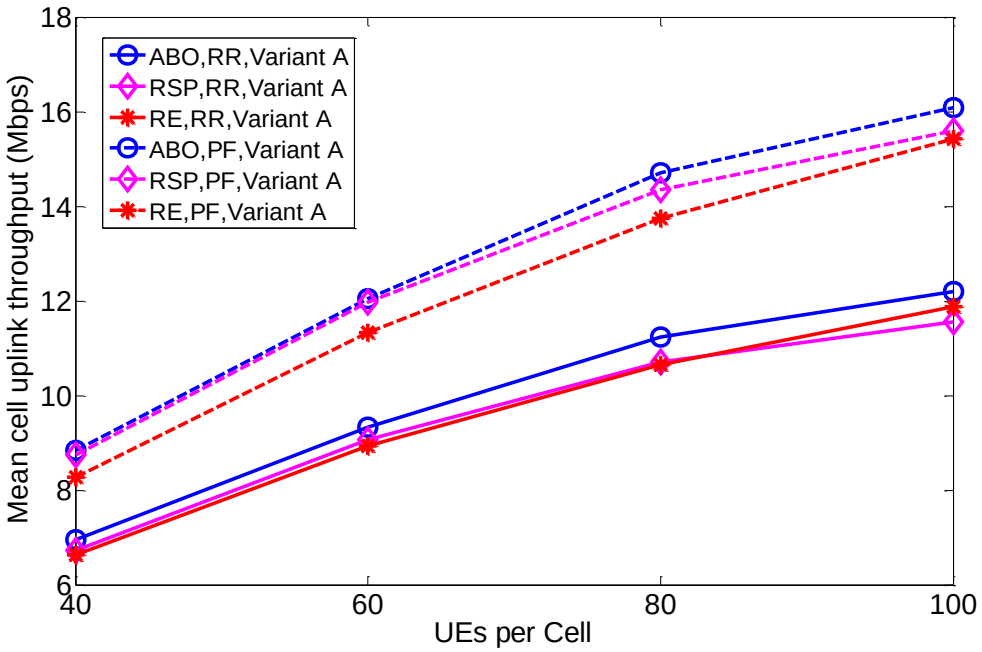

Figure 3.3: Mean cell uplink throughput v.s. the number of users per cell in Variant A

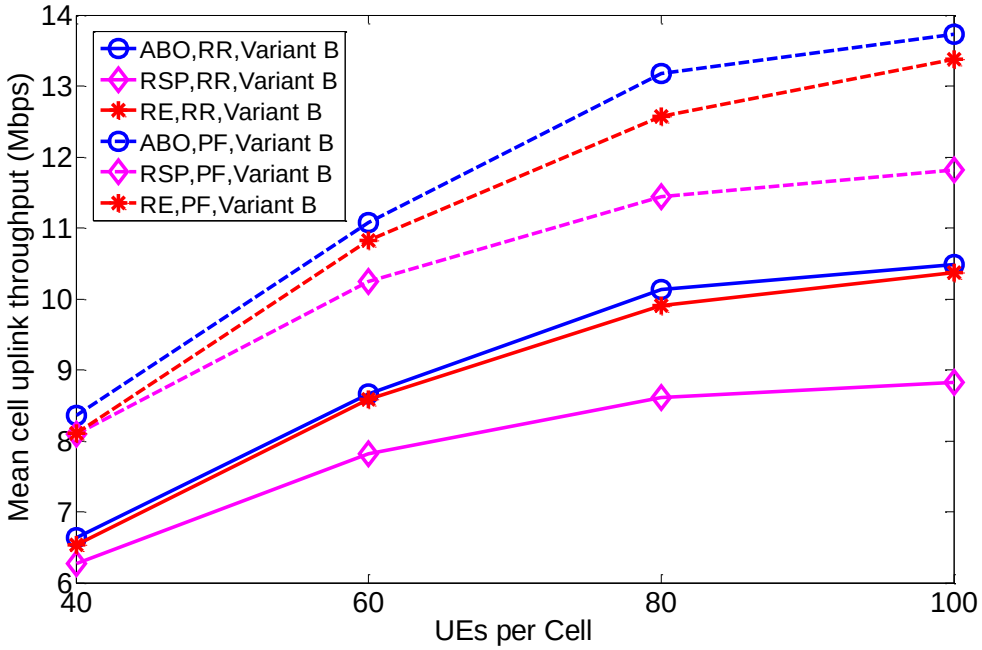

Figure 3.4: Mean cell uplink throughput v.s. the number of users per cell in Variant B

Fig.3.4 shows the average cell uplink throughputs using different route selection strategies in Variant B. The proposed ABO strategy can obtain larger cell uplink throughput than the benchmark strategies with any UE numbers per cell using different scheduling algorithms. The RE strategy is better than the RSP strategy in getter larger cell uplink throughputs in different numbers of UE per cell and different scheduling algorithms. The performance gaps between the ABO strategy and the RE strategy using the PF scheduling algorithm are larger than those using the RR scheduling algorithm.

Table 3.2: Comparison in mean cell uplink throughput

	The UE number per cell			
	40	60	80	100
ABO, RR, VA	3.28%	3.03%	4.81%	5.46%
RE, RR, VA	-1.66%	-1.50%	-0.54%	2.75%
ABO, RR, VB	5.86%	10.61%	17.65%	18.91%
RE, RR, VB	4.19%	9.76%	15.03%	17.61%

The improvements in percentages of the ABO strategy and the RE strategy against the RSP strategy for the mean uplink throughput per cell are depicted in Table 3.2.

In Fig.3.5, the bidirectional throughputs, the sum of the uplink throughputs and the downlink throughputs, in Variant A are presented. The proposed ABO strategy has the best performance in getting larger mean cell bidirectional throughputs among those three strategies. Similar to the relationship in Fig.3.3, the RSP strategy can obtain larger bidirectional throughput than the RE strategy in different RN numbers per cell, no matter which scheduling algorithm is utilised. When the PF scheduling algorithm is used and there are 40 or 60 UEs per cell, approximated bidirectional throughputs can be obtained by the ABO strategy and the RSP strategy.

Fig.3.6 demonstrates the bidirectional throughputs in Variant B v.s. the UE number per cell. Among the route selection strategies, the ABO strategy proposed in this study has the largest average cell bidirectional throughputs. When there are 80 or 100 UEs per cell, the RE strategy is better than the RSP strategy in terms of bidirectional throughputs using different scheduling algorithms. When there are 40 or 60 UEs per cell, the RSP strategy has larger bidirectional throughputs using the PF scheduling algorithm than the RE strategy, and has approximate bidirectional throughputs using the RR scheduling algorithm with the RE strategy.

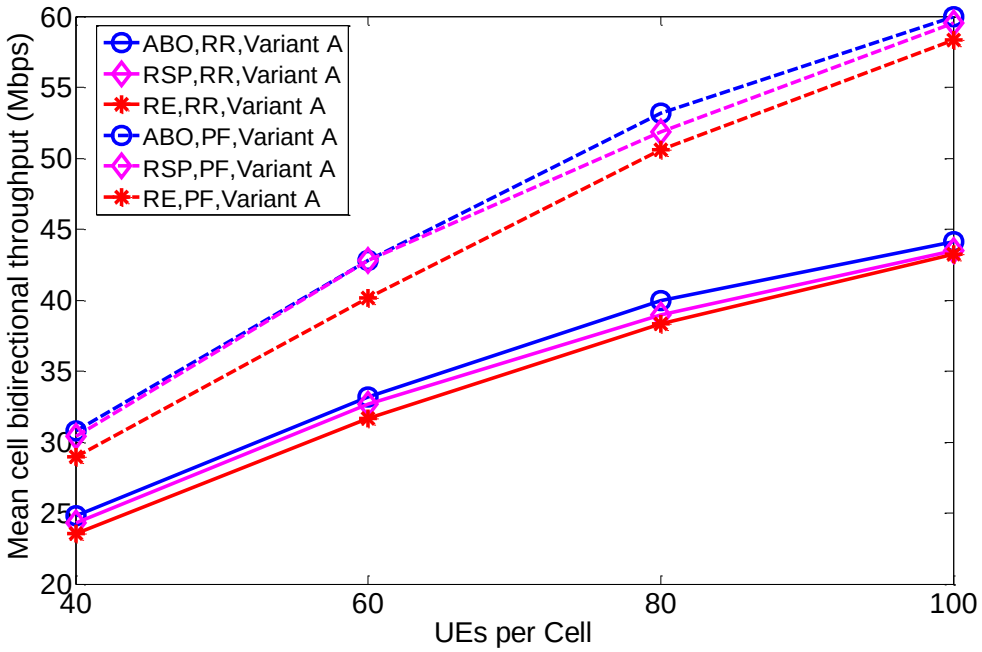

Figure 3.5: Mean cell bidirectional throughput v.s. the number of users per cell in Variant A

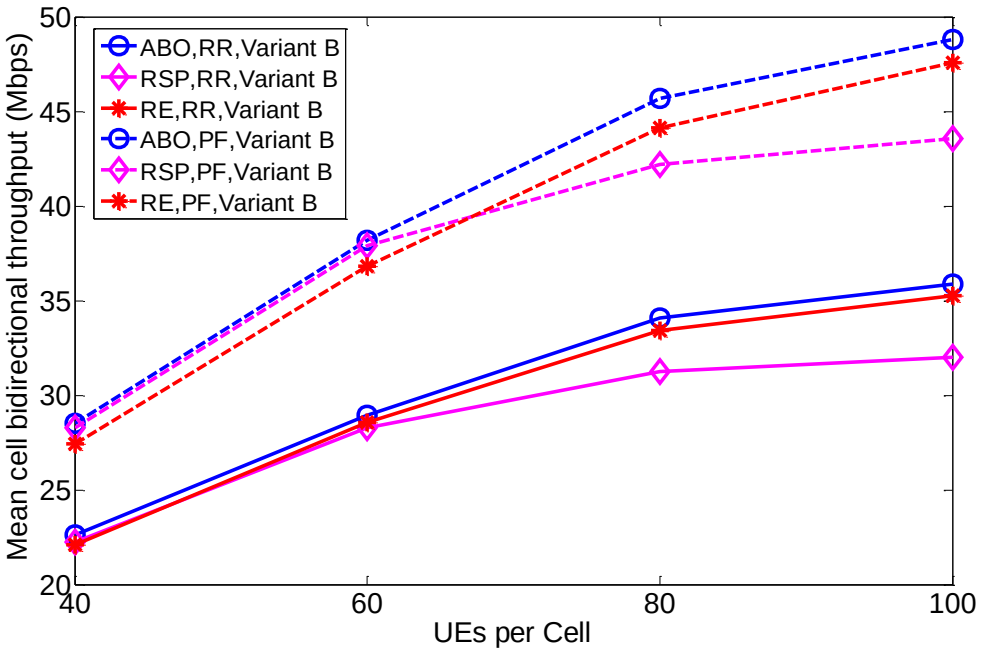

Figure 3.6: Mean cell bidirectional throughput v.s. the number of users per cell in Variant B

Table 3.3: Comparison in mean cell bidirectional throughput

	The UE number per cell			
	40	60	80	100
ABO, RR, VA	2.11%	1.69%	2.54%	1.43%
RE, RR, VA	-3.23%	-3.10%	-1.73%	-0.64%
ABO, RR, VB	1.89%	2.71%	8.82%	11.87%
RE, RR, VB	-0.67%	1.18%	6.80%	10.15%

The improvements in percentages of the ABO strategy and the RE strategy against the RSP strategy for the mean bidirectional throughput per cell are depicted in Table 3.3.

The performance gain in cell bidirectional throughput of the ABO strategy over the RSP and the RE strategies is insignificant, between 1.89% and 11.87%. Nonetheless, the ABO strategy has better performance in optimising the UE throughputs with some types of services due to its ability of adaptively optimising uplink and downlink throughput according to service types.

Since the uplink-biased services are the main concerns in the future traffic, the average uplink throughputs of uplink-biased UEs are presented in Fig.3.7 and Fig.3.8. It is illustrated that the average uplink throughputs of uplink-biased UEs using the ABO strategy are improved much more significantly. The average throughput gains are 6% in Variant A and 14% in Variant B compared with the RSP strategy, and 8.8% in Variant A and 5.8% in Variant B compared with the RE strategy.

Table 3.4: Comparison in mean UE uplink throughput with uplink-biased services

	The UE number per cell			
	40	60	80	100
ABO, RR, VA	7.39%	4.63%	6.45%	6.95%
RE, RR, VA	-3.72%	-4.82%	-3.17%	-0.77%
ABO, RR, VB	10.96%	14.17%	20.85%	20.24%
RE, RR, VB	3.91%	8.01%	11.65%	13.63%

The comparison of the ABO strategy and the RE strategy against the RSP strategy in the mean UE uplink throughput with uplink-biased services is illustrated in Table 3.4.

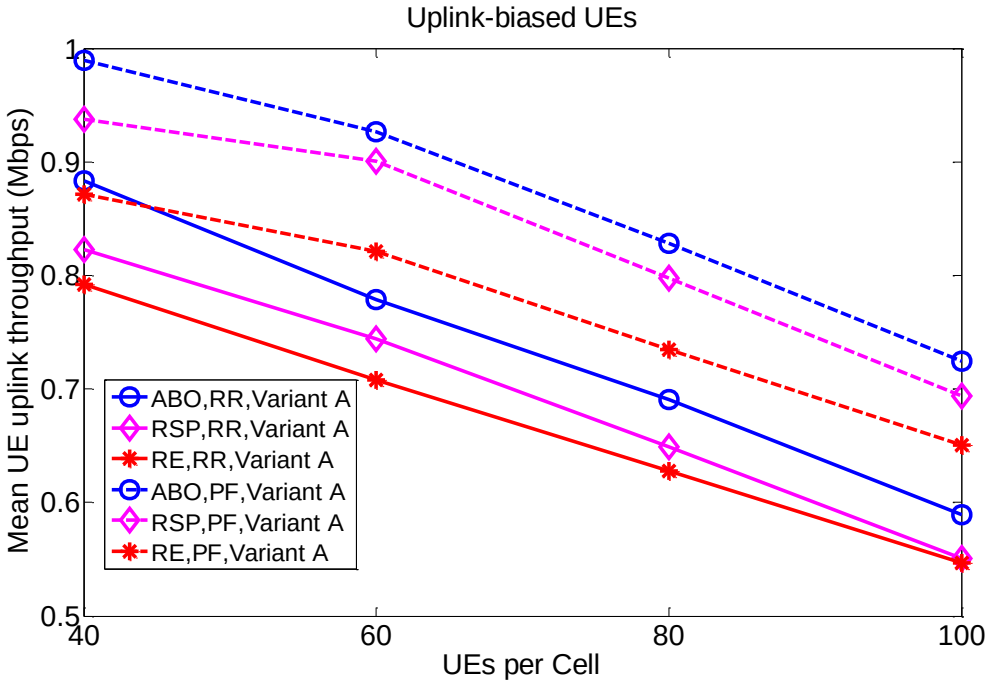

Figure 3.7: Mean uplink throughput of users with uplink-biased service v.s. the number of users per cell in Variant A

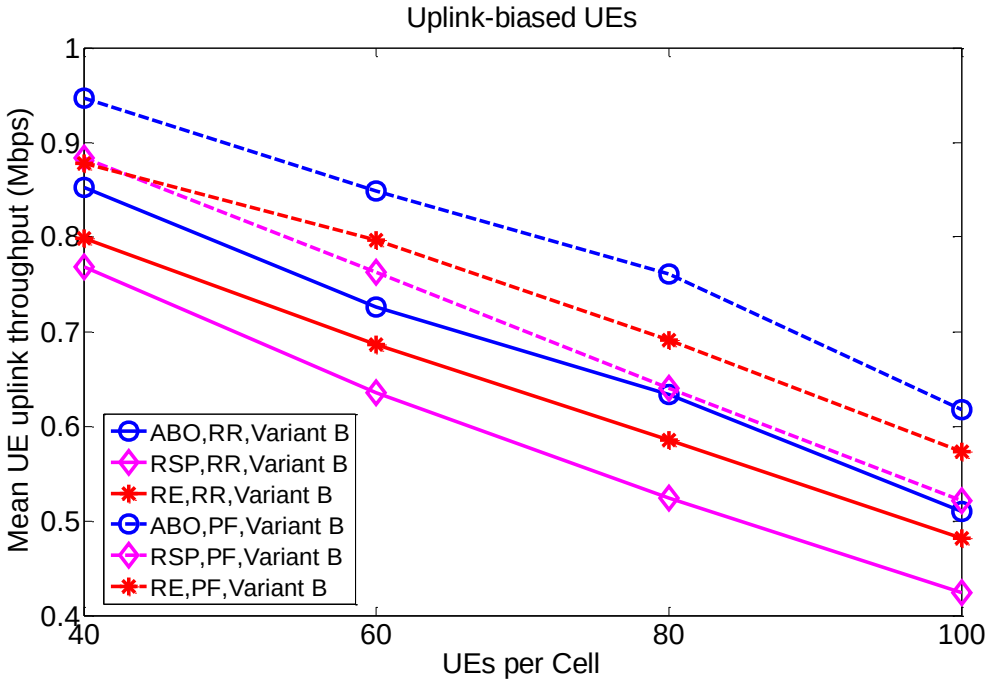

Figure 3.8: Mean uplink throughput of users with uplink-biased service v.s. the number of users per cell in Variant B

It can be noticed in Fig.3.3 to Fig.3.8 is that the RE strategy is better than the RSP strategy in Variant B but worse than the RSP strategy in Variant A. This is because load imbalance prevents the RSP strategy in Variant B and the RE strategy in Variant A from getting better performance, which is caused by the resource assignments in different configurations and their load-independent route selection of UEs. Because of the inherent load balancing feature, the ABO strategy is less influenced by frame configurations.

The throughput patterns of different route selection strategies applying the PF scheduling bear some similarity to the throughput patterns applying the RR scheduling. Nonetheless, a fact can be observed from Fig.3.3, Fig.3.4, Fig.3.7, and Fig.3.8 is that the RE strategy has slightly less PF scheduling gain than the other two strategies.

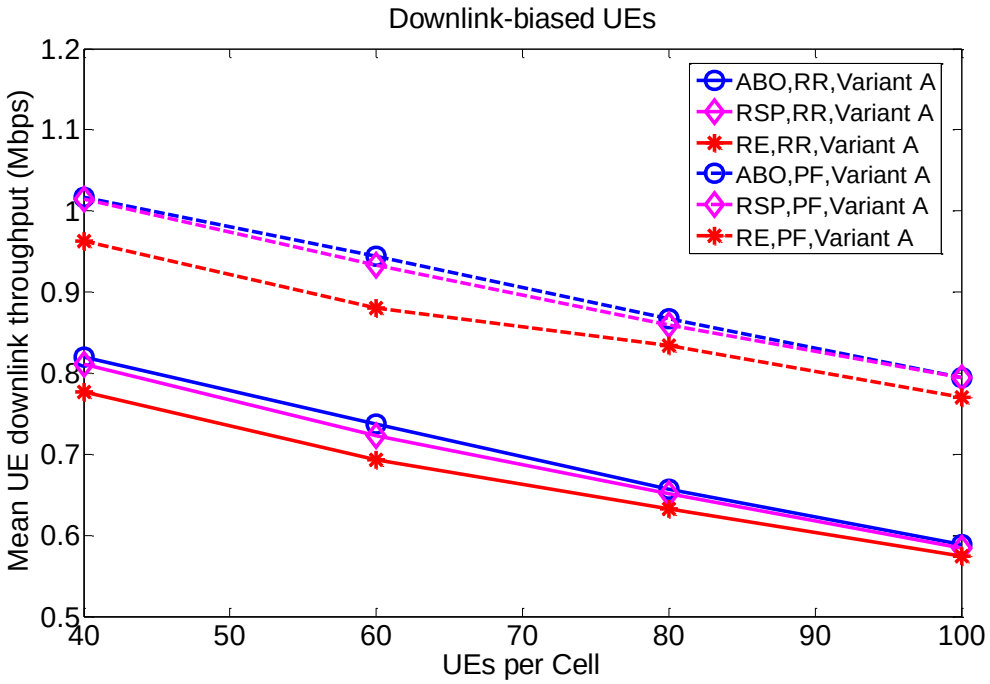

Figure 3.9: Mean downlink throughput of users with downlink-biased service v.s. user number per cell in Variant A

As shown in Fig.3.9 and Fig.3.10, the average downlink throughputs of downlink-biased UEs are improved by a narrow margin using the ABO strategy. Nonetheless, there are some exceptions that when the UE numbers are 80 and 100 per cell in Variant B, the the RE strategy has the largest average downlink throughputs of downlink-biased UEs. Thus, the ABO strategy shows insufficient advantage in optimising downlink-biased UEs.

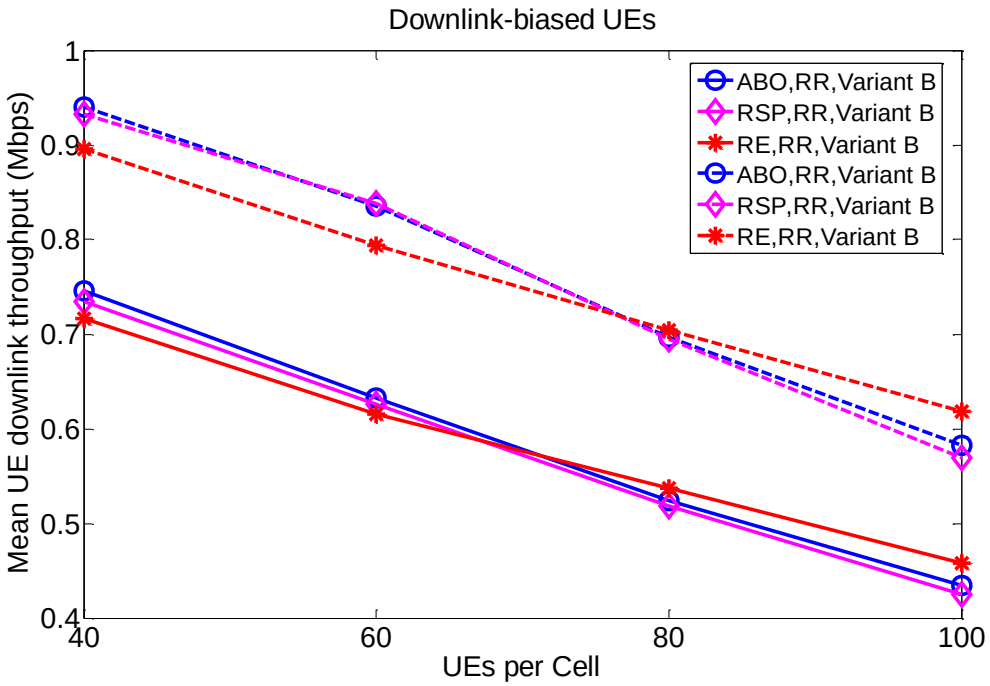

Figure 3.10: Mean downlink throughput of users with downlink-biased service v.s. user number per cell in Variant B

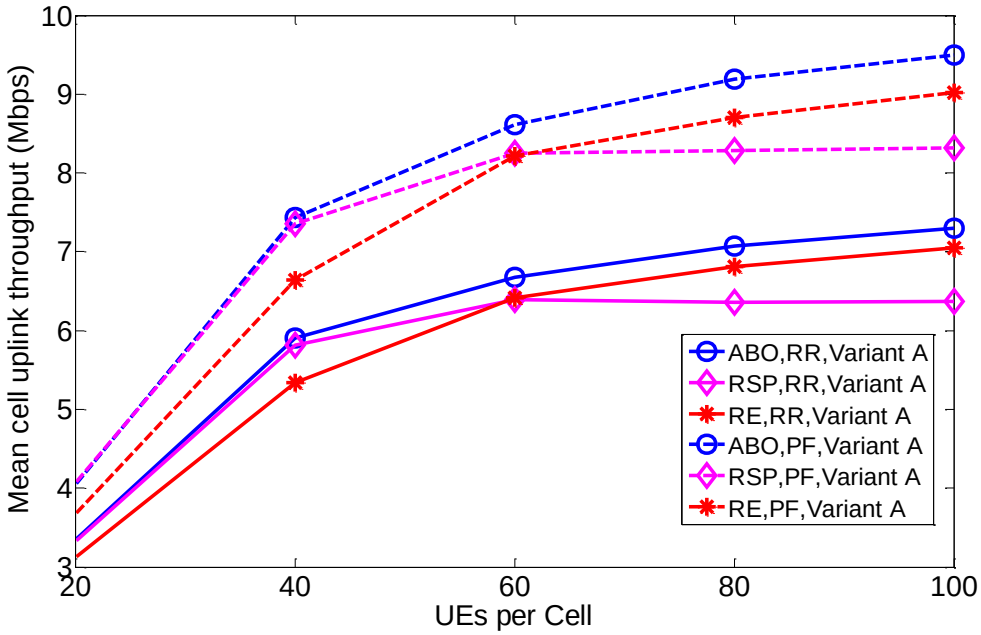

Figure 3.11: Mean cell uplink throughput v.s. the number of users per cell in Variant A in 10 MHz and 50 PRBs

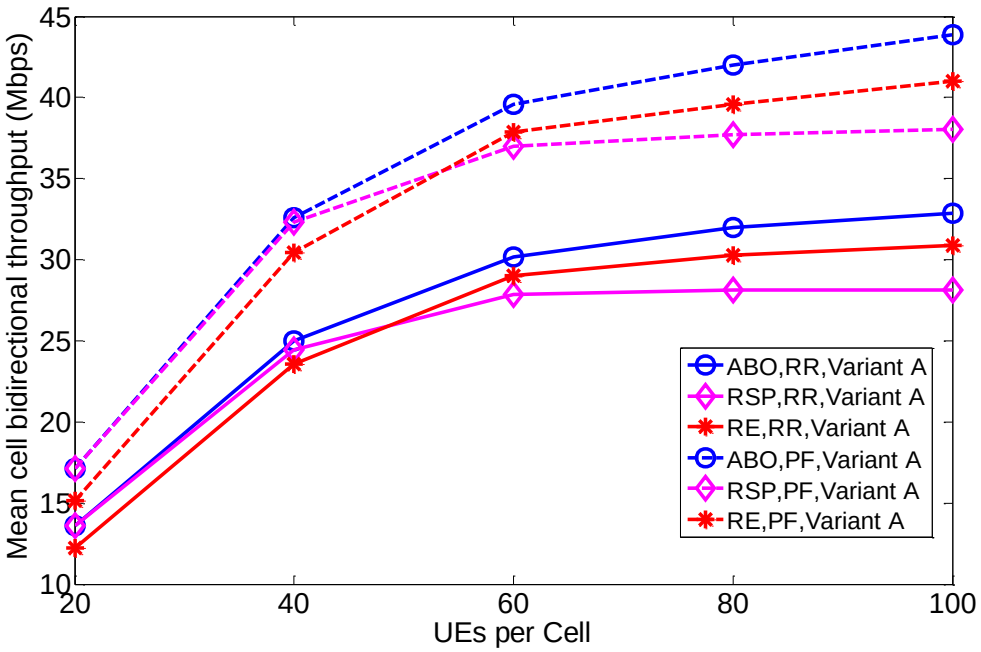

Figure 3.12: Mean cell bidirectional throughput v.s. the number of users per cell in Variant A in 10 MHz and 50 PRBs

In Fig.3.11 and Fig.3.12, three strategies are evaluated in the 10 MHz frequency band with 50 PRBs per time slot. It can be seen that the cell uplink throughputs and bidirectional throughputs increase slowly after the UE number per cell is larger than 60, because the available resources are halved and the cells become heavy-loaded with over 60 UEs per cell. Another fact should be noticed is that the throughputs using the RE strategy is worse than those using the RSP strategy and the ABO strategy, which become larger than the throughputs using the RSP strategy with over 80 UEs per cell. This is caused by the network load imbalance using the RSP strategy and the network load balance using the RE strategy and the ABO strategy, where the network load balance of the ABO strategy is guaranteed by its own load balancing mechanism.

Because uplink performance is given more attention in this study, the statistics of UE uplink throughput are further studied through the Cumulative Distribution Function (CDF) plots shown in Fig.3.13. Using the RE strategy, the uplink throughputs of the worst 5% uplink-biased UEs are less than 200 kbps compared with 350 kbps using the RSP strategy and the ABO strategy. Besides, 50% of the UEs using the RSP strategy can obtain uplink throughput more than 700 kbps, when about 58% of the UEs using the RE strategy and over 60% of the UE using the ABO

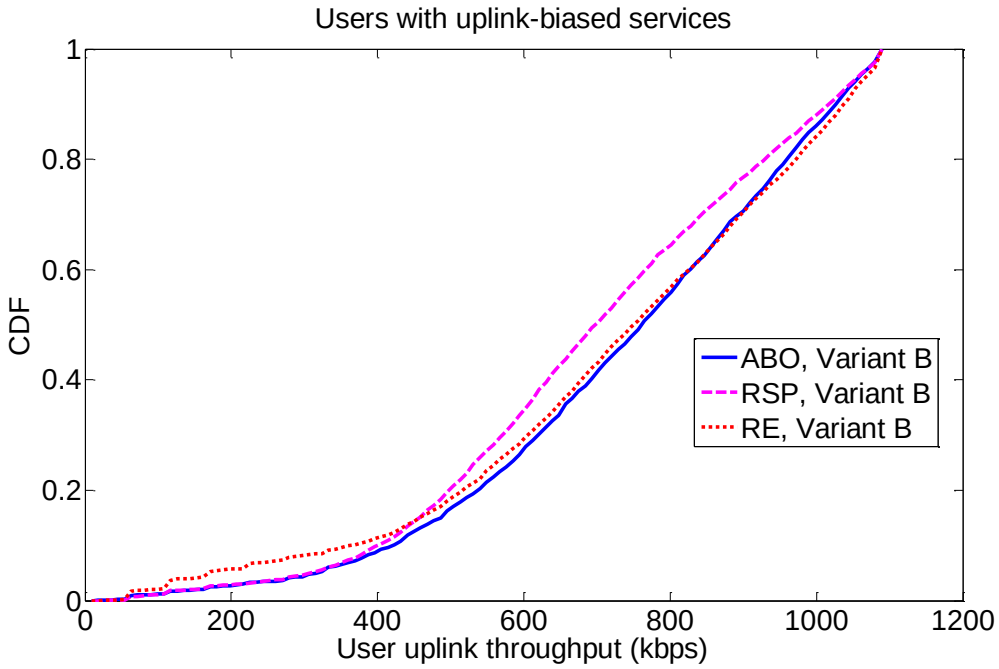

Figure 3.13: CDF of uplink throughputs of uplink-biased UEs (60 UEs per cell)

strategy can get over 700 kbps in uplink throughput. As it is shown, the proposed ABO strategy has larger uplink throughput.

In order to further analyse the effects of these three strategies and eliminate the influence of load balancing feature in the ABO strategy, the relation between mean UE uplink spectral efficiency and UE distance from the cell centre is presented in Fig.3.14. Note that 60 UEs per cell and Variant B frame configuration are assumed. The scatter plots are approximated by the curve fitting to generate curves representing the distance-based conditional mean. It is shown that the average UE uplink spectral efficiency decreases along with growing UE distance from the cell centre. However, the average UE uplink spectral efficiency rises around the RN location resulting from the UEs associating with RNs. This figure implies that when UEs are near the cell centre, the RE strategy can provide higher uplink spectral efficiency for UEs until the UEs are around 110 metres away from the cell centre. Moreover, higher UE uplink spectral efficiency is provided by the ABO strategy than the RSP strategy and the RE strategy in the cell-edge area.

To sum up, the benefits of the ABO strategy compared with the RSP strategy and the RE strategy are listed below:

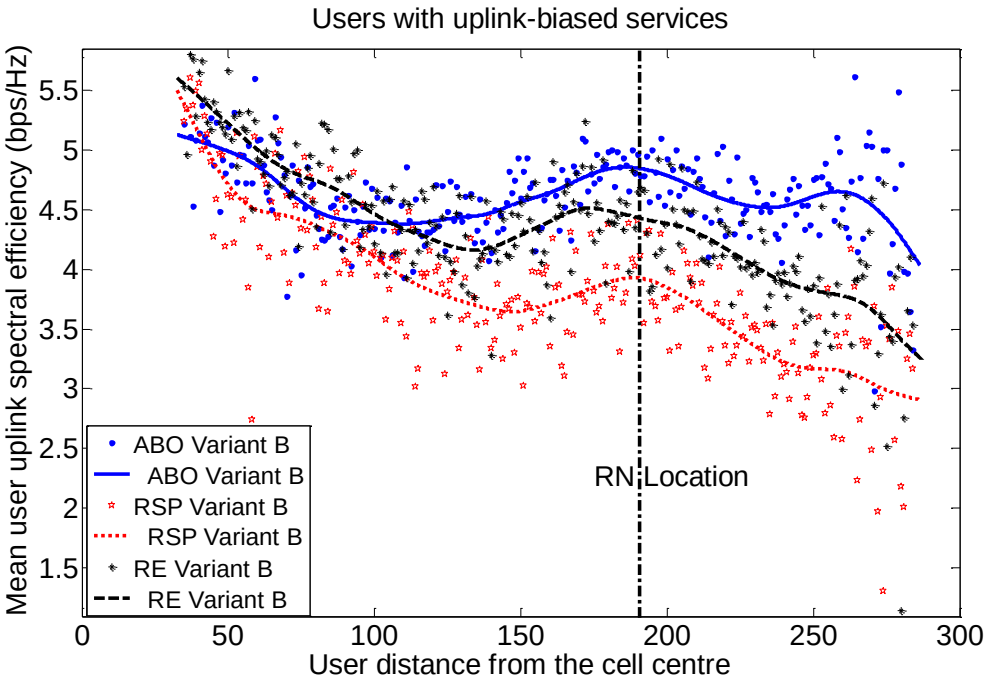

Figure 3.14: Mean uplink throughputs of uplink-biased UEs v.s. distance from the cell centre (60 UEs per cell)

- Cell throughput improvement in different frame configurations because of the inherent load balancing feature.
- Significant gain in the mean throughput of uplink-biased UEs.

3.8 Conclusion

This chapter proposes an adaptive bidirectional optimisation route selection strategy with load balancing aiming at maximising the user bidirectional throughput which is the sum of the uplink throughput and the downlink throughput. Load balancing is considered by its integration in the formulation of the ABO strategy to improve system performance in heavy-loaded scenarios. Through the system-level simulation, the ABO strategy is compared with two benchmark strategies: the received signal power based strategy and the range expansion based strategy. Simulation results show that ABO strategy is superior to the other two strategies in achieving higher cell bidirectional throughput and providing better performance for uplink-biased UEs, achieving up to 14% gain in the mean user uplink throughput.

Chapter 4

Distributed Two-hop Proportional Fair Resource Allocation

4.1 Introduction

This chapter focuses on distributed two-hop Proportional Fair (PF) resource allocation in LTE-Advanced networks with RNs. Resource allocation in LTE-Advanced networks can be divided into two phases: resource partitioning and resource scheduling. As an effective compromise between throughput and fairness, proportional fair resource allocation has been widely studied in conventional single-hop cellular networks[31, 63], OFDMA networks[58] and LTE networks[11]. In recent years, research into PF resource allocation in relay enhanced OFDMA networks is emerging. In relay enhanced LTE-Advanced networks, proportional fair (PF) resource allocation is aimed at guaranteeing two-hop match and optimising global proportional fairness. The two-hop match is defined as equal data rates in the access links and the corresponding backhaul links. The global proportional fairness is between all the UEs served by the evolved Nodes B (eNB) and the RNs. Existing centralised PF resource allocation algorithms achieve these targets at the cost of enormous channel state information (CSI) exchange. For less CSI exchange, distributed approaches to PF resource allocation are also considered. Existing researches about distributed resource allocation focus on designing adaptive resource partitioning while employing a traditional single-hop PF scheduling algorithm in access links. The traditional PF scheduling algorithm maximises single-hop proportional fairness between the data rates in the access links rather than two-hop proportional fairness between the end-to-end data rates in the two hops. In order to reduce CSI exchange and at

the same time to maximise the two-hop proportional fairness, a Distributed Two-Hop PF (DTHPF) resource allocation scheme is proposed. The proposed scheme includes newly designed two-hop resource scheduling algorithms and adjusted resource partitioning algorithms in different two-hop transmission protocols. Since adaptive resource partitioning in different two-hop transmission protocols results in different relations between the resource numbers of access links and backhual links, different two-hop resource scheduling algorithms are proposed. Simulation results demonstrate that the proposed algorithms are better than the existing distributed algorithms in obtaining better proportional fairness and larger cell-edge UE throughputs.

4.2 Related Work

The resource allocation or scheduling techniques in LTE-Advanced networks with RNs can be categorised into two groups, centralised approaches and distributed approaches.

4.2.1 Centralised Approaches

Applying a centralised architecture, the resource scheduling together with the resource partitioning are executed by the donor eNBs. During the resource scheduling of access links, their channel state information (CSI) ought to be collected and fed back by the RNs.

[64] have presented an enhanced proportional fair scheduling algorithm, which combines the resource scheduling of access links and backhaul links. The basic frequency-time resource chuck comprises two equal time slots for the relay users. One time slot is assigned to the access links and the other is occupied by the backhaul links. The end-to-end data rate is calculated as the minimum rate of the two hops. However, some resources are wasted due to the rate differences of the two hops.

In [65], Round-Robin, greedy polling and proportional fair scheduling algorithms are extended to the OFDMA relay networks in the centralised architecture. In each time slot, there are two equal sub-slots to accommodate direct links and backhaul links in the first one and direct links and access links in the second one. In the second sub-slot, a proposed partial proportional fair scheduling algorithm is applied firstly. Based on the scheduling results, the sub-channels are allocated to the relay nodes

until the overall throughput of the access links in the second sub-slot is fulfilled.

[66] proposed a centralised resource allocation scheme with fixed subframe division. This resource allocation scheme includes three parts: 1) the resources are allocated to the relay users to reduce the data stored in the relay nodes; 2) the remaining resources go to the direct users by void filling; 3) the resources are scheduled between direct users and the relay nodes according to the proposed scheduling algorithms. Four scheduling algorithms are extended from the scheduling algorithms used in conventional networks. In two-hop scenarios, the end-to-end data rates are calculated as the minimum rates of the two hops.

The authors in [67] proposed a RRM scheme which combines in-cell routing and resource allocation. Both the queue length and the data rate per subchannel are considered as performance metrics. Fixed two halved subframe division is used. The optimisation of resource allocation in the access subframes is achieved by the Hungarian algorithm, and the resource allocation in the backhaul subframes is based on the queue length stored in the relay nodes. The results show that an efficient comprise between throughput and fairness can be obtained, and the loads of relay nodes can be balanced.

The authors in [68] used different proportional fair scheduling algorithms in two time sub-slots. In the first sub-slot, the resources are scheduled only among the relay users based on the conventional proportional fair scheduling algorithm. In the second sub-slot, a weighted proportional fair scheduling algorithms is used, which considers the two-hop mismatch in the weights. Compared with the partial proportional fair scheduling algorithm in [65], better fairness is achieved at the expense of small throughput loss. In [69], the authors proposed a power allocation scheme for the backhaul links to achieve two-hop match and save energy.

The authors in [70] adopt the traditional proportional fair scheduling algorithm in both eNBs and relay nodes with fixed resource partitioning. The resources of access links constantly occupy 1/3 of the whole frequency band without frequency reuse. The resources assigned to the backhaul links are assumed to match the aggregate throughput of access links. A user routing strategy is proposed to decide the best serving node of each user and balance the loads of serving nodes.

In [71], a two-stage centralised RRM scheme is proposed in OFDMA networks using fixed AF relaying technology. Firstly, the users decide their transmission modes. Sequentially, the joint subcarrier scheduling is executed and the power control is conducted through a geometric programming method. Four interference

coordinated schemes are considered.

[72] proposed a heuristic resource allocation algorithm as a near optimal solution to the formulated proportional fairness problem. The problem is solved by the Lagrangian dual decomposition method, and the algorithm is obtained using Karush-Kuhn-Tucker conditions. A half-to-half subframe division from [73] is assumed. The difference of the data rates of the two-hop links is dealt with by giving different power to the two-hop links In addition, direct links are not considered, since out-band RNs are assumed.

[74] have proposed two resource allocation schemes considering fairness and minimum data rate requirement. In this paper, the subchannels are divided into two phases. The resource allocation problems with both selective phase assignment and non-selective phase assignment are formulated as Lagrangian functions. The two-hop data rate match is achieved through a power allocation algorithm.

The authors in [75] presented two joint routing and resource allocation algorithms and two power allocation algorithms, which can generate three centralised resource allocation schemes. The conditioned subcarrier allocation and mode selection algorithm and the conditioned water filling power allocation algorithm are used in the initial iteration assuming the cochannel interference is assumed to be fixed. The resource allocation and power allocation results are updated by employing a joint subcarrier allocation and mode selection algorithm and a single condensation based geometric programming power allocation algorithm.

[76] presented a semi-distributed resource allocation scheme with adaptive resource partitioning. This scheme consists of two parts: 1) In the backhaul subframes, the resources are allocated to the direct users and the backhaul links based on the priority matrix considering the data rates of the access links at the same subchannel. 2) The resources are allocated to the relay users using the scheduler in the relay nodes.

[77] focused on the resource allocation in relay networks using game theory. The basic principle in this paper is to consider the two hops of relay users together as a bundle. The resources can be scheduled among any two bundles using a Nash bargaining solution. Based on the two-bundle bargaining algorithm, a multi-bundle bargaining algorithm is proposed by applying a Hungarian algorithm to sort the bundles into two-bundle bargaining coalitions. After the resources have been assigned to the bundles of the relay users, the resources are further allocated to the access links and backhaul links in order to maximize the throughput and alleviate

two-hop mismatch.

The authors in [78] provided resource allocation algorithms with adaptive resource partitioning. To guarantee the performance, a scheduling algorithm without access link reuse and a scheduling algorithm with access link reuse are proposed together with the calculation of an approximation guarantee. In addition, a greedy scheduling algorithm is derived by considering the two-hop performance. However, only time-domain resources are considered in this work, and thus, the multi-subcarrier diversity is neglected.

Reference [79] proposed a centralised resource allocation scheme to ensure the proportional fairness between all the UEs associated with eNBs and RNs. In order to simplify the mathematical analysis, the authors assume a virtual PRB for the UEs connected to the RNs. The virtual PRBs are consumed by the backhaul links and the access links. Their proportions are determined by the data rates in the backhaul links and the access links. Using the gradient method and the Karush-Kuhn-Tucker (KKT) conditions, a near-optimal solution is obtained. The impact of backhaul links on the network performance can also be better understood.This centralised resource allocation scheme is conducted in the time-frequency domain, while the time domain is considered in [78].

In [80], a problem to jointly optimise subframe, PRB and power allocation is formulated and solved by a centralised optimal joint allocation algorithm. Using a general Lyapunov optimization framework, the three-dimensional problem is transformed into the minimisation of a Lyapunov drift-plus-penalty function [81]. Then, the main problem is decomposed into three sub-problems. Applying the continuity relaxation and Lagrange dual decomposition in the sub-problems, the joint subframe, PRB and power optimisation problem is solved with acceptable performance and delay.

Fixed resource partitioning between access links and backhaul links will lead to the two-hop mismatch [64, 65, 66, 67], or the proportional fair resource scheduling between backhaul links and direct links is not considered [68, 69, 70]. Power control/allocation algorithms are used in [71, 72, 74, 75] to achieve the two-hop match. However, they will increase complexity and highly depend on the accuracy and immediateness of channel measurements. Adaptive resource partitioning is used in [76, 77, 78, 79, 80]. In [76], the resource scheduling of two-hop links is considered together unless they are in the same subchannel, which cannot utilise channel diversity. In [77], the subframe division between the access links and the backhaul links is not

considered, and the complexity of the multi-bundle bargaining algorithm is too high. Only time-domain resource allocation is considered in [78] without utilising multi-subcarrier diversity. The centralised resource allocation algorithms without power allocation [79] and with power allocation [80] are best solutions so far. However, enormous CSI exchange between the eNBs and the RNs will bring heavy burden to the uplink signalling channels, despite multi-subchannel diversity and multi-user diversity can be exploited using the centralised architecture.

4.2.2 Distributed Approaches

In order to reduce CSI exchange, some PF resource allocation schemes adopt a distributed architecture, in which the resource partitioning and the resource scheduling are processed by different types of serving nodes. Particularly, the resource scheduling of the access links is executed at each RN, which is supported by Type I relay in LTE-Advanced networks; and the resource partitioning is determined by the donor eNBs. In the existing distributed PF resource allocation schemes, great attentions is paid to designing resource partitioning algorithms.

Several distributed resource allocation algorithms are proposed in [82] with adaptive and fixed resource partitioning. The algorithms follow three basic steps: 1) each subchannel in the relay transmission phase is allocated to the user according to the traditional Proportional fair scheduling algorithm; 2) relay nodes send their requests to the eNB based on the throughput of access links; 3) the eNB allocates the resources to the direct users first, and then sorts the resources based on the proportional fairness. The resources with the smallest proportional fairness are allocated to the backhaul links. Fixed time division, fixed frequency division and adaptive time division are considered and evaluated in [82].

The resource allocation algorithm in [83] is comprised of two phases, a sub-carrier allocation phase and an adaptive frame structure setting phase. In the sub-carrier phase, relay nodes allocate the resources for their active users using proportional fair scheduling, and the eNB executes the proportional fair scheduling for the relay nodes and the direct users, in which the relay nodes are considered as special users with requirement information of the relay users. In the second phase, the frame structure is initiated with a calculated pattern based on the average throughput of relay users and adjusted according to the real throughput. The two-hop mismatch problem is of concern, however, the time slots are equally assigned to different relay nodes. No frequency reuse is considered.

[84] presented a backhaul resource allocation scheme based on relay buffer level. The objective of this scheme is to make the backhaul resources assigned to relay nodes meet the traffic demand of the access links. In addition, the backhaul resource partitioning is minimised through a suboptimal algorithm. The distributed RRM architecture is assumed and full reuse of access subframes is applied for the access links and direct links. Based on the half-to-half subframe division and the received signal power based routing, this scheme is compared with a fixed backhaul resource partitioning scheme, which uses half of the backhaul subframes, and a user based scheme, which allocates resources to the relay nodes according to the number of their relay users.

[85] presented two different fair resource partitioning algorithms between backhaul links and access links, Fair-Resource-Unit (Fair-RU) and Fair-Throughput (Fair-TP). In the Fair-RU scheme, the number of resource units for the backhaul link is given according to the relay UEs. In the Fair-TP scheme, the resource number for the backhaul link is assigned to make sure the identical aggregate throughput of access links and direct links. Distributed proportional fair scheduling algorithms are executed at the eNB and RNs separately with full frequency reuse. [86] proposed a scheduling metric based on the delay requirement, the guaranteed bit rate and the service priority index in order to balance the rate and the delay requirement for the service of different QoS level. Reference [87] proposed a new resource partitioning strategy for out-band relaying, called extended proportional fair strategy, which is an extension of the research in [85] and [86]. In this strategy, the relay node is considered as a special user with the proportional fairness metric scaled by the number of the connected relay users.

In [88], a distributed simplified resource allocation algorithm for in-band downlink relay networks is provided to increase the throughput of the UEs with the worst channel conditions. The frame is divided into access subframes and backhaul subframes. In the access subframes, access links and direct links fully reuse the resources. However, the resource number for the direct links and the backhaul links in the backhaul subframes and the resource number of access subframes are calculated based on the objective of maximising the throughput of the worst UEs.

[89] presents a dynamic orthogonal resource partitioning scheme with tunable trade-off between fairness and throughput. No frequency reuse between direct links and access links is assumed. A satisfaction metric is defined in this paper, which is the ratio of the current data rate to the guaranteed bit rate. After the dynamic resource partitioning with different targets is formulated, a parameter O is derived to

show the trade-off between fairness and throughput. Together with the parameters O and the feedback satisfaction levels, different weights are put into the resource partitioning algorithms to achieve better fairness or larger throughput.

The authors in [90] depicted two resource sharing schemes between different backhaul links and two throughput distribution schemes between different access links of one relay node. In the access subframes, full frequency reuse between access links and direct links is assumed. In the backhaul subframes, the resources are only shared between different backhaul links. The resource number of backhaul link is proportional either to the latest throughput of the access links or to the number of relay users. Two throughput distribution schemes between access links based on different metrics are proposed in order to achieve proportional fairness and Max-Min fairness respectively. [91] extends the resource sharing schemes and the throughput distribution schemes to downlink transmission. In addition to [90], a Round-Robin sharing scheme is presented in [91], which gives each active relay node the same number of resources. In [92] and [93], the authors used a co-scheduling strategy in the backhaul subframes, which allows direct users to utilise the remaining resources after the resource demands of backhaul links have been satisfied. In [93], the backhaul subframes are over-provisioned adaptively to ensure the co-scheduling between direct users and relay nodes and to optimise performance. [94] summarised the hard subframe division in [90] and [91] and the flexible subframe division in [92] and [93]. More performance evaluation results are presented in [94]. However the two-hop match and the proportional fairness are not considered.

In [95] [96], the authors use two access/backhaul subframe division algorithms. In these algorithms, only access links can use resources in the access subframes based on the scheduling of the queued packets with the highest AMC level. In the RS-Max with fixed time division algorithm, the whole frame is equally divided into backhaul subframe and access frame. With the adaptive time division, the algorithm change the number of time slots in an iterative manner to maximise the throughput.

Two different backhaul subframe allocation schemes for multiple relay nodes are proposed and compared in [97]. In the backhaul subframes, the Time Division Multiplexed backhaul (TDM-backhaul) scheme allocates different subframes to the backhaul links of different relay nodes, and the frequency division multiplexed backhaul (FDM-backhaul) scheme distributes different resource blocks between the relay nodes. Using the TDM-backhaul scheme, more resources can be used for the access links because a relay node can transmit the signal to its users when the backhaul subframe is not assigned to it. However, due to the limitation of backhaul links, the

TDM-backhaul scheme will not perform better than the FDM-backhaul scheme.

The authors in [98] provided a weighted proportional fair scheduling algorithm to solve the resource waste problem caused by load imbalance between different access links. In this paper, the whole frame is divided into the access intervals for direct links and access links with different lengths and the relay interval for backhaul links. Due to the different channel condition of access links and backhaul links, the resource numbers of access links assigned to different relay nodes are different, which causes inefficient resource usage. Using the proposed scheduling algorithm in each access interval, a user with larger proportional fairness and less resource waste contribution is given higher priority.

Three weighted proportional fair scheduling algorithms for the Multicast Broadcast Single Frequency Network (MBSFN) subframes are proposed in [99]. Both backhaul links and access links are considered to determine how to schedule RNs at the eNB. The weighting factor in PF scheduling algorithm 1 is the number of UEs served by the RN. The weighting factor in PF scheduling algorithm 2 is influenced by the ratio of the channel quality in the access links and the backhaul links, and the overall importance of all the UEs connected to the RNs. The weighting factor in PF scheduling algorithm 3 is derived by the ratio of the data rates in the access links and the backhaul links. However, these schedulers are not proposed to solve the PF resource allocation problem. The PF scheduling for the access links is not discussed.

The authors in [100] proposed a distributed resource allocation scheme. The proposed resource allocation scheme is divided into two sub-tasks, RN resource allocation and eNB resource allocation. Non-cooperative game framework is used to design the RN resource allocation. The authors adopted a strategy to partition less resources for the UEs served by the RNs and keep more resources for single-hop transmission. The proposed scheme is aiming at providing high cell throughput and guaranteeing the minimum data rate requirements of UEs. Simulation results show that this scheme makes a great contribution in improving the cell throughput and reducing the outage probability. However, proportional fairness is not considered.

Semi-static PF-based partition schemes are designed for the full reuse scenario in [101, 102] and none reuse scenario in [54]. Through formulating the generalised PF problem and solving it by the Lagrange multiplier algorithm, these two optimal resource partitioning patterns are derived based on the number of relay users and the average throughputs of access links and backhaul links. Proportional fair scheduling

is adopted at the eNBs and the RNs individually. However, the resource partitioning schemes have not considered the impact of the resource number of access links on the channel quality of direct links.

The distributed resource allocation schemes focus on partitioning resources between direct links, access links and backhaul links in order to achieve two-hop match and improve proportional fairness. However, a traditional proportional fair resource scheduling algorithm used in single-hop networks is still included in all the distributed resource allocation schemes in two-hop networks. The two-hop match ought to be guaranteed and the global proportional fairness should be improved.

4.3 System Model and Assumptions

4.3.1 Network Model

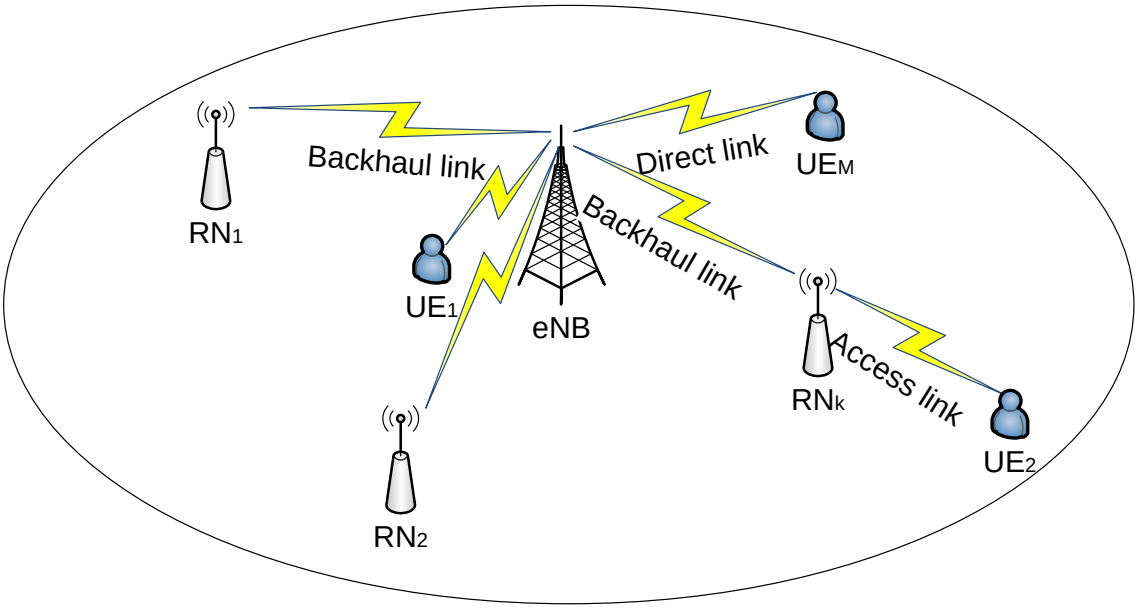

Figure 4.1: Illustration of a LTE-Advanced macro cell

In this chapter, the downlink transmission of a LTE-Advanced network with Type I relay nodes is considered. In a cell of interest shown in Fig.4.1, there are a set of serving nodes (SNs) $\mathcal{K}$, including a donor eNB and multiple RNs. The SN k ($k \in \mathcal{K}$) denotes the eNB when $k = 0$, or an RN otherwise. The RNs are connected to the donor eNB via wireless backhaul links. A set of UEs $\mathcal{M}$ can be either served by the donor eNB directly or via an RN through two hops. It is assumed that all the data in the wireless backhaul links is decoded and forwarded by the RNs to the

relay UEs in the access links, since the RNs are incapable of buffering excess data. The UEs associated with SN k create a subset $\mathcal{M}_k$ of $\mathcal{M}$. Multiple SN connection and cooperative transmission are not considered in this study.

A physical resource block (PRB) is a basic OFDMA resource allocation unit, comprising a constant number of subcarriers and OFDM symbols. Assume that there is a set of PRBs $\mathcal{N}$ for data transmission in each radio frame. With a certain resource partitioning pattern, SN k can obtain a PRB subset $\mathcal{N}_k$, which is further divided into an access PRB subset $\mathcal{N}_k^a$ for access links and a backhaul PRB subset $\mathcal{N}_k^b$ for backhaul links. Note that $|\mathcal{N}_k^a|$ and $|\mathcal{N}_k^b|$ need to be integers, where $|\bullet|$ means the cardinality of a set, and the backhaul PRB size $|\mathcal{N}_0^b|$ is defined as 0 for the donor eNB. The relationship between the access PRBs and the backhaul PRBs can be given by

$$\begin{aligned} &\mathcal{N}_k^a \cap \mathcal{N}_k^b = \emptyset, \quad \mathcal{N}_k^a \cup \mathcal{N}_k^b = \mathcal{N}_k, \\ &\forall \mathcal{N}_k^a \in \mathcal{N}_k, \quad \forall \mathcal{N}_k^b \in \mathcal{N}_k \end{aligned} \tag{4.1}$$

4.3.2 Channel Model Assumptions

In direct links and access links, it is assumed that all UEs have independent multi-path frequency-selective Rayleigh fading channels and their instantaneous channel gains are flat over each PRB. In addition, based on the calculation given in [60], the Doppler time-selective Rayleigh fading channels result in flat channel gains within a radio frame, when the speeds of UEs are under 60 km/s. For backhaul links, flat fading channels are assumed under the fixed line-of-sight condition, and the instantaneous data rates are constant over all PRBs. A multi-cell scenario is considered in this study. Through PRB pre-assignments in subframes, the inter-cell interference is predictable in order to maintain a stable interference environment and make the problem formulation feasible. In addition, fixed transmitting power per PRB is assumed for all the links to reduce the complexity of transmitters.

4.3.3 Two-hop Transmission Protocols

Two typical two-hop transmission protocols are considered in this research, Orthogonal Two-Hop (OTH) transmission protocol and Simultaneous Two-Hop (STH) transmission protocol, which are illustrated in Fig.4.2 and Fig.4.3. In the two-hop transmission protocols, each radio frame is divided into backhaul subframes and access subframes. The access PRBs in the access subframes and the backhaul PRBs in

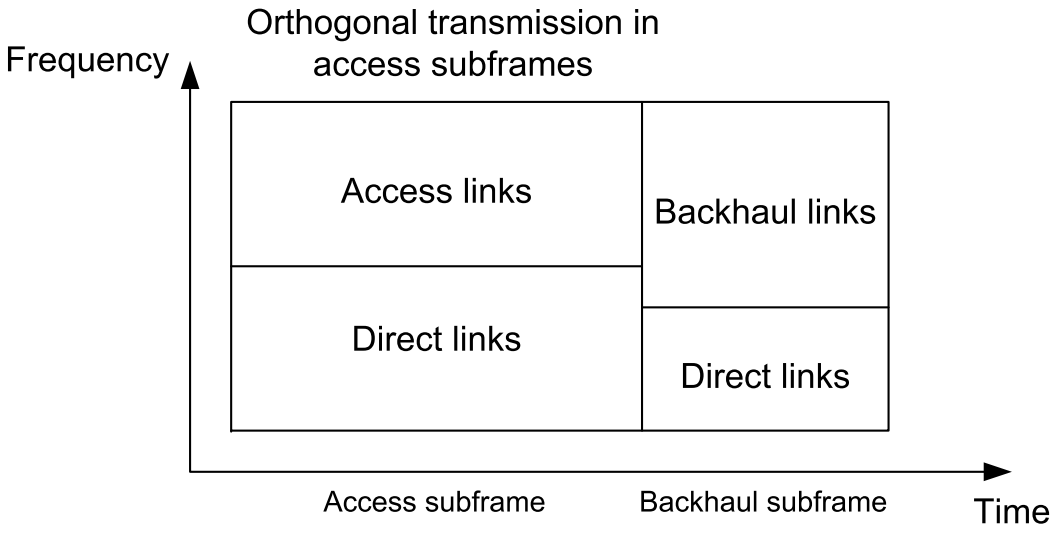

Figure 4.2: Orthogonal two-hop transmission protocol

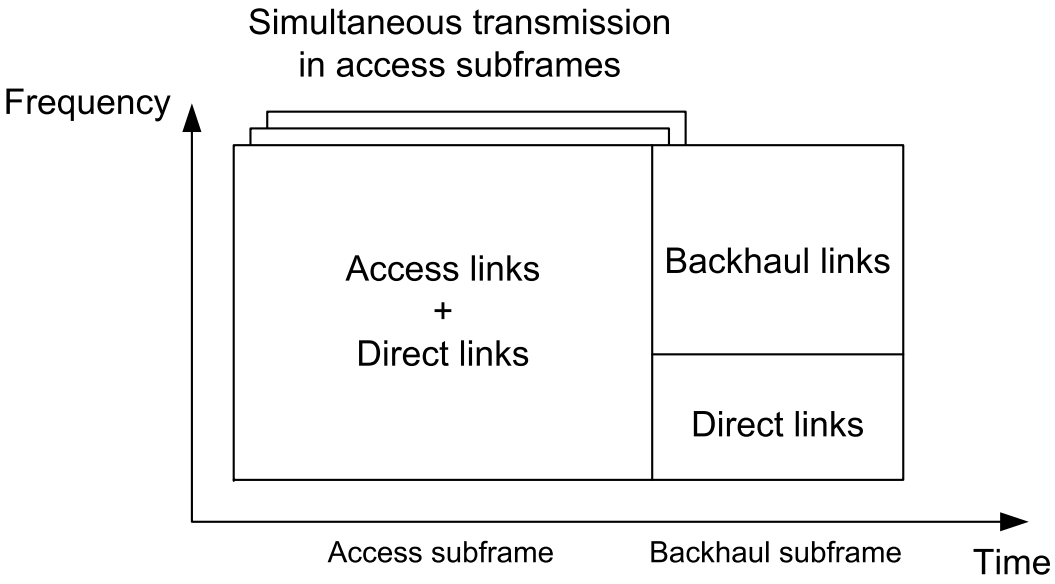

Figure 4.3: Simultaneous two-hop transmission protocol

the backhaul subframes are allocated to the two-hop relay UEs. For the single-hop direct UEs, the remainder of the backhaul subframes can be used. Whether the PRBs in the access subframes are reused or not by the two-hop relay UEs and the single-hop direct UEs depends on different two-hop transmission protocols.

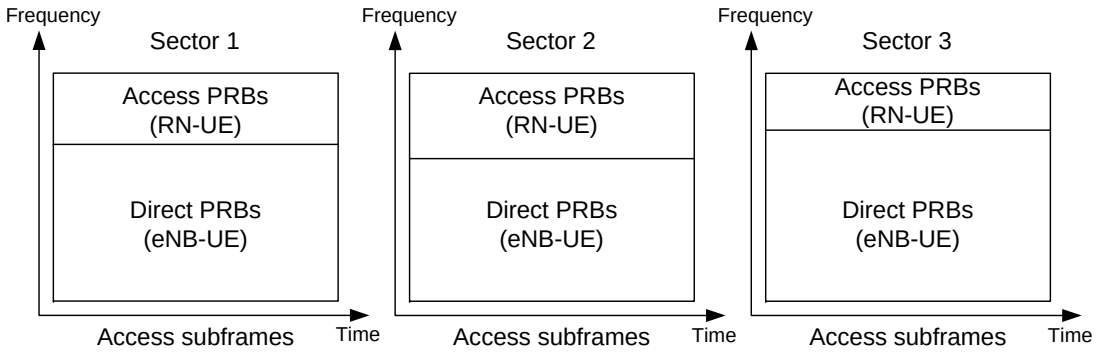

Figure 4.4: An orthogonal reuse pattern in the orthogonal protocol

In the orthogonal two-hop (OTH) transmission protocol, the single-hop direct UEs and the two-hop relay UEs share all the PRBs in the access subframes without any overlapping. No intra-cell interference is generated. An Orthogonal Reuse (OR) pattern in the access subframes is used. The main inter-cell interference experienced by the relay UEs is from the RNs in the adjacent cells, and the main inter-cell interference received by the direct UEs is from the surrounding eNBs. The OR pattern deployed in different sectors of a macro cell is shown in Fig.4.4.

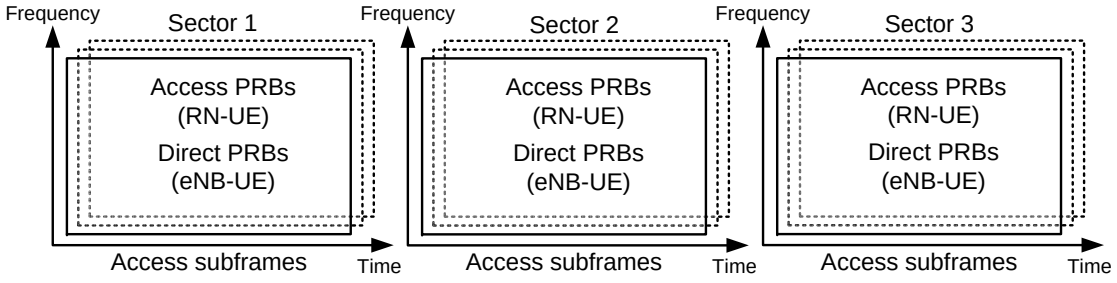

Figure 4.5: Full reuse pattern in the simultaneous protocol

Using the simultaneous two-hop (STH) transmission protocol, a Full Reuse (FR) pattern and two fixed Partial Reuse (PR) patterns are considered as shown in Fig.4.5, Fig.4.6 and Fig.4.7. In the FR pattern, the whole PRBs in the access subframes are available for the direct links and the access links. The intra-cell and inter-cell interference suffered by the UEs are consistent from all the unattached SNs. In the 2/3 PR pattern, the access links are allowed to reuse 2/3 of the resources for the direct links. In the 1/3 PR pattern, the access links are allowed to reuse 1/3 of

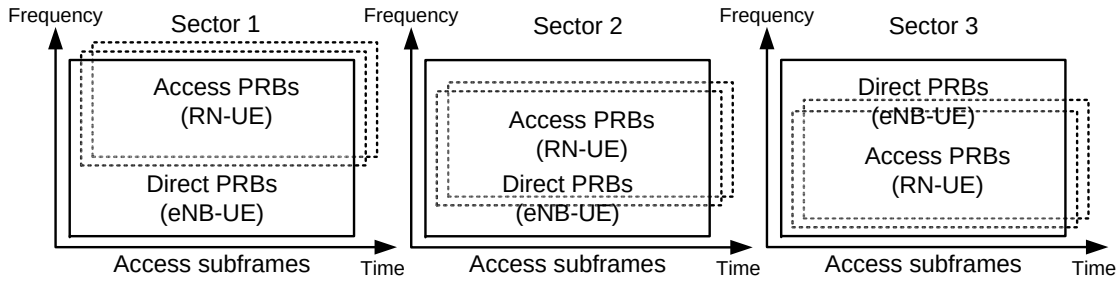

Figure 4.6: 2/3 partial reuse pattern in the simultaneous protocol

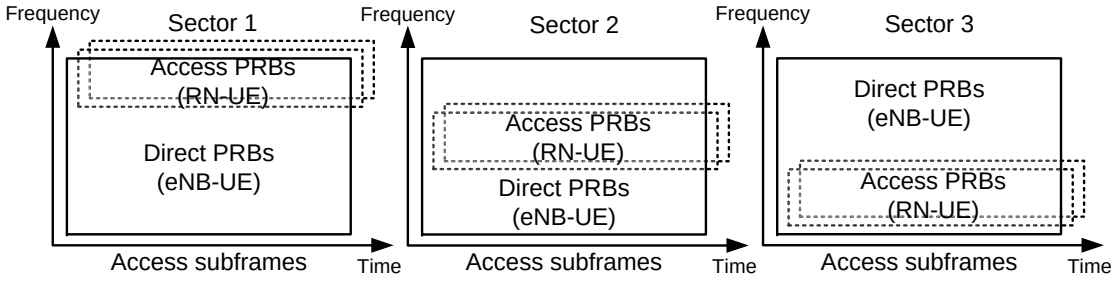

Figure 4.7: 1/3 partial reuse pattern in the simultaneous protocol

the resources for the direct links. Thus, the intra-cell and inter-cell interference is reduced and the available resources of the relay UEs for the access links are also diminished, compared with the FR pattern.

The relationship of the access PRBs, backhaul PRBs and direct PRBs in different two-hop transmission protocols can be summarised below

$$\text{in the OTH protocol,} \quad \bigcup_{k=0}^{K} \mathcal{N}_k = \mathcal{N} \tag{4.2}$$

$$\text{in the STH protocol,} \quad \bigcup_{k=1}^{K} \mathcal{N}_k^b + \mathcal{N}_0^a = \mathcal{N}, \quad \mathcal{N}_{k\neq 0}^a \leq \phi \mathcal{N}_0^a \tag{4.3}$$

where ϕ indicates 1, 2/3 and 1/3 in the FR, 2/3 PR and 1/3 PR patterns respectively.

4.4 Problem Formulation

Without loss of generality, the downlink transmission is considered frame-by-frame. The PF resource allocation problem with adaptive resource partitioning in LTE-Advanced networks with Type I relay nodes is formulated as the equivalence of

maximising the following utility function [17]

$$\max \sum_{m \in \mathcal{M}} \log R_m \tag{4.4}$$

where R_m is the data rate of UE m within a radio frame.

Since the UE association relationship has been decided by a certain route selection algorithm, the data rate of UE m served by SN k in a radio frame can be expressed as

$$R_m = \sum_{n \in \mathcal{N}_k^a} \lambda_{m,n} r_{k,m,n} \tag{4.5}$$

where $\lambda_{m,n}$ is the binary resource allocation variable, and $r_{k,m,n}$ is the instantaneous data rate achieved by UE m connected to SN k on PRB n. If PRB n is allocated to UE m associated with SN k, then $\lambda_{m,n} = 1$, otherwise, $\lambda_{m,n} = 0$. Note that only the throughputs finally received by the UEs in the access PRBs should be included in the expression.

Considering time multiplexing and two-hop match required in the LTE-Advanced standards, the GPF problem in the OTH protocol can be formulated as

$$\max \sum_{k \in \mathcal{K}} \sum_{m \in \mathcal{M}_k} \log \sum_{n \in \mathcal{N}_k^a} \lambda_{m,n} r_{k,m,n} \tag{4.6}$$

subject to

$$\textit{C1:} \sum_{m \in \mathcal{M}_k} \sum_{n \in \mathcal{N}_k^a} \lambda_{m,n} r_{k,m,n} = |\mathcal{N}_k^b| r_{0,k}, \forall k \in \mathcal{K}, k \neq 0$$

$$\textit{C2:} \ |\mathcal{N}_0^a| \leq |\mathcal{N}| - \sum_{k \in \mathcal{K}, k \neq 0} |\mathcal{N}_k^a| - \sum_{k \in \mathcal{K}, k \neq 0} |\mathcal{N}_k^b|$$

and the GPF problem in the STH protocol can be formulated as

$$\max \sum_{k \in \mathcal{K}} \sum_{m \in \mathcal{M}_k} \log \sum_{n \in \mathcal{N}_k^a} \lambda_{m,n} r_{k,m,n} \tag{4.7}$$

subject to

$$\textit{c1:} \sum_{n \in \mathcal{M}_k} \sum_{n \in \mathcal{N}_k^a} \lambda_{m,n} r_{k,m,n} = |\mathcal{N}_k^b| r_{0,k}, \forall k \in \mathcal{K}, k \neq 0$$

$$\textit{c2:} \ |\mathcal{N}_0^a| \leq |\mathcal{N}| - \sum_{k \in \mathcal{K}, k \neq 0} |\mathcal{N}_k^b|$$

In different reuse patterns, constraints *C1* and *c1* are the same, which implies the two-hop match. Additionally, the constraints *C2* and *c2* show how to segment the

entire PRBs in a radio frame.

The Generalised Proportional Fairness (GPF) problems in (4.6) and (4.7) are not convex optimisation problems, since UEs' data rates R is not a convex set with binary variables $\lambda \in \{0, 1\}$. In order to make the GPF problem tractable, the binary variables λ are allowed to take any value between 0 and 1, $\lambda \in [0, 1]$, so that R is a convex set and the GPF problems in (4.6) and (4.7) become convex optimisation problem[103]. The method of Lagrange multipliers can then be used to solve the GPF problems.

4.5 Problem Relaxation

In this section, our aim is to solve the formulated GPF problem in different two-hop transmission protocols. Using a distributed architecture, the GPF problem can be decomposed into two sub-problems, i.e., a resource portioning problem with given scheduling results, and a resource scheduling problem considering the known two-hop resource segments.

4.5.1 Adaptive PF Resource Partitioning

According to the findings in [31, 58] and the system model defined in this chapter, the throughput of UE m in a PF scheduler can be approximated by its average data rate per PRB, the average allocated PRB number and a PF scheduling gain $G_{m,k}$. The PF scheduling gain is based on the throughput comparison between the PF scheduling the Round-robin scheduling, which are scheduling the same UEs on the same PRBs.

$$R_m \approx G_{m,k} \frac{|\mathcal{N}_k|}{|\mathcal{M}_k|} \bar{r}_{m,k} \tag{4.8}$$

where $G_{m,k}$ depends on the channel states of all the UEs in the scheduler and are independent of the PRB numbers to be scheduled.

In [54, 102], the resource partitioning problems in the OTH and STH transmission protocols are simplified into a PRB number-related logarithmic sum maximisation function through substituting (4.8) into (4.6) and (4.7)

$$\max \sum_{k \in \mathcal{K}} |\mathcal{M}_k| \log |\mathcal{N}_k^a| \tag{4.9}$$

Besides, the relationship between the backhaul PRB numbers and the access PRB numbers can be derived by substituting (4.8) into constraint *C1* or *c1*. A backhaul-to-access ratio θ_k is defined for every RN k as

$$\theta_k = \frac{|\mathcal{N}_k^b|}{|\mathcal{N}_k^a|} = \frac{\sum_{m \in \mathcal{M}_k} G_{m,k} \bar{r}_{m,k}}{|\mathcal{M}_k| r_{0,k}} \tag{4.10}$$

where θ_k indicates the ratio of the data rates per PRB of the backhaul link to the aggregate access links of RN k. Note that the backhaul-to-access ratios can be estimated by the previous average data rates.

Two adaptive resource partitioning algorithms in the OTH and STH protocols have been proposed in [54, 102]. However, these algorithms are based on OFDMA networks without considering the integrated subframe division, which is not practical for relay enhanced LTE-Advanced networks. In what follows, these adaptive resource partitioning algorithms are adjusted for the LTE-Advanced networks, considering the integrated subframe division indicator α with only a slight increase in complexity.

In the OTH protocol The adaptive PF resource partitioning algorithm in the OTH protocol is described in the following steps.

Step 1: By only considering constraint *C2* and solving (4.9) by the Lagrange multiplier algorithm, perfect resource partitioning results in the OTH protocol can be readily derived [54].

$$\begin{aligned} |\mathcal{N}_0^a| =& \frac{|\mathcal{M}_0||\mathcal{N}|}{|\mathcal{M}|} \\ |\mathcal{N}_k^a| =& \frac{|\mathcal{M}_k||\mathcal{N}|}{(1+\theta_k)|\mathcal{M}|} = \frac{|\mathcal{N}_k^b|}{\theta_k}, \forall k \in \mathcal{K}, k \neq 0 \end{aligned} \tag{4.11}$$

Step 2: The backhaul subframe number α is determined by the minimum integer which fulfils all the requirements of backhaul PRB.

$$\alpha = \min(T-1, \lceil \sum_{k \in \mathcal{K}, k \neq 0} \frac{|\mathcal{M}_k| T}{|\mathcal{M}|} \frac{\theta_k}{1+\theta_k} \rceil) \tag{4.12}$$

where T is the subframe number in a radio frame and $\lceil \bullet \rceil$ means rounding up to the nearest integer.

Step 3: The access subframe number is determined by calculating Δ.

$$\Delta = \frac{\sum\limits_{k\in\mathcal{K},k\neq 0} |\mathcal{N}_k^a|}{(1-\frac{\alpha}{T})|\mathcal{N}|} \geq 1, \forall k \in \mathcal{K}, k \neq 0 \tag{4.13}$$

If the Δ is below 1, the algorithm ends with perfect resource partitioning results. Otherwise, the imperfect resource partitioning results will be obtained as

$$\begin{aligned} |\mathcal{N}_k^a|_{new} =& \frac{|\mathcal{N}_k^a|}{\Delta}, |\mathcal{N}_k^b|_{new} = \frac{|\mathcal{N}_k^b|}{\Delta}, \forall k \in \mathcal{K}, k \neq 0 \\ |\mathcal{N}_0^a|_{new} =& |\mathcal{N}| - \sum_{k\in\mathcal{K},k\neq 0} (1+\theta_k)|\mathcal{N}_k^a| \end{aligned} \tag{4.14}$$

This algorithm has a low computational complexity of $\mathcal{O}(K)$, the same as the algorithm in [54]. It needs at most $2K$ basic resource partitioning operations, when there are excessively large number of relay UEs, as described in equation (4.13).

In the STH protocol Through the following steps, the adaptive PF resource partitioning algorithm in the STH protocol is described as:

Step 1: Considering constraint *c2* and function (4.9), perfect results can be readily obtained using the Lagrange multiplier algorithm [102] as

$$\begin{aligned} |\mathcal{N}_0^a| =& \frac{|\mathcal{M}_0||\mathcal{N}|}{|\mathcal{M}|} \\ |\mathcal{N}_k^a| =& \frac{|\mathcal{M}_k||\mathcal{N}|}{\theta_k|\mathcal{M}|} = \frac{|\mathcal{N}_k^b|}{\theta_k}, \forall k \in \mathcal{K}, k \neq 0 \end{aligned} \tag{4.15}$$

Step 2: The backhaul subframe number α is calculated as the minimum integrated value to satisfy the requirements of backhaul PRB.

$$\alpha = \min(T-1, \lceil \sum_{k\in\mathcal{K},k\neq 0} |\mathcal{M}_k| \frac{T}{|\mathcal{M}|} \rceil) \tag{4.16}$$

where $\lceil \bullet \rceil$ means rounding up to the nearest integer.

Step 3: In order to satisfy the PRB requirements of access links, Δ_k is calculated as

$$\Delta_k = \frac{|\mathcal{N}_k^a|}{(1-\frac{\alpha}{T})|\mathcal{N}|} \geq \phi, \forall k \in \mathcal{K}, k \neq 0 \tag{4.17}$$

where ϕ is 1 in the FR pattern, 2/3 in the 2/3 PR pattern and 1/3 in the 1/3 PR

pattern. If Δ_k of some RNs are more than ϕ, their access PRB numbers are fixed at $\phi(1-\frac{\alpha}{T})|\mathcal{N}|$ and the backhaul PRB numbers are calculated as $\phi(1-\frac{\alpha}{T})|\mathcal{N}|\theta_k$. Then, these RNs and their backhaul PRBs are excluded from the SN set $\mathcal{K}$ and the backhaul PRB set $\mathcal{N}^b$ respectively. Accordingly, the remaining PRB number $|\mathcal{N}|$ and the remaining UE number $|\mathcal{M}|$ are renewed.

Step 4: Repeat Step 1 and Step 3 by substituting the new PRB number $|\mathcal{N}|$ and the new UE number $|\mathcal{M}|$ into equations (4.15), until all the remaining RNs fulfil the requirement (4.17). Therefore, we can obtain the access PRB numbers and backhaul PRB numbers of all SNs, $|\mathcal{N}_k^a|$ and $|\mathcal{N}_k^b|$.

Compared with the algorithms in [102], our algorithm applies a more practical subframe division and has the same maximum complexity. Besides, potential shorter operation time can be achieved by the proposed algorithm, since multiple RNs can be dealt with in parallel in Step 3.

Integral resource segments In the real LTE-Advanced systems, the actual PRB number should be integers. Some simple rounding operations are required.

$$\begin{aligned} |\hat{\mathcal{N}}_k^a| =& [|\mathcal{N}_k^a|], \forall k \in \mathcal{K} \\ |\hat{\mathcal{N}}_k^b| =& [\theta_k|\mathcal{N}_k^a|], \forall k \in \mathcal{K}, k \neq 0 \end{aligned} \tag{4.18}$$

where $[\bullet]$ denotes rounding to the nearest integers no less than 0.

4.5.2 Two-hop PF Resource Scheduling

Having obtained resource partitioning results, the resource scheduling sub-problem at each SN can be deduced from the GPF problem. Since the resource scheduling problem at donor eNB can be solved by the conventional resource scheduling algorithm [11], we focus on the resource scheduling problem at RNs, which can be formulated as

$$\max \sum_{m \in \mathcal{M}_k} \log \sum_{n \in \mathcal{N}_k^a} \lambda_{m,n} r_{k,m,n} \tag{4.19}$$

this is a $\lambda_{m,n}$-related 0-1 integer programming problem in the given PRBs. Since the access PRBs are assumed to be identical for the RNs in channel fading characteristics, the problem is subject to the access PRB numbers, which are obtained by the resource partitioning algorithms. Since the backhaul-to-access ratios θ_k are the values determined by the resource scheduling itself, no access PRB sizes including

θ_k can be directly used to solve the problem. In order to obtain low-complexity resource scheduling algorithms for the OTH protocol and the STH protocol, we solve the resource scheduling problem in a PRB-by-PRB manner.

In the OTH protocol The two-hop PF resource scheduling problem in the OTH protocol can be formulated as

$$\max \quad \sum_{m\in\mathcal{M}_k} \log \sum_{n\in\mathcal{N}_k^a} \lambda_{m,n} r_{k,m,n} \tag{4.20}$$

$$\text{subject to} \quad |\mathcal{N}_k^a| = \frac{|\mathcal{M}_k||\mathcal{N}|}{(1+\theta_k)|\mathcal{M}|} = \frac{|\mathcal{N}_k^b|}{\theta_k} \tag{4.21}$$

$$\sum_{m\in\mathcal{M}_k} \lambda_{m,n} \leq 1, \forall n \in \mathcal{N}_k^a \tag{4.22}$$

$$\lambda_{m,n} \geq 0, \forall n \in \mathcal{N}_k^a, \forall m \in \mathcal{M}_k \tag{4.23}$$

The access PRB number and backhaul PRB number of each RN are calculated in equation (4.11). Both of them are related to the backhaul-to-access ratio θ_k and cannot be directly used for obtaining the scheduling results. It can be observed that the sum of the number of the access PRBs and the number of the backhaul PRBs is constant without any relation to θ_k. Therefore, a constraint based on two-hop resources are considered instead of (4.21), which is

$$\sum_{n\in\mathcal{N}_k^a} \sum_{m\in\mathcal{M}_k} (\lambda_{m,n} + \lambda_{m,n} \frac{r_{k,m,n}}{r_{0,k}}) \leq \frac{|\mathcal{M}_0||\mathcal{N}|}{|\mathcal{M}|} \tag{4.24}$$

For the solution to the problem (4.20) with constraints, a Lagrangian function is written as follows

$$\begin{aligned}
&L(\boldsymbol{\lambda}, \mu, \boldsymbol{\nu}, \boldsymbol{\xi}) \\
&= \sum_{m\in\mathcal{M}_k} \log \sum_{n\in\mathcal{N}_k^a} \lambda_{m,n} r_{k,m,n} \\
&+\mu \left[\frac{|\mathcal{M}_0||\mathcal{N}|}{|\mathcal{M}|} - \sum_{n\in\mathcal{N}_k^a} \sum_{m\in\mathcal{M}_k} (\lambda_{m,n} + \lambda_{m,n} \frac{r_{k,m,n}}{r_{0,k}}) \right] \\
&+ \sum_{n\in\mathcal{N}_k^a} \nu_n \left[1 - \sum_{m\in\mathcal{M}_k} \lambda_{m,n} \right] \\
&+ \sum_{n\in\mathcal{N}_k^a} \sum_{m\in\mathcal{M}_k} \xi_{m,n} \lambda_{m,n}
\end{aligned} \tag{4.25}$$

where μ, $\boldsymbol{\nu}$ and $\boldsymbol{\xi}$ are the Lagrangian multipliers and non-negative numbers to satisfy the KarushKuhnTucker (KKT) conditions.

By letting the differentiation of L with regard to $\lambda_{m,n}$ equal 0, the following equation can be obtained for each $\lambda_{m,n}$.

$$\begin{aligned}&\frac{\partial L}{\partial \lambda_{m,n}}\\&= \frac{r_{k,m,n}}{\sum_{n\in\mathcal{N}_k^a}\lambda_{m,n}r_{k,m,n}} - \mu(1+\frac{r_{k,m,n}}{r_{0,k}})\\&-\nu_n+\xi_{m,n}=0\end{aligned} \tag{4.26}$$

We find that

$$\begin{aligned}&\nu_n-\xi_{m,n}=\\&(1+\frac{r_{k,m,n}}{r_{0,k}})(\frac{\frac{r_{k,m,n}r_{0,k}}{r_{k,m,n}+r_{0,k}}}{\sum_{n\in\mathcal{N}_k^a}\lambda_{m,n}r_{k,m,n}}-\mu)\end{aligned} \tag{4.27}$$

We then use $\beta_{k,m,n}$ and $\eta_{k,m,n}$ to simplify the above equation.

$$\nu_n-\xi_{m,n} = (1+\beta_{k,m,n})(\eta_{k,m,n}-\mu) \tag{4.28}$$

$$\beta_{k,m,n} = \frac{r_{k,m,n}}{r_{0,k}} \tag{4.29}$$

$$\eta_{k,m,n} = \frac{\frac{r_{k,m,n}}{1+\beta_{k,m,n}}}{\sum_{n\in\mathcal{N}_k^a}\lambda_{m,n}r_{k,m,n}} \tag{4.30}$$

Considering the KKT conditions for the Lagrangian function (4.25), if the $\lambda_{m,n}$ is chosen more than 0, $\xi_{m,n}$ should be chosen as 0. Unless only one UE is chosen in PRB n with $\lambda_{m,n}=1$, ν_n should be chosen as 0.

For different $\eta_{k,m,n}$, the following expression of $\lambda_{m,n}$ can be derived.

$$\lambda_{m,n}=\begin{cases}0, & \text{if } \eta_{\mathrm{k,m,n}}<\mu\\(0,1], & \text{if } \eta_{\mathrm{k,m,n}}\geq\mu\end{cases} \tag{4.31}$$

In order to round $\lambda_{m,n}$ to 0 or 1 and to guarantee there is only one UE selected for the PRB n, the sub-optimal greedy solution in each PRB n should be the UE m^* with the following maximum value

$$m^*=\arg\max_{\mathcal{M}_k}\frac{\frac{r_{k,m,n}r_{0,k}}{r_{k,m,n}+r_{0,k}}}{\sum_{n\in\mathcal{N}_k^a}\lambda_{n,m}r_{k,m,n}} \tag{4.32}$$

By replacing $\sum_{n\in\mathcal{N}_k^a}\lambda_{n,m}r_{k,m,n}$ with the historical data rate $\bar{R}_{m,k}(t-1)$ of UE m associated with RN k, a distributed two-hop resource scheduling algorithm for the OTH protocol is proposed as

$$m = \arg\max_{\mathcal{M}_k} \frac{\frac{r_{k,m,n}r_{0,k}}{r_{k,m,n}+r_{0,k}}}{\bar{R}_{m,k}(t-1)}, \forall n \in \mathcal{N}_k^a \tag{4.33}$$

After each time interval, $\bar{R}_{m,k}(t-1)$ is updated as

$$\begin{aligned}\bar{R}_{m,k}(t) =&(1-\frac{1}{W})\bar{R}_{m,k}(t-1)+\\ &\frac{1}{W}\sum_{n\in\mathcal{N}_k^a}\lambda_{n,m}r_{k,m,n}\end{aligned} \tag{4.34}$$

where W is the average filter window length.

Using the proposed resource scheduling algorithm, the proportional fairness of end-to-end data rates is supposed to be maximised. Thus, based on the findings in [31, 58], the end-to-end data rate of each relay UE can be approximated as

$$R_m \approx G_{m,k}^* \frac{|\mathcal{N}_k^a|+|\mathcal{N}_k^b|}{|\mathcal{M}_k|}\frac{\bar{r}_{m,k}r_{0,k}}{\bar{r}_{m,k}+r_{0,k}} \tag{4.35}$$

where $G_{m,k}^*$ is the scheduling gain of the proposed algorithm compared with the Round-Robin scheduling. It can be seen from the approximation in (4.35) that the difference between the end-to-end data rates of relay UEs can be reduced compared with the conventional single-hop PF scheduling algorithm.

In the STH protocol Based on the adaptive resource partitioning in the STH protocol, the two-hop resource scheduling problem for the STH protocol is subject to four independent constraints

$$\max \quad \sum_{m\in\mathcal{M}_k}\log\sum_{n\in\mathcal{N}_k^a}\lambda_{m,n}r_{k,m,n} \tag{4.36}$$

$$\text{subject to} \quad |\mathcal{N}_k^a| \le \phi(1-\frac{\alpha}{T})|\mathcal{N}| \tag{4.37}$$

$$|\mathcal{N}_k^b| \le \frac{|\mathcal{M}_k||\mathcal{N}|}{|\mathcal{M}|} \tag{4.38}$$

$$\sum_{m\in\mathcal{M}_k}\lambda_{m,n} = 1, \forall n \in |\mathcal{N}_k^a| \tag{4.39}$$

$$\lambda_{m,n} \ge 1, \forall n \in \mathcal{N}_k^a, \forall m \in \mathcal{M}_k \tag{4.40}$$

In order to solve this resource scheduling problem, We consider the Lagrangian function with the KKT conditions

$$\begin{aligned}
&L(\boldsymbol{\lambda}, \xi, \mu, \boldsymbol{\nu}) \\
&= \sum_{m \in \mathcal{M}_k} \log \sum_{n \in \mathcal{N}_k^a} \lambda_{m,n} r_{k,m,n} \\
&+\sigma \left[\phi(1 - \frac{\alpha}{T})|\mathcal{N}| - \sum_{n \in \mathcal{N}_k^a} \sum_{m \in \mathcal{M}_k} \lambda_{m,n} \right] \\
&+\mu \left[\frac{|\mathcal{M}_0||\mathcal{N}|}{|\mathcal{M}|} - \sum_{n \in \mathcal{N}_k^a} \sum_{m \in \mathcal{M}_k} \lambda_{m,n} \frac{r_{k,m,n}}{r_{0,k}} \right] \\
&+ \sum_{n \in \mathcal{N}_k^a} \nu_n \left[1 - \sum_{m \in \mathcal{M}_k} \lambda_{m,n} \right] \\
&+ \sum_{n \in \mathcal{N}_k^a} \sum_{m \in \mathcal{M}_k} \xi_{m,n} \lambda_{m,n}
\end{aligned} \tag{4.41}$$

where $\boldsymbol{\lambda}$, σ, μ, $\boldsymbol{\nu}$ and $\boldsymbol{\xi}$ are the Lagrangian multipliers and non-negative numbers to satisfy the KKT conditions.

By letting the differentiation of L with regard to $\lambda_{m,n}$ equal 0, the following equation can be obtained for each $\lambda_{m,n}$.

$$\begin{aligned}
&\frac{\partial L}{\partial \lambda_{m,n}} = \\
&\frac{r_{k,m,n}}{\sum_{n \in \mathcal{N}_k^a} \lambda_{m,n} r_{k,m,n}} - \sigma - \mu \frac{r_{k,m,n}}{r_{0,k}} - \nu_n + \xi_{m,n} = 0
\end{aligned} \tag{4.42}$$

If the constraint (4.38) is not satisfied, μ can be any number not less than 0. We have

$$\nu_n - \xi_{m,n} = \frac{r_{k,m,n}}{r_{0,k}} \left(\frac{r_{0,k}}{\sum_{n \in \mathcal{N}_k^a} \lambda_{n,m} r_{k,m,n}} - \mu \right) - \sigma \tag{4.43}$$

Similar to the solution of the resource scheduling problem in the OTH protocol, the chosen UE should maximise the following value.

$$m = \arg\max_{\mathcal{M}_k} \frac{r_{0,k}}{\sum_{n \in \mathcal{N}_k^a} \lambda_{n,m} r_{k,m,n}} \tag{4.44}$$

If the constraint (4.38) is satisfied, μ should be 0 to satisfy the KKT condition.

Therefore, the UE should be chosen according to the following metric.

$$m = \arg\max_{\mathcal{M}_k} \frac{r_{k,m,n}}{\sum_{n\in\mathcal{N}_k^a} \lambda_{n,m} r_{k,m,n}} \tag{4.45}$$

In order to solve the PF scheduling problem with two constraints, a two-hop schedule-and-confirm algorithm with two stages is proposed.

Stage 1: The initial scheduling results accounting for constraint (4.37) can be obtained easily through similar procedures as in the OTH protocol. As for PRB n, it is scheduled to UE m with the highest ratio of the current data rate to the history data rate.

$$\begin{aligned} m &= \arg\max_{\mathcal{M}_k} \frac{r_{k,m,n}}{\sum\limits_{n\in\mathcal{N}_k^a} \lambda_{m,n} r_{k,m,n}} \\ &= \arg\max_{\mathcal{M}_k} \frac{r_{k,m,n}}{\bar{R}_{k,m}(t-1)} \end{aligned} \tag{4.46}$$

and the preliminary variable $\hat{\lambda}_{m,n}$ is set to 1. For those UEs that are not chosen, $\hat{\lambda}_{m^*,n}$ is 0.

Stage 2: After all the access PRBs have been scheduled according to (4.46), they should be confirmed by the scheduling of the backhaul PRBs. Because of constraints (4.38) and (*C1*), the access PRB n allocated to UE m is confirmed by

$$\begin{aligned} m &= \arg\max_{\mathcal{M}_k} \frac{r_{0,k}}{\sum\limits_{n\in\mathcal{N}_k^b} \lambda_{n,m}^b r_{0,k}} \\ &= \arg\max_{\mathcal{M}_k} \frac{r_{0,k}}{\sum\limits_{n\in\mathcal{N}_k^a} \lambda_{m,n} r_{k,m,n}} \end{aligned} \tag{4.47}$$

where $\lambda_{n,m}^b$ is the resource allocation variable in the backhaul links. If the access PRB scheduling is confirmed, the final resource allocation variable $\lambda_{m,n}$ and the corresponding $\lambda_{n,m}^b$ are set to 1, otherwise, the confirmation of the next access PRB will begin. Stage 2 repeats until the scheduling of all access PRBs are confirmed or all the backhaul PRBs are scheduled. After each time interval, $\bar{R}_{m,k}(t-1)$ is updated as

$$\begin{aligned} \bar{R}_{m,k}(t) =& (1-\frac{1}{W})\bar{R}_{m,k}(t-1) + \\ & \frac{1}{W}\sum_{n\in\mathcal{N}_k^a} \lambda_{n,m} r_{k,m,n} \end{aligned} \tag{4.48}$$

where W is the average filter window length.

Since the PF resource scheduling problem in the STH protocol is constrained by the resources of both hops, the end-to-end data rates of relay UEs are between two values, R_m^{Access} and $R_m^{Backhaul}$, for the two hops.

$$\begin{aligned} R_m^{Access} &\approx G_{m,k} \frac{|\mathcal{N}_k^a|}{|\mathcal{M}_k|} \bar{r}_{m,k} \\ R_m^{Backhaul} &\approx \frac{|\mathcal{N}_k^b|}{|\mathcal{M}_k|} r_{0,k} \end{aligned} \tag{4.49}$$

where $G_{m,k}$ is the scheduling gain of the conventional PF scheduling algorithm compared with the Round-Robin scheduling algorithm. Which value the end-to-end data rates are closer to depends on which constraint is stricter.

CSI exchange analysis By using the distributed resource allocation scheme proposed in this chapter, the CSI exchange between the donor eNBs and the RNs can be reduced significantly. In the centralised resource allocation schemes, the channel information of the relay UEs in all the PRBs should be transmitted to the donor eNB periodically by each RN, and the resource scheduling decision of relay UEs in the assigned PRBs are transmitted to each RN by the donor eNB. In the proposed scheme, only the sum of data rates of the attached relay UEs in the access links should be transmitted by each RN, and the donor eNBs inform the RNs about the PRBs partitioned for them. Thus, the occupied resources in the control channels of backhaul links by the CSI exchange using the centralised scheme is $|\mathcal{M}_k| \times |\mathcal{N}|$ times that for the proposed distributed scheme.

4.6 Performance Evaluation

4.6.1 Simulation Scenarios

According to the LTE self-evaluation methodology [14], a semi-static system-level Matlab simulation platform is developed to evaluate downlink performance. Using the wrap-around technique, seven 3-sectored macro cells are generated with a fixed numbers of UEs randomly dropped in them. In each cell, a fixed number of RNs are located on the fringe of the cell with the same distance of half of the inter-site distance from the eNB. The simulated network is illustrated in Fig.4.8. The details of simulation parameters are listed in Table 4.1.

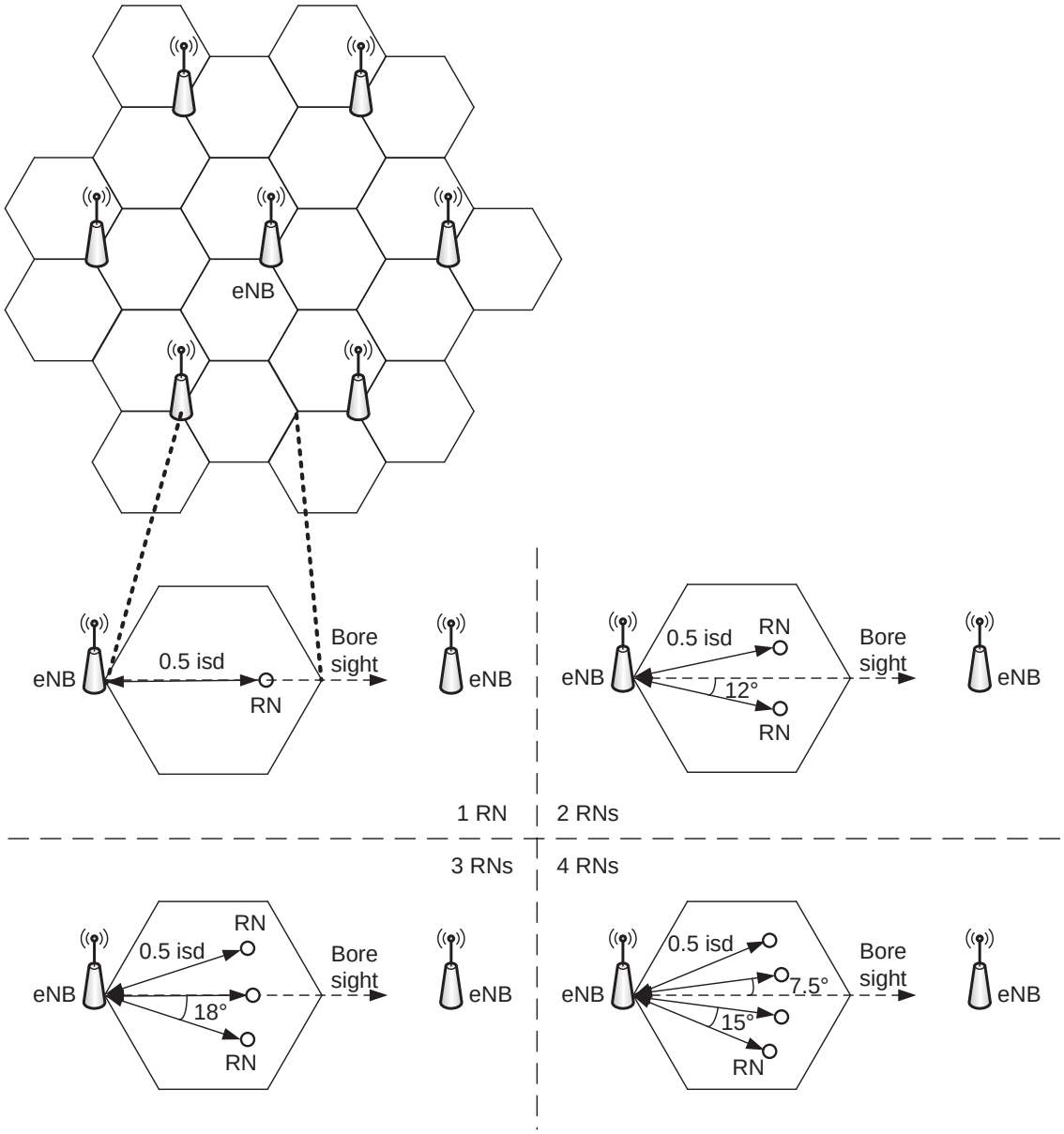

Figure 4.8: Cellular network layout and RN deployment

Table 4.1: Simulation parameters

Parameters	Values
Carrier/Bandwidth	2GHz /FDD 10MHz
Subframe number	10/radio frame
PRB number	50/subframe
UE number	30/sector
Inter-site distance	500 m
Transmitting power	eNB: 46 dBm RN: 30 dBm
Antenna configuration	eNB: 14 dBi, 70 directional RN: 5 dBi, omni UE: 0 dBi, omni
Thermal noise density	-174 dBm/Hz
Noise figure	9 dB at UE, 5 dB at RN
Channel model	3GPP case 1 for relay [14]
Shadowing standard deviations	Log-normal distribution eNB-RN: 6 dB eNB-UE: 8 dB RN-UE: 10 dB
Fast fading model	SUI-5 channel [104]
Traffic model	Full buffer
AMC scheme	15 levels according to [59]

The end-to-end optimal routing strategy [53] is utilised in this simulation. Each UE m is connected to SN k with the maximum end-to-end data rate per PRB.

$$k = \arg\max(SE_{0,m}, \frac{SE_{0,k}SE_{k,m}}{SE_{0,k} + SE_{k,m}}) \tag{4.50}$$

where $SE_{k,m}$ represents the estimated average data rate per PRB between SN k and UE m, and $SE_{0,k}$ denotes the backhaul data rate per PRB of RN k.

The OR pattern in the OTH protocol and the FR, 2/3 PR and 1/3 PR patterns in the STH protocol are considered as the scenarios of the performance evaluations. Although these patterns have been mentioned in the previous sections, more details about the PRB assignment in different sectors of a macro cell are illustrated in Fig.4.4, Fig.4.5, Fig.4.6 and Fig.4.7. In the OR pattern, the access PRBs are assigned firstly in different sectors to avoid more inter-cell interference from the

eNBs in the adjacent cells. In the 2/3 PR and 1/3 PR patterns, the access PRBs in different sectors are reusing different parts of the whole PRBs to reduce inter-cell interference as well as intra-cell interference.

The proposed resource allocation scheme in each reuse pattern includes two algorithms: an adaptive proportional fair resource partitioning algorithm and an end-to-end proportional fairness based resource scheduling algorithm. Apart from the PF scheduling scheme without relays, a distributed PF resource allocation scheme was considered for comparison. The distributed PF-based Adaptive Resource Partitioning and the Conventional Resource Scheduling (ARP+CRS) scheme used in [54, 102] is the most valuable benchmark of the proposed scheme. In the ARP+CRS scheme, the resource partitioning is similar to the proposed scheme, and the resource scheduling algorithm of access links is given by

$$m = \arg\max_{\mathcal{M}_k} \frac{r_{k,m,n}}{\bar{R}_{m,k}(t-1)}, \forall n \in \mathcal{N}_k^a \tag{4.51}$$

$$\begin{aligned} \bar{R}_{m,k}(t) =& (1 - \frac{1}{W})\bar{R}_{m,k}(t-1) + \\ & \frac{1}{W} \sum_{n \in \mathcal{N}_k^a} \lambda_{n,m} r_{k,m,n} \end{aligned} \tag{4.52}$$

where $r_{k,m,n}$ is the data rate in the access links and W is the average filter window length.

In this simulation, the downlink performance of all the UEs in the macro cell is evaluated. The performance of the relay UEs attached to the RNs are also assessed. Macro UEs are defined as the UEs in the macro cell, including the direct UEs and the relay UEs in the same macro cell. The metrics of the evaluation include the GPF factor, the average UE throughput and the 5% worst UE throughput. Besides the GPF factor is required to show the effectiveness of the solutions to the GPF problem in 4.4, it is a commonly used metric [31] to show the trade-off between average throughput and fairness, which is expressed as:

$$GPF\ factor = \frac{1}{|\mathcal{M}|} \sum_{m \in \mathcal{M}} \log R_m \tag{4.53}$$

The 5% worst UE throughput is the largest throughput of the 5% UEs with worst throughputs, as defined in 3GPP standard [14]. This metric is also used to indicate the cell-edge performance.

4.6.2 Performance Comparison in the OTH Protocol

4.6.2.1 GPF factor

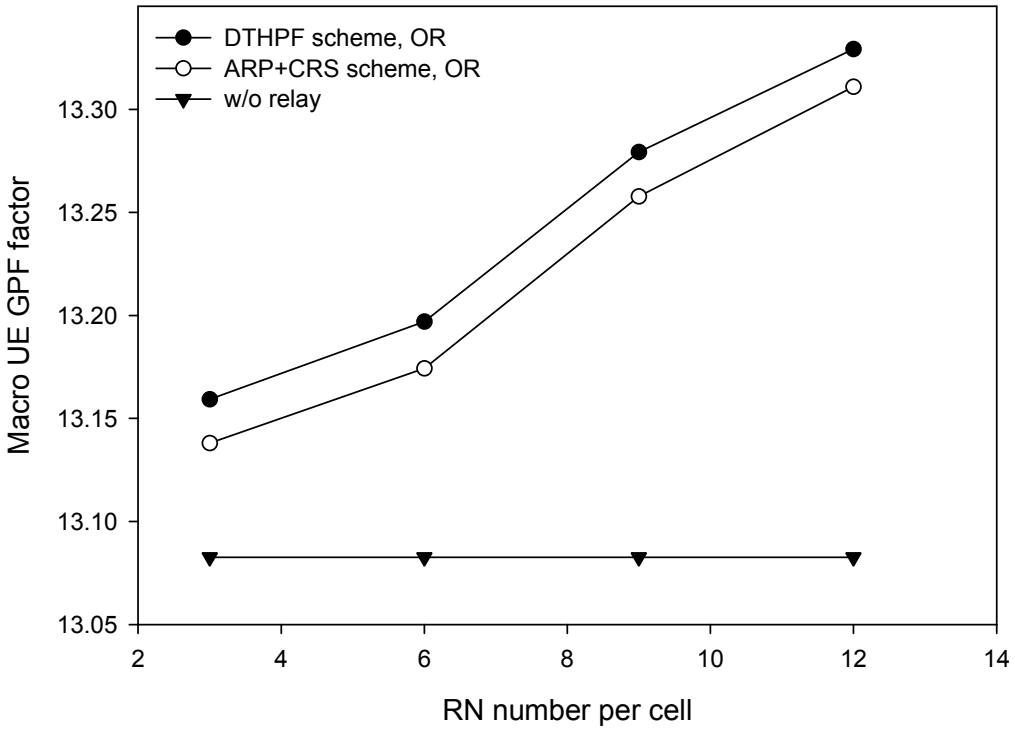

Figure 4.9: GPF factor (Macro UEs) v.s. RN numbers per cell in the OTH protocol

Fig.4.9 shows the GPF factors of macro UEs using different resource allocation schemes versus the RN number in the OR pattern of the OTH protocol. The GPF factors in the proposed DTHPF scheme and the benchmark ARP+CRS scheme increase with the increase of the number of RNs per cell. When the number of RNs per cell is 12, the largest GPF factor in this simulation with the OR pattern is achieved, and 0.3 larger than that without relay, which is equivalent to 30% gain. The reason of this observation is that more RNs have more opportunities of obtaining better channel quality for the cell-edge UEs. At different numbers of RNs pers cell, the proposed DTHPF scheme outperforms the ARP+CRS scheme in getting larger GPF factor, which implies better trade-off between throughput and fairness for the macro UEs. The performance gain of the DTHPF scheme over the ARP+CRS scheme seems to be a constant in different RN numbers per cell.

The macro UEs include the UEs attached to the RNs and the UEs served by the eNBs. For the UEs attached to the RNs, their performance is impacted by the

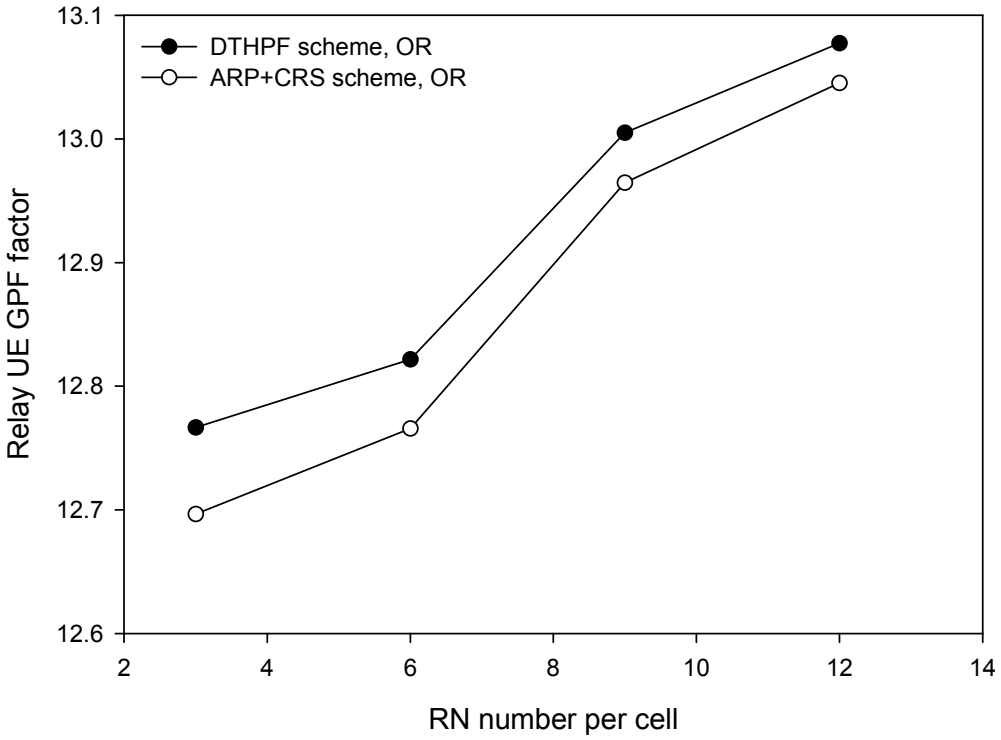

Figure 4.10: GPF factor (relay UEs) v.s. RN numbers per cell in the OTH protocol

different resource allocation schemes used for them. As is displayed in Fig.4.10, the GPF factors increase with more RNs per cell. The reason of the increasing is that the diversity of multiple RNs improve the access link conditions, and thus increase the GPF factors. The proposed DTHPF scheme can obtain more relay UE GPF factors than the benchmark scheme in different RN numbers per cell. The gap between these two schemes is getting closer when the number of RNs per cell is increasing. With increasing RNs per cell, the relay UEs served by each RN are getting less, and thus the performance gain of relay UEs brought by the proposed DTHPF scheme is reducing. Although the performance gain of relay UEs is getting smaller in larger number of RNs per cell, the performance gain of macro UEs is still unchanged, because the number of relay UEs is growing.

4.6.2.2 Average UE throughput

In Fig.4.11, it is illustrated that the average UE throughputs using different schemes increase with the increase of the number of RNs. In the OR pattern, both the DTHPF scheme and the ARP+CRS scheme can achieve higher average throughput for the macro UEs than the average throughput without any relay. The benchmark

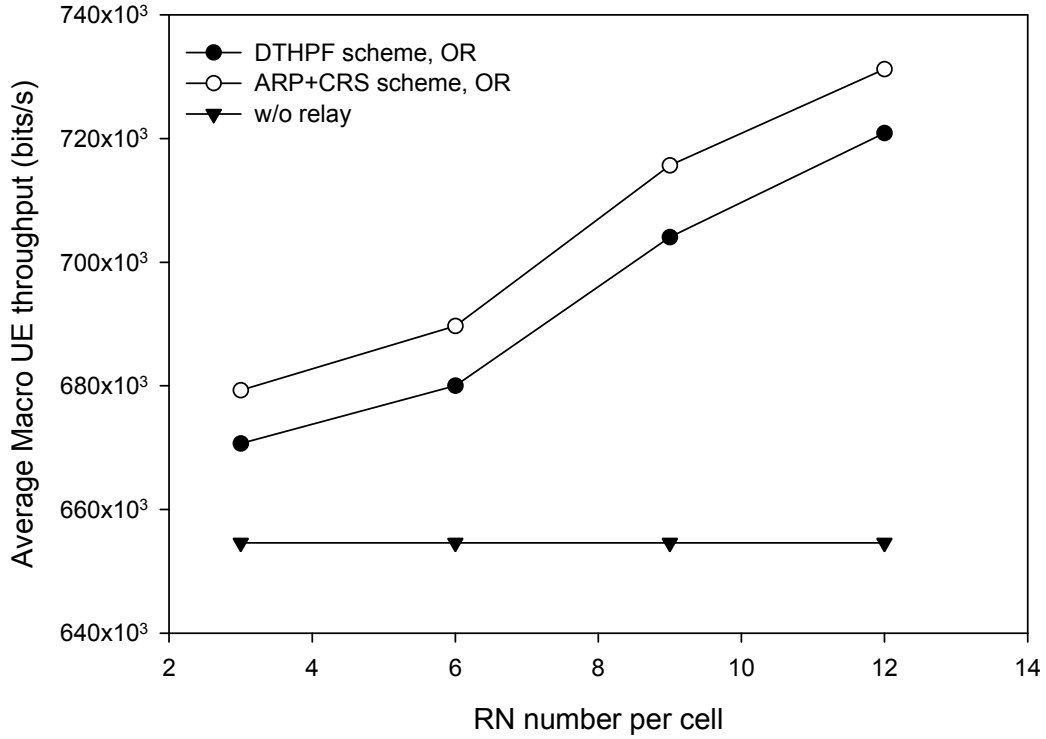

Figure 4.11: Average macro UE throughput v.s. RN numbers per cell in the OTH protocol

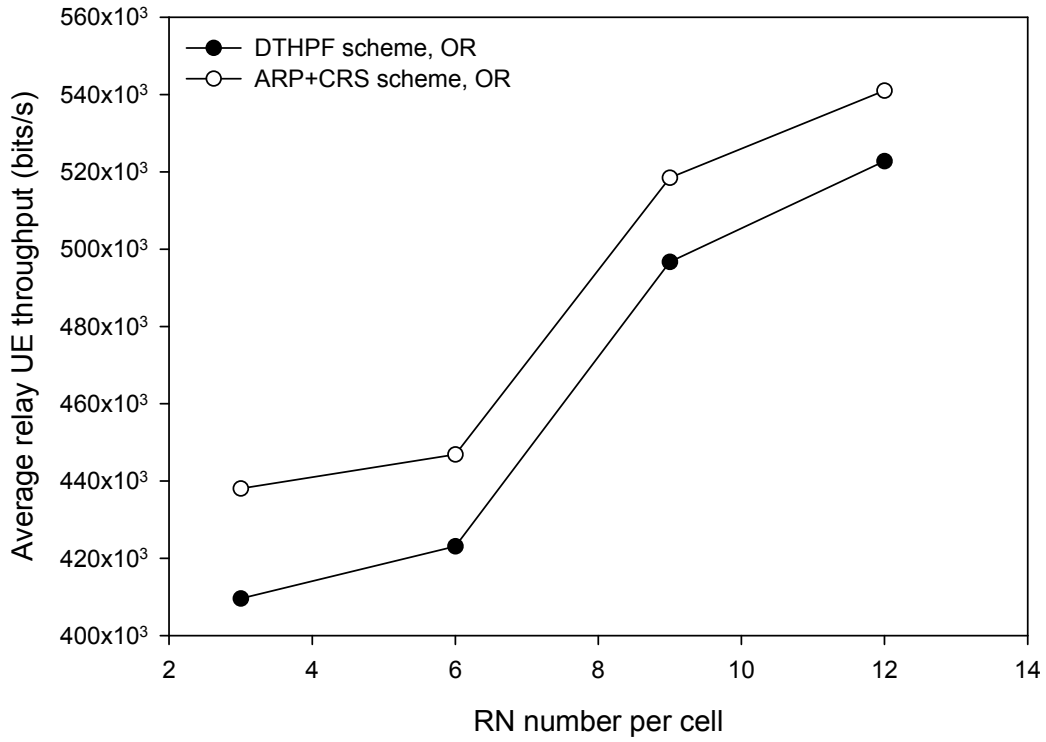

Figure 4.12: Average relay UE throughput v.s. RN numbers per cell in the OTH protocol

ARP+CRS scheme can obtain larger average throughputs for the UEs than the proposed DTHPF scheme. Since the proposed DTHPF scheme is aiming at providing better compromise between throughput and fairness, it can be seen that the benchmark ARP+CRS scheme achieves larger throughputs at cost of neglecting fairness. The performance gaps in average macro UE throughput between these two resource allocation schemes are changed only insignificantly.

It can be observed from Fig.4.12 that the average throughputs of relay UEs achieved by the proposed DTHPF resource allocation scheme are smaller than that in the ARP+CRS scheme in the OR pattern. The average throughputs of relay UEs increase with the increase of the number of RNs per cell due to the wider diversity of multiple RNs. It also can be seen that the performance gap in average relay UE throughput between the proposed scheme and the benchmark scheme reduces with increasing number of RNs per cell. This fact implies that the proposed DTHPF scheme has lower impact on the average throughput of relay UEs when there are more RNs per cell and less relay UEs per RN.

4.6.2.3 5% worst UE throughput

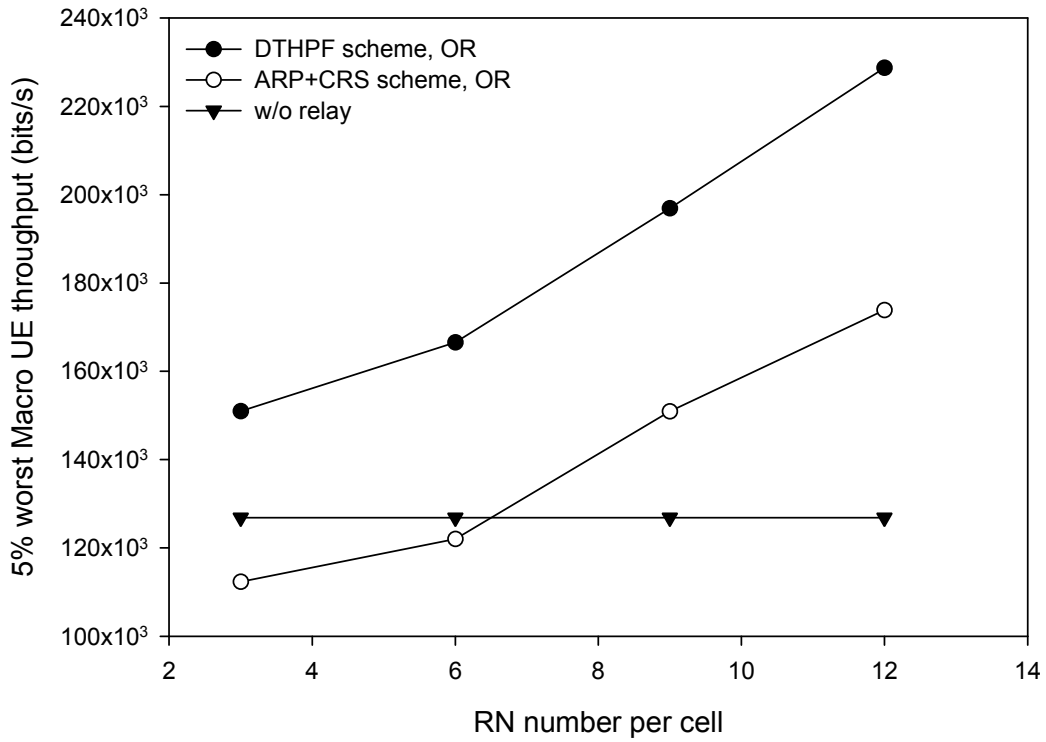

Figure 4.13: 5% worst macro UE throughput v.s. RN numbers per cell in the OTH protocol

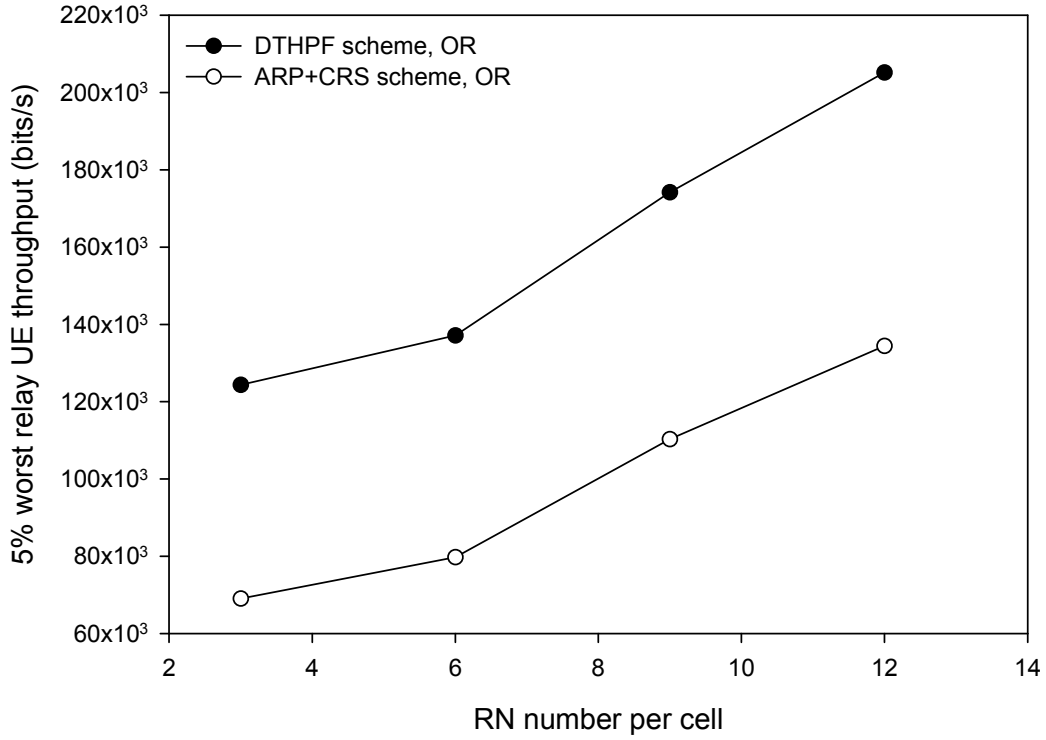

Figure 4.14: 5% worst relay UE throughput v.s. RN numbers per cell in the OTH protocol

The 5% worst throughputs of macro UEs are demonstrated in Fig.4.13. In the OR pattern, the 5% worst macro UE throughput achieved by the proposed DTHPF scheme obtains significant gain over the ARP+CRS scheme for different RN numbers per cell, and is much higher than the value without relays. The 5% worst macro UE throughputs in the benchmark ARP+CRS scheme is lower than the reference value without relays, when the RN number is below 6 per cell. What can be inferred from this fact is that the benchmark PF resource allocation scheme cannot achieve the two-hop proportional fairness maximisation and cannot guarantee fairness between macro UEs. Another fact which can be observed is that the performance gain of the proposed DTHPF scheme over the ARP+CRS scheme in the 5% worst macro UE throughputs is slightly larger when there are more RNs per cell

Fig.4.14 presents the 5% worst throughput of relay UEs against different RN numbers per cell. The 5% worst relay UE throughputs increase with more RNs per cell using both resource allocation schemes considered in this chapter. As shown in Table 4.2, they increase sharply in the OR pattern by 60%-80% from 3 RNs per cell to 12 RNs per cell. This fact is because with more RNs in a cell, the cell-edge UEs with bad channel conditions have more chances to choose one of multiple RNs to improve their performance.

Table 4.2: The gains of the DTHPF scheme over the ARP+CRS scheme in the OTH protocol

	RN number per cell			
	3	6	9	12
Macro UE GPF factor	0.0212	0.0227	0.0216	0.0183
Relay UE GPF factor	0.0701	0.0559	0.0404	0.0322
Average Macro UE Throughput	-1.28%	-1.42%	-1.65%	-1.43%
Average Relay UE Throughput	-6.94%	-5.61%	-4.38%	-3.49%
5% worst Macro UE Throughput	25.57%	26.73%	23.36%	23.97%
5% worst Relay UE Throughput	79.95%	71.94%	57.93%	52.57%

Table 4.2 shows the gains of the DTHPF scheme over the ARP+CRS scheme in the OTH protocol. From this table, it can be seen that although the average throughputs of macro UEs and relay UEs decrease using the proposed scheme, the UEs with 5% worst channel conditions can obtain up to around 80% more throughputs compared with the benchmarking scheme.

4.6.3 Performance Comparison in the STH Protocol

4.6.3.1 GPF factor

Fig.4.15 show the GPF factor versus the RN number per cell using different resource allocation schemes with the FR pattern, the 2/3 PR pattern and the 1/3 PR pattern. In all patterns, the proposed DTHPF scheme outperforms the ARP+CRS scheme in achieving larger GPF factors, which means a better trade-off between throughput and fairness. Due to less resources being reused for the access links in the 2/3 PR pattern and the 1/3 PR pattern, the GPF factor gain of the proposed DTHPF scheme over the benchmark ARP+CRS scheme is smaller. This is because stricter resource constraints of the access links make the proposed two-hop PF resource scheduling algorithm in the STH protocol closer to the conventional PF scheduling algorithm. With a growing number of RNs per cell, the GPF factors using both schemes increases. The GPF factors in the 2/3 PR pattern and 1/3 PR pattern are larger than the GPF factors in the FR pattern. The GPF factors in the 2/3 PR pattern are almost the same as the GPF factors in the 1/3 PR pattern, when there are 3 RNs per cell, and larger than the GPF factors in the 1/3 PR pattern, when there are 12 RNs per cell. Reduced intra-cell interference leads to larger GPF

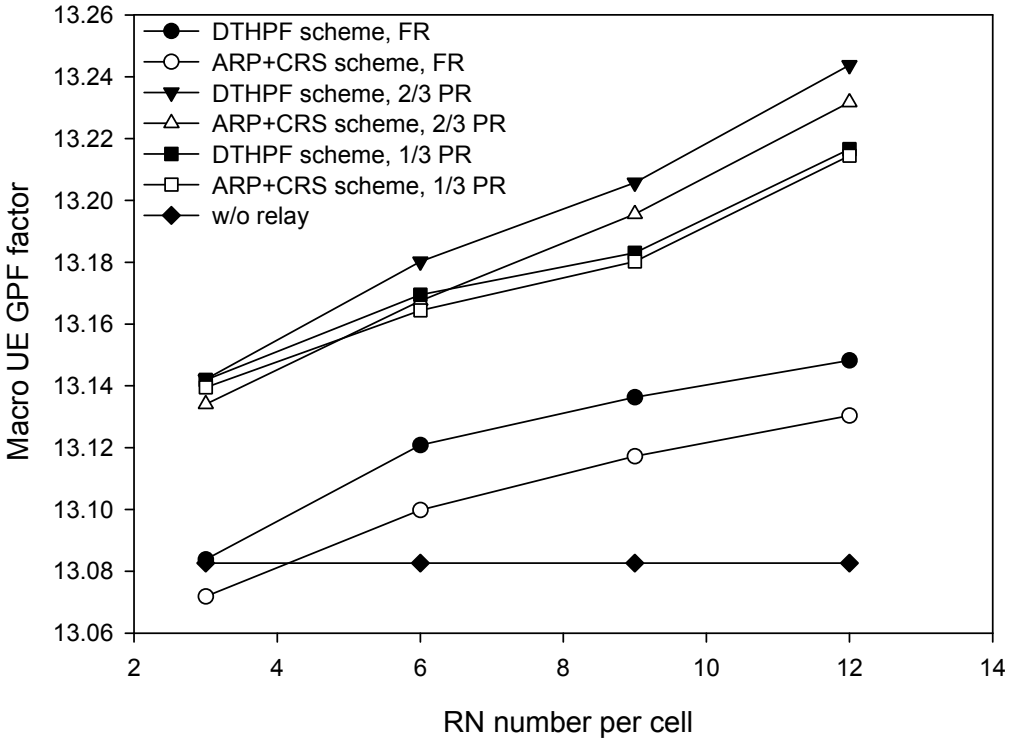

Figure 4.15: GPF factor (Macro UEs) v.s. RN numbers per cell in the STH protocol

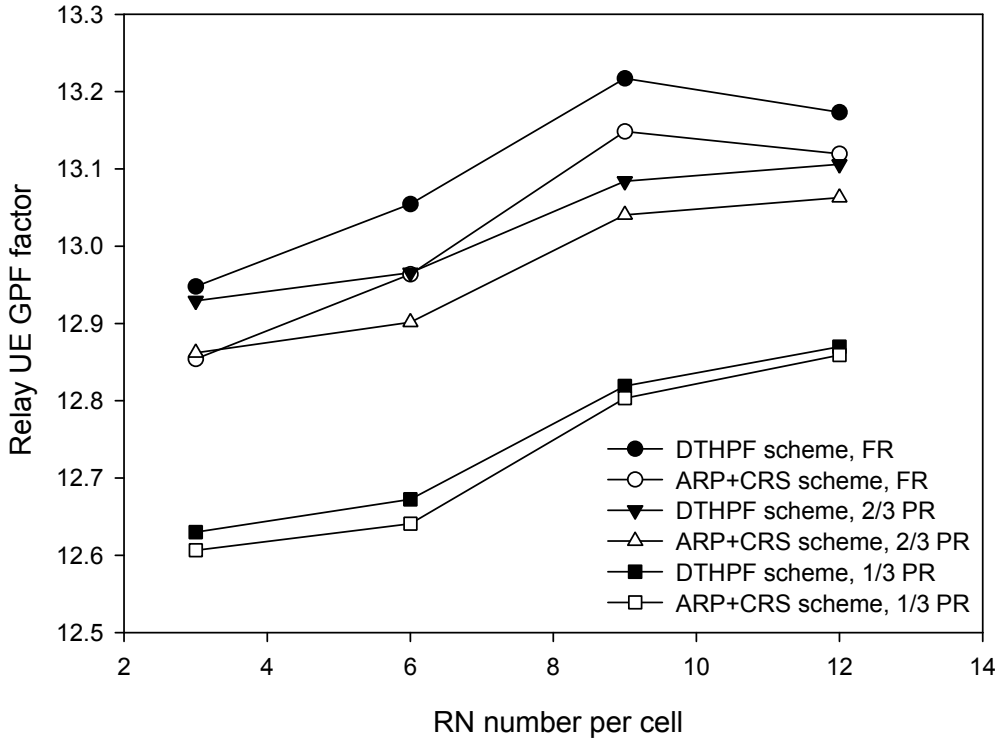

Figure 4.16: GPF factor (relay UEs) v.s. RN number per cell in the STH protocol

factors in the 2/3 PR and the 1/3 PR patterns than in the FR pattern. However, less resources for the access links causes smaller GPF factors in the 1/3 PR pattern than in the 2/3 PR pattern, especially when the RN number per cell is large and many UEs are associated with RNs.

As displayed in Fig.4.16, the proposed DTHPF resource allocation scheme can obtain larger GPF factors for relay UEs than the benchmark ARP+CRs scheme with the FR pattern, the 2/3 PR pattern and the 1/3 PR pattern. It can be noticed that along with less resource reuse for the access links in the 2/3 PR pattern and the 1/3 PR pattern, the relay UE GPF factor gain of the proposed DTHPF scheme over the benchmark ARP+CRS scheme is smaller. This is because the proposed two-hop PF resource scheduling algorithm in the STH protocol is closer to the conventional PF scheduling algorithm due to stricter resource constraints of the access links. The relay UE GPF factors in the FR pattern are larger than those in the 2/3 PR pattern and much larger than those in the 1/3 PR pattern. This is because there are less resources for the access links used by the relay UEs in the 2/3 PR pattern and the 1/3 PR pattern. When the RN numbers per cell grow from 9 to 12, the relay UE GPF factors in the FR pattern drop due to the aggravating inter-RN interference brought by the increasing number of RNs and full frequency reuse.

4.6.3.2 Average UE throughput

In Fig.4.17, it is illustrated that along with growing RN numbers in each cell, most of the average macro UE throughputs using both resource allocation schemes in all patterns rise. The exceptional situation exists when the number of RNs per cell goes up from 9 to 12 per cell in the FR pattern. With the FR pattern, the 2/3 PR pattern and the 1/3 PR pattern, the average UE throughputs achieved by the proposed DTHPF scheme can be hardly differentiated from those achieved by the benchmark ARP+CRS scheme. This is because the average throughputs of relay UEs are constrained by the backhaul PRB numbers, which are decided by the similar adaptive resource partitioning algorithms of these two schemes. When the number of RNs in a cell is 3, the throughputs of the 2/3 PR pattern are almost the same as those with the 1/3 PR pattern. When the number of RNs in a cell is 12, the throughput of the 2/3 PR patter are much larger than those with the 1/3 PR pattern. The throughputs with the 2/3 PR pattern and the 1/3 PR pattern are significantly more than those with the FR pattern with any numbers of RNs per cell, due to less intra-cell interference between direct links and access links.

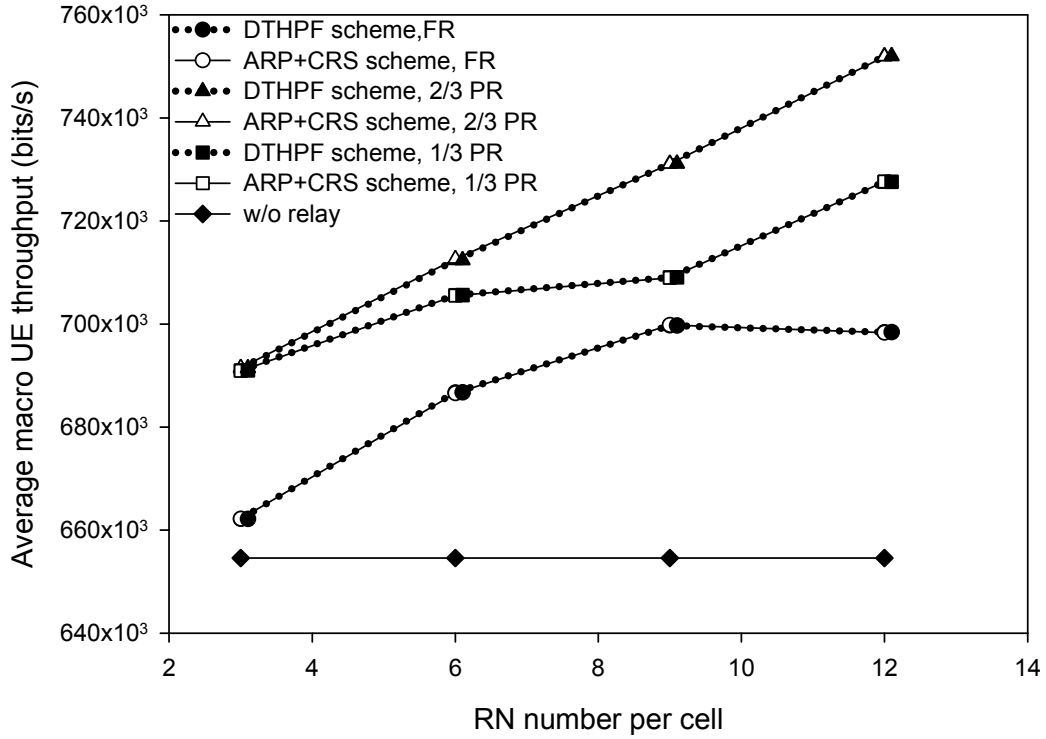

Figure 4.17: Average macro UE throughput v.s. RN number per cell in the STH protocol

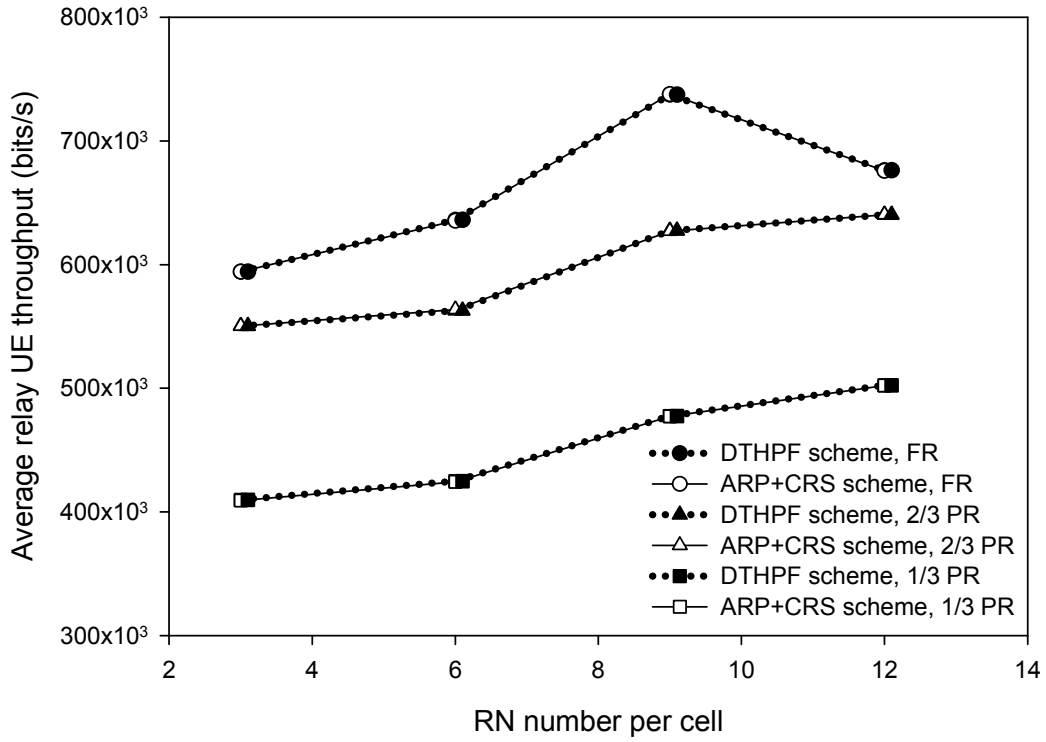

Figure 4.18: Average relay UE throughput v.s. RN number per cell in the STH protocol

From Fig.4.18, the average relay UE throughputs achieved by the proposed DTHPF scheme and the ARP+CRS scheme with the FR pattern, the 2/3 PR pattern and the 1/3 PR pattern can be observed. Due to similar reasons, the average relay UE throughputs achieved by the proposed DTHPF scheme and the benchmark ARP+CRS scheme in all patterns are almost identical. The average throughputs of relay UEs in the FR pattern are larger than those with the 2/3 PR pattern. The average throughputs of relay UEs in the FR and the 2/3 PR patterns are larger than those with the 1/3 PR pattern. Their relationship is proportional to the amount of resources assigned to the relay UE in the access links. When the RN number per cell goes up from 9 to 12, the average relay UE throughputs in the FR pattern falls, because of increasing interference between multiple RNs.

4.6.3.3 5% worst UE throughput

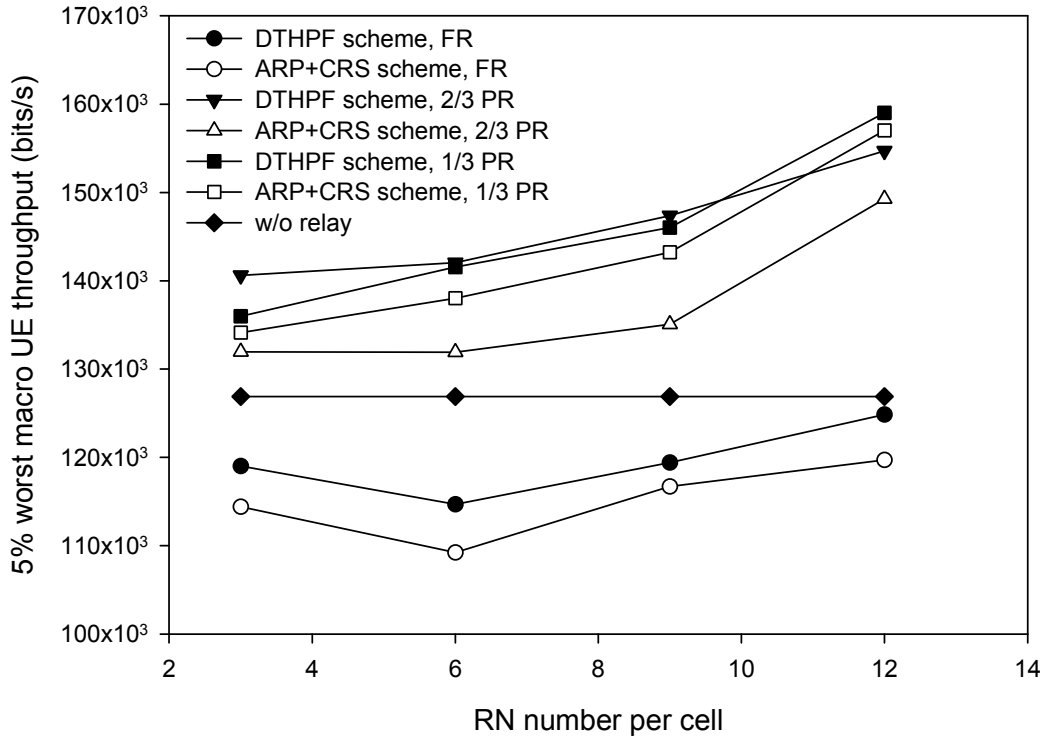

Figure 4.19: 5% worst macro UE throughput v.s. RN number per cell in the STH protocol

The 5% worst throughputs of macro UEs are demonstrated in Fig.4.19. In the FR pattern, the 5% worst throughputs are less than those without relays in different RN numbers per cell, and the proposed scheme performs better than the ARP+CRS scheme. The reason of this situation is that all the UEs in the macro cell are fully

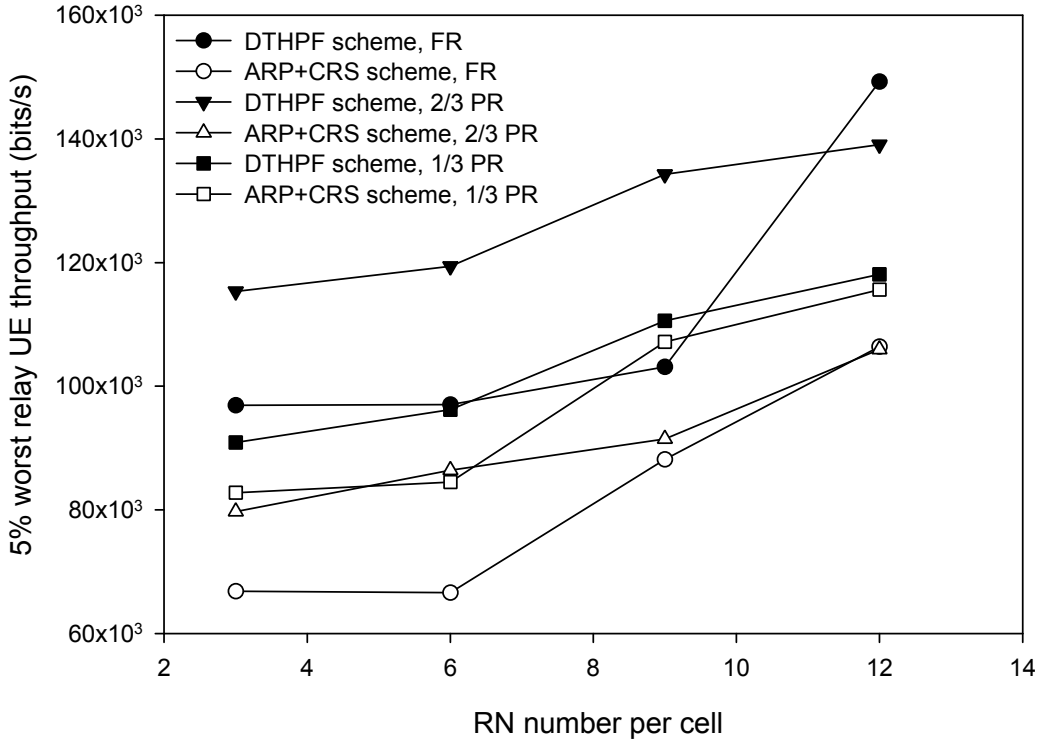

Figure 4.20: 5% worst relay UE throughput v.s. RN number per cell in the STH protocol

reusing all the PRBs in the access subframes, and thus are experiencing severe intra-cell interference from the eNB and the RNs. With alleviated intra-cell interference in the 2/3 PR pattern and 1/3 PR pattern, the 5% worst throughputs are larger than those in the single-hop networks without relays and those with the FR pattern. It can be observed that the difference between the proposed DTHPF scheme and the ARP+CRS scheme is the smallest with the 1/3 PR pattern.

Fig.4.20 depicts the 5% worst throughput of relay UEs against different RN numbers. The 5% worst throughputs increase with more RNs per cell. They increase slowly with the FR pattern. With more RNs in a cell, cell-edge UEs with bad channel conditions have more chances of choosing one of multiple RNs to improve their performance. However, with the FR pattern, increasing intra-cell interference caused by multiple RNs weakens the diversity gain of routing between multiple RNs. When the intra-cell interference decreases, the 5% worst throughputs using the ARP+CRS scheme are better with the 2/3 PR pattern and 1/3 PR pattern than with the FR pattern with small RN number per cell. Using the proposed scheme with 12 RNs per cell, the 5% worst throughput with the FR pattern is larger that that with the 2/3 PR pattern and the 1/3 PR pattern.

Table 4.3: The gains of the DTHPF scheme over the ARP+CRS scheme in the OTH protocol

		RN number per cell			
		3	6	9	12
FR	Macro UE GPF factor	0.012	0.021	0.019	0.0179
	Relay UE GPF factor	0.0939	0.0907	0.0684	0.0537
	Average Macro UE Throughput	0.00%	0.02%	-0.01%	0.02%
	Average Relay UE Throughput	0.00%	0.12%	-0.06%	0.05%
	5% worst Macro UE Throughput	4.03%	4.99%	2.33%	4.29%
	5% worst Relay UE Throughput	44.95%	45.62%	16.97%	40.27%
2/3 PR	Macro UE GPF factor	0.0081	0.0127	0.0102	0.0121
	Relay UE GPF factor	0.0674	0.0641	0.0435	0.0431
	Average Macro UE Throughput	-0.01%	-0.03%	0.01%	0.01%
	Average Relay UE Throughput	0.03%	-0.15%	0.05%	0.00%
	5% worst Macro UE Throughput	6.57%	7.69%	9.09%	3.64%
	5% worst Relay UE Throughput	44.68%	38.16%	46.81%	31.26%
1/3 PR	Macro UE GPF factor	0.0024	0.0051	0.0028	0.0021
	Relay UE GPF factor	0.0233	0.0318	0.0158	0.0109
	Average Macro UE Throughput	0.01%	0.01%	0.02%	0.00%
	Average Relay UE Throughput	0.13%	0.12%	0.06%	0.04%
	5% worst Macro UE Throughput	1.39%	2.56%	1.96%	1.27%
	5% worst Relay UE Throughput	9.85%	13.85%	3.18%	2.15%

Table 4.3 shows the gains of the DTHPF scheme over the ARP+CRS scheme in the STH protocol. From this table, it can be seen that although the average throughputs of macro UEs and relay UEs are almost the same using the proposed scheme and the benchmarking scheme, the UEs with 5% worst channel conditions can obtain up to around 45% more throughputs by using the proposed scheme compared with the benchmarking scheme.

4.6.4 Cumulative Distribution Function

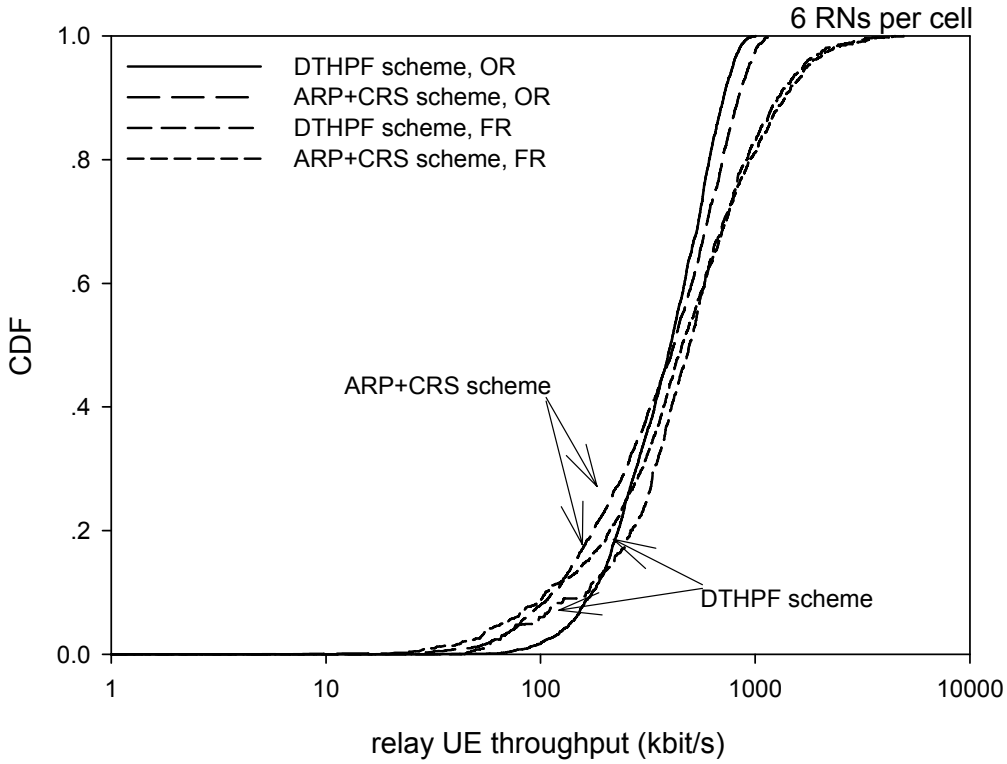

Figure 4.21: CDF of relay UE throughput

The Cumulative Distribution Functions (CDF) of relay UE throughputs with 6 RNs per cell in the OR pattern and the FR pattern are shown in Fig.4.21. For the 40% relay UEs with worst throughputs, they can achieve better throughputs in the proposed scheme. For the relay UEs with the top 20% throughput, the ARP+CRS scheme performs significantly better than the proposed scheme in the OR pattern, but has no advantage in the FR pattern.

4.6.5 Summary

In summary, the proposed DTHPF resource allocation scheme has better GPF factors and better 5% worst UE throughputs, for different RN numbers in all the reuse patterns. The performance of macro UEs with the OR pattern is better than that with the FR pattern, because extra intra-cell interference is generated by reusing the same PRB in direct links and access links with the FR pattern. However, the performance of relay UEs is better with the FR pattern than with the OR pattern. With less intra-cell interference and less resources for the access links with the 1/3 PR pattern, the performance is better than that for the FR pattern using the proposed scheme and the benchmark scheme. The performance gain achieved by the proposed DTHPF scheme compared to the benchmark ARP+CRS scheme is small. As the compromise between the FR pattern and the 1/3 PR pattern, the 2/3 PR pattern can achieve better performance and significant performance gain using the proposed scheme.

Since the proposed DTHPF resource allocation scheme considers the channel conditions of access links and backhaul links together, the UEs with bad channel conditions can have more opportunities to occupy the resources partitioned for the access links. Compared with the OTH protocol, the DTHPF resource allocation scheme has worse performance of the UEs with bad channel conditions in the STH protocol. This is because in the STH protocol, the two-hop resource scheduling is constrained by the resource number of backhaul links.

The two-hop resource scheduling and the adaptive resource partitioning in the proposed DTHPF resource allocation scheme will not request extra control channels in backhaul links. The proposed two-hop resource scheduling at the RNs needs the channel information of their backhaul links, which can be easily obtained and will consume few computation resources of the RNs.

4.7 Conclusion

The existing distributed PF resource allocation schemes, using the conventional single-hop PF scheduling algorithm at RNs, fail to ensure the two-hop end-to-end proportional fairness of relay UEs. This chapter proposes a distributed two-hop proportional fair (DTHPF) resource allocation scheme that can achieve better two-hop end-to-end proportional fairness in LTE-Advanced networks with Type I relay

nodes. The contributions in this chapter are that the GPF problem is formulated and decomposed into two related sub-problems, i.e., a resource partitioning sub-problem and a resource scheduling sub-problem; orthogonal and simultaneous two-hop transmission protocols are considered in solving the sub-problems; the existing adaptive resource partitioning algorithms are adjusted for LTE-Advanced networks; and two algorithms are proposed for two-hop resource scheduling subject to different resource partitioning constraints. The simulation results show that the proposed DTHPF resource allocation schemes have achieved better compromise between throughput and fairness.

Chapter 5

Two-Hop Adaptive Partial Frequency Reusing

5.1 Introduction

In this chapter, two-hop adaptive partial frequency reusing (APFR) in relay enhanced LTE-Advanced networks is studied. In the LTE-Advanced standards on relay node, access links of two-hop transmission are allowed to be allocated in the same subframes with direct links. There are three possible relations between the access links and the direct links. The time-frequency resources, i.e. PRBs, could be fully reused, partially reused or orthogonally shared by the access links and direct links, which can be marked as Full Frequency Reusing (FFR), Partial Frequency Reusing (PFR) and None Frequency Reusing (NFR). When the resources are fully reused, the maximum resources are utilised, but severe interference is generated; when the resources are orthogonally shared, better spectral efficiency can be obtained without interference, however the available resource numbers cannot increase. In order to make a trade-off between increasing available resource numbers and alleviating interference, PFR is considered for deciding a proper number of reused resources. In LTE-Advanced two-hop networks, the resource numbers of access links and direct links should be decided adaptively according to the number of relay UEs and direct UEs. Therefore, APFR is considered to avoid load imbalance and guarantee the fairness between relay UEs and direct UEs.

In what follows, the literature related to the method of determining the frequency reusing and reducing interference in the reused resources are firstly reviewed. Then,

proportional fairness is used as the performance metric of APFR, which can make an effective compromise between increasing throughput and guaranteeing fairness. Thus, the APFR problem for maximising proportional fairness is formulated as a Generalised Proportional Fairness (GPF) problem. After the route selection is determined for each UE, the GPF problem can be decomposed into a resource partitioning problem. By solving the resource partitioning problem, a near-optimal result of the reused PRB number for APFR can be achieved. In order to achieve better system performance, a proportional fair joint route selection and resource partitioning algorithm is proposed. Finally, the performance of the proposed APFR based algorithm and the benchmarking FFR based algorithm are evaluated and compared. The evaluation results show that the proposed APFR based algorithm can achieve both larger throughput and better fairness with different RN transmitting power and different RN distances than the benchmarking FFR based algorithm.

5.2 Related Work

Frequency reuse has been considered by many researchers in different approaches. Different frequency reuse schemes are designed for maximising the system performance with regard to different metrics. In the field of frequency reuse in two-hop cellular networks, recent contributions are introduced and reviewed briefly.

Three inter-cell frequency planning schemes are proposed in [105] together with a intra-cell resource partitioning solution. The proposed resource partitioning solution is based on the numbers and the channel quality of the UEs in each kind of link. The UE numbers are calculated according to the coverage of the eNB and the RN under a uniform distribution of UEs. Through this solution, the whole frequency band is orthogonally shared by the access links and the direct links in the same cell. For inter-cell interference coordination, partial frequency reuse is utilised in the proposed frequency planing schemes, including the cell partitioning based scheme, the virtual-sector based scheme and the virtual-sector enhanced cell-partitioning based scheme. Furthermore, more stringent constraints of resource partitioning are imposed by the cell partitioning method for interference mitigation. The simulation results prove their advantages in providing better performance with channel-dependent resource partitioning. However, the same frequency band is reused in each cell, and the None Frequency Reusing (NFR) is considered in the intra-cell resource partitioning.

In [106], a soft frequency reuse scheme based on power control is proposed in

order to mitigate the interference between adjacent sectors. Any sector can reuse all the resources of the neighbouring sectors to achieve a frequency reuse factor of 1. The direct UEs and relay UEs share the resources orthogonally. Three sectors in adjacent cells constitute a virtual cell. The transmitting power of eNBs and RNs is adjusted to meet the Signal-to-Interference-Ratio (SIR)-balance principle in the virtual cells. Besides, the resource allocation is based on the UE distribution and their target throughput.

In [107], a modified fractional frequency partitioning scheme is proposed for inter-cell interference coordination in relay enhanced cellular networks. Compared with the traditional fractional frequency reuse scheme without relays, the resources for the cell edge are assigned to the RNs. In order to maximise proportional fairness, the numbers of the resources allocated to the eNB and the RNs are proportional to the dynamic traffic load of the eNB and the RNs respectively. Both centralised and distributed approaches are proposed to achieve load balancing. The proposed scheme can provide better performance compared with the static resource partitioning. However, the frequency resources are not reused within the same cell.

Researches in [105, 106, 107] focus on applying adaptive partial frequency reuse in inter-cell interference coordination.

Path selection rules with different frequency reuse patterns and frame transmission patterns are investigated in [53]. The proposed path selection rules in [53] consider the spectral efficiencies of access links and backhaul links. When more than two RNs are deployed and they are reusing the same resources, the effective spectral efficiencies of access links are multiplied by the number of RNs and then divided by the reuse factor. Simulation results not only provide an insight into the appropriate RN distance, frequency reuse factors and frame transmission patterns, but also prove that the proposed path selection rules are better than traditional path selection rules. However, the calculation of effective spectral efficiency is based on an equal UE distribution and static resource partitioning.

In [108], the spectral efficiency in the downlink of cellular relay networks is analysed with opportunistic scheduling and spectrum reuse. The analysed spectral efficiency is validated by a framework based on extreme-value theory and a system-level simulation. Hence, this study provides an insight into the possible performance enhancements from multi-hop transmission and frequency reuse with opportunistic scheduling. The simulation results show that simultaneous transmission protocols can achieve significantly better spectral efficiency than the orthogonal transmission

protocols. However, fair resource partitioning between eNB and RN is not considered. As the authors also suggest, relay-related frequency reuse policies should be generalised by incorporating fractional frequency reuse techniques.

The problems of resource partitioning in orthogonal sharing and co-channel reusing are considered in [109]. In both scenarios, one subframe is divided into two equal time slots. The resource configuration scheme proposed in [109] is aimed at achieving two principles. One is to ensure allocation fairness among the UEs across the whole cell, not only the direct UEs served by the macro eNB but also the relay UEs attached to the RNs. The other principle is to guarantee the same throughput in the access links and corresponding backhaul links. By estimating the coverage area of the macro eNB and the expectation values of SINR in different positions, the system spectrum efficiency can be calculated. In the simulations, the system performance is evaluated with different path loss factors and eNB coverage areas along different RN positions. The co-channel reusing scenario is recommended by the authors.

Paper [101] focuses on allocating resources between access links, backhaul links and direct links in order to obtain a better compromise between fairness and throughput. In this paper, the access links can reuse all the resources of direct links in the backhaul subframes. The authors formulate the resource allocation problem as the GPF problem. Aimed at achieving the GPF objective, i.e. maximising the sum logarithmic UE data rate, the GPF resource allocation problem is divided into two steps: resource partitioning and resource scheduling. This paper proposes an adaptive proportional fair resource partitioning algorithm. This algorithm calculates the resources of backhaul links and direct links as directly proportional to the number of UEs served by the eNB and the RNs, unless the resource numbers of access links exceed the resource number of direct links. However, interference between access links and direct links is not considered. Increasing the number of resources for the access links will increase the interference of the direct links and thus decrease the performance of direct UEs. In [102], a proportional fair based routing algorithm is proposed jointly with an adaptive resource partitioning algorithm. The proposed routing algorithm considers both the received signal quality and the number of resources assigned to the UEs.

In [53, 101, 102, 108, 109], the performance with different intra-cell frequency reuse scenarios is studied. The performance evaluations using full frequency reuse and no frequency reuse have been given and their results are discussed. However, intra-cell fractional frequency reuse is not investigated adequately.

[98] proposes a Load-Balancing Opportunistic (LoBO) scheduling algorithm that improves the overall system throughput in a weighted proportional fairness manner. At the same time, the traffic loads are balanced among the access links of all RNs. The main contribution of [98] is the proposal of an effective subframe division algorithm to determine the boundaries of access subframes and backhaul subframes as part of opportunistic resource allocation. The concept of Resource Allocation Gap (RAG) is introduced in order to represent the overall resource waste in the access subframes. The RAG is used as the inverse weighting factor in the proportional fair scheduling. In this way, the proposed LoBO scheduling algorithm is aimed at reducing resource waste. A system evaluation demonstrates a 30% gain compared with a conventional proportional fair scheduling algorithm in [17] with fixed subframe division. Although adaptive resource reuse between the direct links and the access links is considered, the intra-cell interference is not discussed or quantified. The interference will influence the system performance significantly.

A low-complexity joint sub-carrier allocation, scheduling and power control scheme is proposed in [71] by considering potential interference among neighbouring cells. The joint resource allocation problem is solved by decomposing it into two stages. In the first stage, subcarrier scheduling is conducted by a local search. In the second stage, power is allocated for all of the scheduled subcarriers. By leveraging geometric programming, the authors prove that optimal power control can be achieved in the high SIR region. Simulation results show that by utilizing the proposed joint resource allocation scheme, the aggregated throughput of OFDMA-based relay networks can be improved. However, partial frequency reuse is not considered.

In [110], an optimal two-hop resource allocation scheme is proposed in order to maximise the system throughput under max-min fairness constraints. This scheme is compared with two well-known schemes [108], the orthogonal two-hop scheme and the overlapped two-hop scheme. The authors formulate the optimisation problem for each scheme, and solve it by using linear programming. The results show that high cell throughput can be achieved by the proposed optimal scheme, while guaranteeing fairness and low outages. However, the complexity of the proposed scheme is higher than the benchmarking schemes in [108], and route selection and resource partitioning are not considered.

In [78], a time-domain resource scheduling algorithm with reuse in access subframes is proposed. Based on the proposed scheduling algorithm without reuse, subsets of UEs containing at most one of the UEs associated with each RNs are considered. Then, the UE relay hop weighted flow is translated into an equivalent

weighted flow of the subsets for reuse. Hence, the scheduling problem with reuse is transformed into a generic scheduling problem without reuse. Further, in the downlink, the authors consider subsets of RNs instead of the subsets of UEs in order to get a low- complexity scheduling algorithm. The algorithms in this paper should be run for many iterations, and the scenario that the access links and the direct links are reusing the same resources is not considered.

[111] addresses the problem of interference coordination in relay-aided cellular OFDMA systems, aimed at exploiting the benefits of RNs while alleviating interference. The authors propose an Integrated Interference Coordination Scheme (IICS) for relay enhanced OFDMA systems. The IICS is composed of two phases. Each of the two phases executes a specific resource assignment algorithm, namely Semi-Static Allocation Algorithm (SSAA) and Dynamic Allocation Algorithm (DAA). When the offered load is not very heavy, the low-complexity SSAA is used to allocate orthogonal resources to UEs served by the eNB and the RNs. When the traffic load is heavy, DAA is used for more efficient resource scheduling and more resource reuse. The basic idea of SSAA is to guarantee one resource block for each UE, and to allocate more resources to the UEs with low interference level. The DAA assigns the UEs to individual clusters using a graph method. The UEs in a cluster can reuse the same resource blocks with low interference. The resource blocks can by utilised more efficiently by the DAA. The simulation results show that the proposed IICS scheme can obtain improved system throughputs compared with resource allocation schemes without adequate interference coordination.

In [112], a Pre-Configuration Algorithm (PCA) is added to the SSAA and DAA to form a resource allocation with interference coordination scheme. PCA is used when the traffic load is light and there are enough orthogonal resource blocks for the UEs. The interference level can be reduced by PCA.

[113] proposes a game-theoretic framework called the Interference Coordination Game (ICG) in order to further address the same problem in [111] and [112]. The ICG is decomposed into two sub-games, the Resource Block Assignment Game (RBAG) and the Power Allocation Game (PAG). RBAG allocates resource blocks with alleviated interference. Furthermore, PAG is based on resource block assignment for further reducing interference and improving system pay-off. In [113], the existence and uniqueness of a Nash Equilibrium in ICG is proven. Simulation results show that the proposed framework can guarantee the Nash Equilibrium of ICG. Compared with the fractional reuse scheme and the scheme without interference coordination, better SINR and higher system throughput can be achieved.

In [71, 78, 98, 110, 111, 112, 113], centralised resource allocation algorithms are proposed in order to achieve better performance under the adaptive partial frequency reuse. However, these algorithms require many iterations and have high complexity.

In [88], the access links fully reuse the resources of direct links in the access subframes. In the backhaul subframes, the resources used by the direct links and backhaul links are orthogonal. The direct UEs with the worst channel quality may be scheduled in the backhaul subframes in order to avoid severe interference from the RNs. However, it can reduce the reuse efficiency and potentially decrease the system throughput. In this paper, the authors propose a simple resource partitioning algorithm to maximise the throughput while guaranteeing the minimum throughput for each UE. However, the degree of interference between direct links and access links is not considered in the resource partitioning problem. In addition, the routing problem affected by the proposed resource partitioning algorithm is not studied.

The authors in [114] propose an interference coordination strategy to mitigate the intra-cell co-channel interference between the RNs and the eNB. The concept of an interference zone is introduced in this paper. In the interference zones, the interference level from some serving nodes is within a small range from the received signal level. Otherwise, the UEs are in the non-interference zone. Based on the centralised approach, two variants of resource partitioning algorithm are considered. In Variant I, the fractional frequency reuse method is used. Using this method, the UEs in the interference zones are assigned orthogonal resources. In Variant II, the resources for the interference zones are reused by the UEs in the non-interference zone. The number of resources assigned to the interference zones and the non-interference zones are determined by a per-zone resource partitioning algorithm based on the UE numbers.

In [115], the resource partitioning problem for fractional frequency reuse, i.e. PFR, is studied. A Cell-colouring based Distributed Frequency Allocation (C-DFA) method is described. The C-DFA in cellular networks can easily turn the resource partitioning problem based on PFR in relay enhanced cellular networks into a distributed scheme without considering inter-cell interference. To validate the C-DFA, a Dynamic Fractional Frequency Allocation (DDFFA) algorithm is proposed for the relay enhanced OFDMA networks with two steps, channel grouping and channel borrowing. Simulation results show that better system throughput can be achieved by the DDFFA algorithm. The limitation of C-DFA and DDFFA is also discussed. The distributed planar graph colouring algorithm cannot guarantee different colours for neighbouring cells. Thus, severe inter-cell interference may happen to force the DDFFA to increase computation and inter-node signal exchange.

In [116] and [117], a new frequency reuse scheme for heterogeneous networks is proposed in addition a non-reuse scheme, a full-reuse scheme and a partial-reuse scheme. The UEs which have low or medium SINR and experience main interference from intra cell are indicated as the reserved UEs. Some resources are allocated to these UEs in proportion to the number of UEs without reuse. The remaining UEs can reuse the same resources. Using the frequency reservation method, the intra-cell interference can be reduced by 50% in theory. The simulation results show that better system capacity and cell-edge SINR can be achieved with this scheme. However, fairness between UEs in the macro cell is not considered and an effective compromise between throughput and fairness cannot be guaranteed.

In [118], a novel fractional frequency reuse scheme, i.e. PFR, is proposed based on a no frequency reuse (NFR) scheme with interference coordination. In the NFR scheme similar to [106], the eNB and the RNs in the same sector share the whole frequency band, and the RNs in adjacent sectors use different frequency bands. In the PFR scheme, the eNB can reuse part of the resources assigned to the RNs to obtain more resources for direct links. Based on the proposed PFR scheme, a load balancing algorithm is proposed. When the eNB is overloaded, some direct UEs can reuse part of the resources assigned to the relay UEs with lower transmitting power. When the RNs are overloaded, some relay UEs are handed over to the eNB in the same cell. Moreover, the scheduling algorithm is revised to ensure the outer zone UEs have priority to obtain resources.

In [119], a novel two-hop frequency reuse method is discussed with proportional fairness consideration and cooperative relaying. Some resources are reused by the eNB and the RNs for cooperative transmission to some UEs. Cooperative transmission can improve the spectral efficiency, which can be considered as another form of increasing the number of resources. The RNs need to decide whether their UEs are served independently or cooperatively with the eNB. The authors formulate the resource allocation problem as an optimisation problem. By solving this problem, an asymptotically optimal solution is derived to allocate resources among the cooperative transmission UEs and the UEs independently served by the eNB and the RNs. However, this paper doesn't provide a method of determining the cooperative UEs.

In [114, 115, 116, 117, 118, 119], the adaptive partial frequency reuse is realised by deciding which UEs can occupy reused resources and which UEs can use non-reused resources. The methods of determination are the interference-zone in [114], the channel grouping and borrowing in [115, 118], the frequency reservation in [116, 117]

and cooperative transmission in [119]. However, the degree of interference between direct links and access links is not considered and the metrics of determination is not a value based on the current networks.

5.3 System Model

In this thesis, the downlink transmission in a LTE-Advanced network with Type I relay nodes is considered. In the cell of interest, a donor eNB is deployed in a centre with three sectors, while single or multiple RNs are located on the fringe of each sector. In this study, the single RN scenario is considered for analytical simplicity, though the analysis can be readily extended to multi-RN scenarios. Randomly distributed UEs $\mathcal{M}$ are either served by the donor eNB directly or connected the RN using two-hop transmission. The UEs served by the eNB are direct UEs $\mathcal{M}_d$, and the UEs served by the RN are relay UEs $\mathcal{M}_r$. There are $|\mathcal{M}_d|$ direct UEs and $|\mathcal{M}_r|$ relay UEs. Note that, $|\bullet|$ means the cardinality of a set. The transmission between the eNB and the direct UEs is called direct links, the transmission between the eNB and the subscribed RNs is represented as backhaul links and the transmission between the RNs and their associated relay UEs is named as access links.

A radio frame is divided into backhaul subframes and access subframes. In the backhaul subframes, the resources are assigned to the backhaul links first, and the rest of the resources are allocated to the direct UEs. In the access subframes, the resources are partly reused by the direct links and the access links, and there are some resources only occupied by direct UEs. In the reused resources, the average data rate per PRB of a direct link in the presence of interference from RNs is denoted as $\bar{E}_{d,m}^{w/i}$. In the non-reused resources, the average data rate per PRB of a direct link in the absence of interference from RNs is represented as $\bar{E}_{d,m}^{w/oi}$, and the average data rate per PRB of an access link can be expressed as $\bar{E}_{r,m}$. The PRB number of the access subframes is N_a, including the number of reused PRBs denoted as $N^{w/i}$ and the number of non-reused PRBs as $N^{w/oi}$.

$$N_a = N^{w/i} + N^{w/oi} \tag{5.1}$$

5.4 Generalised Proportional Fairness (GPF) Problem Formulation

In this thesis, how to maximise the proportional fairness with adaptive PFR (PF-APFR) can be formulated as a generalised proportional fair (GPF) problem. The objective of this GPF problem is to maximise the utility of the sum of the logarithmic data rates as:

$$\max \sum_{m \in \mathcal{M}_d \cap \mathcal{M}_r} \log R_m = \max(\sum_{m \in \mathcal{M}_d} \log R_{d,m} + \sum_{m \in \mathcal{M}_r} \log R_{r,m}) \tag{5.2}$$

where $R_{d,m}$ and $R_{r,m}$ are denoted as the data rate of a direct UE and the data rate of a relay UE.

By assuming that a Proportional Fair (PF) based scheduling algorithm is utilised for direct UEs and relay UEs, each of them has a fixed scheduling gain over the Round-Robin scheduling algorithm, according to the findings in [31, 58]. Therefore, the data rates of UEs can be simplified into the values only related to the resource number and the average spectral efficiency. Considering the reused resources and the non-reused resources occupied by the direct UEs, the data rate of each direct UE can be expressed as:

$$R_{d,m} = (\frac{N^{w/oi}}{|\mathcal{M}_d|} \bar{E}^{w/oi}_{d,m} + \frac{N^{w/i}}{|\mathcal{M}_d|} \bar{E}^{w/i}_{d,m}) G_d(|\mathcal{M}_d|) \tag{5.3}$$

where $G_d(|\mathcal{M}_d|)$ indicates the gain of the PF scheduling algorithm over Round-Robin scheduling algorithm, which is related to the number of the scheduled UEs; $\bar{E}^{w/oi}_{d,m}$ and $N^{w/oi}$ denote the average data rate per PRB without reusing and the non-reused PRB number respectively; $\bar{E}^{w/i}_{d,m}$ and $N^{w/i}$ represent the average data rate per reused PRB and the number of reused PRBs separately. Since the relay UEs only occupy reused resources, their data rates can be expressed as:

$$R_{r,m} = \frac{N^{w/i}}{|\mathcal{M}_r|} \bar{E}_{r,m} G_r(|\mathcal{M}_r|) \tag{5.4}$$

Since the data rates of relay UEs should also be transmitted in the backhaul links, the backhaul PRB numbers used by these relay UEs can be calculated as:

$$N^b = \frac{\sum_{m \in \mathcal{M}_r} R_{r,m}}{E_{r,0}} = N^{w/i} \frac{\sum_{m \in \mathcal{M}_r} \bar{E}_{r,m}}{|\mathcal{M}_r| E_{r,0}} G_r(|\mathcal{M}_r|) = N^{w/i} \theta \tag{5.5}$$

where $E_{r,0}$ denotes the average data rate per PRB in the backhaul link between the RN r and the donor eNB, and θ represents the backhaul-to-access ratio, which is defined as

$$\theta = \frac{\sum_{m \in \mathcal{M}_r} \bar{E}_{r,m}}{|\mathcal{M}_r| E_{r,0}} G_r(|\mathcal{M}_r|) \tag{5.6}$$

By substituting (5.3) and (5.4) into (5.2), the GPF problem can be rewritten as:

$$\begin{aligned} \max\{ & |\mathcal{M}_r| \log N^{w/i} + \sum_{m \in \mathcal{M}_r} \log \frac{G_r(|\mathcal{M}_r|) \bar{E}_{r,m}}{|\mathcal{M}_r|} \\ & + \sum_{m \in \mathcal{M}_d} \log(N^{w/i} + N^{w/oi} \frac{\bar{E}^{w/i}_{d,m}}{\bar{E}^{w/oi}_{d,m}}) + \sum_{m \in \mathcal{M}_d} \log \frac{G_d(|\mathcal{M}_d|) \bar{E}^{w/oi}_{d,m}}{|\mathcal{M}_d|} \} \end{aligned} \tag{5.7}$$

After all the UEs have selected their serving nodes, their average data rates per PRB can be measured. Thus, the GPF problem can be transformed into the problem of determining an optimal PRB number for each set of links. Since the sum of PRBs for different usages is a constant value N, this is also a resource partitioning problem. The resource partitioning problem for PF-APFR can be described as

$$\begin{aligned} & \max U(N^{w/i}) \\ = & \max\{|\mathcal{M}_r| \log N^{w/i} + \sum_{m \in \mathcal{M}_d} \log(N^{w/oi} + N^{w/i} \frac{\bar{E}^{w/i}_{d,m}}{\bar{E}^{w/oi}_{d,m}})\} \\ s.t. \ & N^{w/i} + N^{w/oi} + N^b = N \end{aligned} \tag{5.8}$$

5.5 Proportional Fair Joint Route Selection and Resource Partitioning Algorithm for APFR

5.5.1 A Near-Optimal Resource Partitioning Algorithm

In order to solve the resource partitioning problem for PF-APFR, the method of Lagrange multiplier is utilised. The Lagrange function of the problem (5.8) is given

as

$$\begin{aligned} L(N^{w/i}, N^{w/oi}, \lambda) =& |\mathcal{M}_r| \log N^{w/i} + \sum_{m \in \mathcal{M}_d} \log(N^{w/oi} + N^{w/i} \frac{\bar{E}_{d,m}^{w/i}}{\bar{E}_{d,m}^{w/oi}}) \\ &+ \lambda(N^{w/i} + N^{w/oi} + N_b - N) \\ =& |\mathcal{M}_r| \log N^{w/i} + \sum_{m \in \mathcal{M}_d} \log(N^{w/oi} + N^{w/i} \frac{\bar{E}_{d,m}^{w/i}}{\bar{E}_{d,m}^{w/oi}}) \\ &+ \lambda(N^{w/i} + N^{w/oi} + N^{w/i}\theta - N) \end{aligned} \tag{5.9}$$

The gradients of the Lagrange function with respect to $N^{w/i}$ and $N^{w/oi}$ can be obtained respectively as

$$\frac{\partial L(N^{w/i}, N^{w/oi}, \lambda)}{\partial N^{w/i}} = \frac{|\mathcal{M}_r|}{N^{w/i}} + \sum_{m \in \mathcal{M}_d} \frac{\frac{\bar{E}_{d,m}^{w/i}}{\bar{E}_{d,m}^{w/oi}}}{N^{w/oi} + N^{w/i} \frac{\bar{E}_{d,m}^{w/i}}{\bar{E}_{d,m}^{w/oi}}} + \lambda(1+\theta) \tag{5.10}$$

$$\frac{\partial L(N^{w/i}, N^{w/oi}, \lambda)}{\partial N^{w/oi}} = \sum_{m \in \mathcal{M}_d} \frac{1}{N^{w/oi} + N^{w/i} \frac{\bar{E}_{d,m}^{w/i}}{\bar{E}_{d,m}^{w/oi}}} + \lambda \tag{5.11}$$

By setting the gradients in (5.10) and (5.11) equal to 0, the following equations can be derived.

$$\frac{|\mathcal{M}_r|}{N^{w/i}} + \sum_{m \in \mathcal{M}_d} \frac{\frac{\bar{E}_{d,m}^{w/i}}{\bar{E}_{d,m}^{w/oi}}}{N^{w/oi} + N^{w/i} \frac{\bar{E}_{d,m}^{w/i}}{\bar{E}_{d,m}^{w/oi}}} = (1+\theta) \sum_{m \in \mathcal{M}_d} \frac{1}{N^{w/oi} + N^{w/i} \frac{\bar{E}_{d,m}^{w/i}}{\bar{E}_{d,m}^{w/oi}}} \tag{5.12}$$

$$|\mathcal{M}_r| = \sum_{m \in \mathcal{M}_d} \frac{1 + \theta - \frac{\bar{E}_{d,m}^{w/i}}{\bar{E}_{d,m}^{w/oi}}}{\frac{N^{w/oi}}{N^{w/i}} + \frac{\bar{E}_{d,m}^{w/i}}{\bar{E}_{d,m}^{w/oi}}} \tag{5.13}$$

The value range of $\frac{N^{w/oi}}{N^{w/i}}$ is between 0 and positive infinity, and the value of

$\frac{\bar{E}_{d,m}^{w/i}}{\bar{E}_{d,m}^{w/oi}}$ is between 0 and 1. It can be proven that in the case that the number of direct UEs is larger than the relay UE number, there is always a value of $\frac{N^{w/oi}}{N^{w/i}}$ to satisfy the equation (5.13). Hereafter, a near-optimal resource partitioning, $N^{w/i}$, N_b and N_a, can be obtained.

For different direct UEs, $\frac{\bar{E}_{d,m}^{w/i}}{\bar{E}_{d,m}^{w/oi}}$ has different values, reflecting different degrees of interference. It can be readily observed that the optimal value of $\frac{N^{w/oi}}{N^{w/i}}$ cannot be directly calculated through equation (5.13). Besides, it can also be seen that with larger $\frac{\bar{E}_{d,m}^{w/i}}{\bar{E}_{d,m}^{w/oi}}$, the right side of equation (5.13) becomes smaller, and the ratio $\frac{N^{w/oi}}{N^{w/i}}$ should be smaller to hold the balance of the equation.

In general, the distribution of $\frac{\bar{E}_{d,m}^{w/i}}{\bar{E}_{d,m}^{w/oi}}$ cannot be estimated. By intentionally designing $\frac{\bar{E}_{d,m}^{w/i}}{\bar{E}_{d,m}^{w/oi}}$, no frequency reuse (NFR) and full frequency reuse (FFR) can be generated as two special situations of APFR.

No frequency reuse the NFR situation indicates a situation that all the direct UEs have $\frac{\bar{E}_{d,m}^{w/i}}{\bar{E}_{d,m}^{w/oi}} = 0$. It always implies the case that PRBs in the access subframes are not reused by the direct links and the access links, but shared orthogonally.

The resource partitioning of NFR has been discussed in [54]. Through equation (5.13), $\frac{N^{w/oi}}{N^{w/i}}$ can be derived as

$$\frac{N^{w/oi}}{N^{w/i}} = (1+\theta)\frac{|\mathcal{M}_d|}{|\mathcal{M}_r|} \tag{5.14}$$

After several steps of calculation, the optimal resource partitioning can be obtained

as

$$N^{w/i} = \frac{1}{1+\theta}\frac{|\mathcal{M}_r|}{|\mathcal{M}|}N \tag{5.15}$$

$$N_b = \frac{\theta}{1+\theta}\frac{|\mathcal{M}_r|}{|\mathcal{M}|}N \tag{5.16}$$

$$N^{w/oi} = \frac{|\mathcal{M}_d|}{|\mathcal{M}|}N \tag{5.17}$$

$$\tag{5.18}$$

where $N^{w/oi}$ represents the PRB number occupied only by the direct UEs, and $N^{w/i}$ is the the PRB number occupied only by the relay UEs in the access links.

Full frequency reuse the FFR situation denotes a situation that all the PRBs in the access subframes are reused by the direct links and the access links. However, the throughput balance between access links and backhaul links is not considered. It also suggests a case that all the direct UEs are not impacted by the interference from the relay UEs in different PRBs. In both situations, $\frac{\bar{E}^{w/i}_{d,m}}{\bar{E}^{w/oi}_{d,m}} = 1$ for every direct UE.

The resource partitioning in this situation has been discussed in [102]. Through equation (5.13), $\frac{N^{w/oi}}{N^{w/i}}$ can be derived as

$$\frac{N^{w/oi}}{N^{w/i}} = \theta\frac{|\mathcal{M}_d|}{|\mathcal{M}_r|} - 1 \tag{5.19}$$

After several steps of calculation, the optimal resource partitioning can be obtained as

$$N^{w/i} = \frac{1}{\theta}\frac{|\mathcal{M}_r|}{|\mathcal{M}|}N \tag{5.20}$$

$$N_b = \frac{|\mathcal{M}_r|}{|\mathcal{M}|}N \tag{5.21}$$

$$N_a = \frac{|\mathcal{M}_d|}{|\mathcal{M}|}N \tag{5.22}$$

where N_a represents the number of PRBs occupied by the direct UEs, and $N^{w/i}$ is the number of PRBs occupied by the relay UEs in the access links.

Since N_a should be no less than $N^{w/i}$, the following inequality can be given.

$$|\mathcal{M}_d| \geq \frac{|\mathcal{M}_r|}{\theta} \tag{5.23}$$

Proposed Algorithm In the FFR situation, the largest values of $\frac{\bar{E}_{d,m}^{w/i}}{\bar{E}_{d,m}^{w/oi}}$ are considered for all direct UEs. Thus, the largest ratio of $\frac{N^{w/oi}}{N^{w/i}}$ can be obtained. Using this initial ratio, a resource partitioning algorithm for PF-APFR is proposed to decide the integrated values of $N^{w/i}$, N_b and N_a. A near-optimal value of $\frac{N^{w/oi}}{N^{w/i}}$ satisfying equation (5.13) can also be achieved.

Algorithm 2 A resource partitioning algorithm for PF-APFR

Input: $|\mathcal{M}_r|$, $|\mathcal{M}_d|$: the numbers of relay UEs and direct UEs; θ : the backhaul-to-access ratio; $\frac{\bar{E}_{d,m}^{w/i}}{\bar{E}_{d,m}^{w/oi}}$: the ratio of the data rate per non-reused PRB to the data rate per reused PRB of each direct UE $\forall m \in \mathcal{M}_d$

Output: $N^{w/i}$, N_b and N_a

1: Initialise $N^{w/i} = \lceil \frac{1}{\theta} \frac{|\mathcal{M}_r|}{|\mathcal{M}|} N \rceil$
2: **repeat**
3: $N^{w/i} = N^{w/i} - 1$;
4: Calculate $N_a = \lceil N - \theta N^{w/i} \rceil$;
5: Calculate $N^{w/oi} = N_a - N^{w/i}$;
6: **for all** $m \in \mathcal{M}_d$ **do**
7: Calculate $temp1$ according to equation (5.13);
8: **end for**
9: **until** $temp1 \leq |\mathcal{M}_r|$, or $N^{w/i} \leq \frac{1}{1+\theta} \frac{|\mathcal{M}_r|}{|\mathcal{M}|} N$
10: **return** $N^{w/i}$; $N_a = \lceil N - \theta N^{w/i} \rceil$; $N_b = N - N_a$

Complexity analysis The complexity of this algorithm is based on the number of possible integrated values of $N^{w/i}$. Ranging from $\frac{1}{1+\theta} \frac{|\mathcal{M}_r|}{|\mathcal{M}|} N$ to $\frac{1}{\theta} \frac{|\mathcal{M}_r|}{|\mathcal{M}|} N$, there are $\frac{1}{\theta+\theta^2} \frac{|\mathcal{M}_r|}{|\mathcal{M}|} N$ possible integrated values for $N^{w/i}$. As the calculation of $temp1$ based on equation (5.13) needs $|\mathcal{M}_d|$ times the basic operations, the complexity of Algorithm 2 is $\mathcal{O}(\frac{|\mathcal{M}_d|}{\theta^2} \frac{|\mathcal{M}_r|}{|\mathcal{M}|} N)$.

5.5.2 A Route Selection Algorithm for PF-APFR

According to what is shown in equation (5.13), the resource partitioning for PF-APFR is related to the number of UEs, e.g., $|\mathcal{M}_d|$ and $|\mathcal{M}_r|$, and the spectral efficiency of direct UE $E_{d,m}$, which are decided by route selection. Therefore, the joint processing of route selection and resource partitioning can improve the proportional fairness further.

Assume that new coming UEs arrive one at a time. Firstly, for each new UE m, a sector with an eNB and a RN is selected according to received signal power. There are two routes to be further chosen, either a direct route to the eNB or a relay route via an RN to the eNB. Secondly, the resource partitioning results of choosing these two routes can be calculated through the proposed resource partitioning algorithms. By substituting the resource partitioning results into equation (5.8), the possible utility of choosing either of the routes can be obtained. Finally, after the comparison between these two candidate routes, the route with larger possible utility is selected. The detail of the route selection algorithm for PF-APFR is described below

Algorithm 3 A route selection algorithm for PF-APFR

Input: $P_{m,k}, \forall m \in \mathcal{M}, \forall k \in \mathcal{K}$: the received signal power of UE m in $\mathcal{M}$ from sector k in $\mathcal{K}$; $|\mathcal{M}_r|$, $|\mathcal{M}_d|$: the current numbers of relay UEs and direct UEs; θ : the backhaul-to-access ratio; $\frac{\bar{E}^{w/i}_{d,m}}{\bar{E}^{w/oi}_{d,m}}$: the ratio of the data rate per non-reused PRB to the data rate per reused PRB of each direct UE $\forall m \in \mathcal{M}_d$

Output: k : the selected sector; s : the selected route, either the eNB d or the RN r

1: For a new arriving UE m,
2: $k = \arg\max_{\mathcal{K}} P_{m,k}$;
3: Update $\mathcal{M}_r = \{\mathcal{M}_r, m\}$;
4: Calculate $N^{w/i}$, N_a and N_b using Algorithm 2;
5: Calculate U_r using equation (5.8);
6: Update $\mathcal{M}_d = \{\mathcal{M}_d, m\}$;
7: Calculate $N^{w/i}$, N_a and N_b using Algorithm 2;
8: Calculate U_d using equation (5.8);
9: $s = \arg\max(U_r, U_d)$;
10: **return** k; s.

The complexity of the proposed route selection algorithm is the number of UEs times the sum of the number of sectors plus the complexity of the proposed resource partitioning algorithm, which can be depicted as $\mathcal{O}(|\mathcal{M}| \times (|\mathcal{K}| + \frac{|\mathcal{M}_d|}{\theta^2}\frac{|\mathcal{M}_r|}{|\mathcal{M}|}N))$.

5.6 Performance Evaluation

5.6.1 Simulation Parameters

According to the LTE self-evaluation methodology [14], a semi-static system-level Matlab simulation platform is developed to evaluate downlink performance. Using the wrap-around technique, seven 3-sectored macro cells are generated with fixed numbers of UEs randomly dropped in them. In each cell, a fixed number of RNs are located at the cell edge with the same distance from the eNB. The details of the simulation parameters are listed in Table 5.1.

Table 5.1: Simulation parameters

Parameters	Values
Carrier/Bandwidth	2GHz /FDD 10MHz
Subframe number	10/radio frame
PRB number	50/subframe
UE number	30/sector
Inter-site distance	500 m
Transmitting power	eNB: 46 dBm RN: 30 dBm
Antenna configuration	eNB: 14 dBi, 70 directional RN: 5 dBi, omni UE: 0 dBi, omni
Thermal noise density	-174 dBm/Hz
Noise figure	9 dB at UE, 5 dB at RN
Channel model	3GPP case 1 for relay [14]
Shadowing standard deviations	Log-normal distribution eNB-RN: 6 dB eNB-UE: 8 dB RN-UE: 10 dB
Fast fading model	SUI-5 channel [104]
Traffic model	Full buffer
AMC scheme	15 levels according to [59]

In this simulation, the network topology considers single-RN scenarios, which is illustrated in Fig. 5.1. In each sector, there is one RN located at the bore sight towards the adjacent eNB. The Inter-Site Distance (ISD) between two adjacent

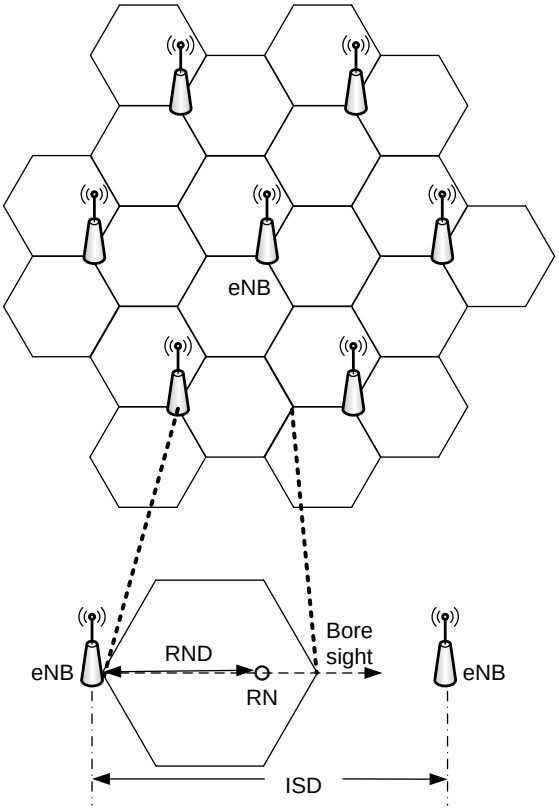

Figure 5.1: Cellular network layout with one RN

eNBs is 500 meters. The RN Distances (RNDs) from the central eNB in the same sector are the ISD multiplied by different values in this thesis. Different RNDs may impact the performance comparison. In addition, the performance with different RN transmitting power will be evaluated as well.

The joint route selection and resource partitioning algorithm proposed in this chapter is based on the analysis of APFR, called "APFR based alg." in the simulation results. Chosen as the benchmarking scheme, the route selection and resource partitioning scheme given in [102] is based on the scenario of Full Frequency Reuse (FFR), called "FFR based alg.". In addition, the simulation results of the LTE-Advanced networks without relays are also shown.

In this simulation, the downlink performance of all the UEs in the macro cell is evaluated. The performance of the relay UEs attached to the RNs are also assessed. Macro UEs are defined as the UEs in the macro cell, including the direct UEs and the relay UEs in the same macro cell. The metrics of the evaluation include the GPF factor, the average UE throughput, the 5% worst UE throughput and Jain's fairness [120]. Besides the GPF factor showing the effectiveness of the solutions to the GPF problem in equation (4.4), it is a commonly used metric [31] to show the

trade-off between average throughput and fairness, which is expressed as:

$$GPF\ factor = \frac{1}{|\mathcal{M}|} \sum_{m \in \mathcal{M}} \log R_m \tag{5.24}$$

Jain's fairness index proposed in [120] is also a quantitative measure of fairness for resource allocation, which can identify the proportion of under-allocation. Jain's fairness of n users with x_i throughput is described as:

$$\mathcal{J}(x_1, x_2, \ldots, x_n) = \frac{(\sum_{i=1}^{n} x_i)^2}{n \cdot \sum_{i=1}^{n} x_i^2} \tag{5.25}$$

The 5% worst UE throughput is the largest throughput of the 5% UEs with the worst throughputs, as defined in 3GPP standard [14]. This metric is also used to indicate the cell-edge performance.

5.6.2 Simulation Results

The performance using the proposed Joint Route Selection and Resource Partitioning (JRSRP) algorithm based on APFR and the benchmarking JRSRP algorithm based on FFR is evaluated when different values are given to the transmitting power of each RN. The RN transmitting power of 30 dBm, 33 dBm, 36 dBm and 39 dBm are used in the simulations.

Fig.5.2 shows the GPF factors using different JRSRP algorithms with different RN transmitting powers. With two-hop relaying, the GPF factors using both the proposed APFR based JRSRP algorithm and the FFR based algorithm are larger than those in the LTE-Advanced networks without relays. With the increase of transmitting power of RNs, better downlink performance of access links can be achieved, but more severe interference will be generated to the direct links. Because it is better able to deal with this situation, the APFR based algorithm improves the GPF factors for different RN transmitting powers, compared with the FFR based algorithm. It can be observed that the GPF factors using the FFR based JRSRP algorithm are increasing gently, especially when the RN transmitting power grows from 36 dBm to 39 dBm. However, the increment of GPF factor using the APFR based algorithm is more significant between these two RN transmitting powers. Therefore, the APFR based algorithm may support a larger transmitting power of RNs in the LTE-Advanced networks in order to provide better proportional fairness.

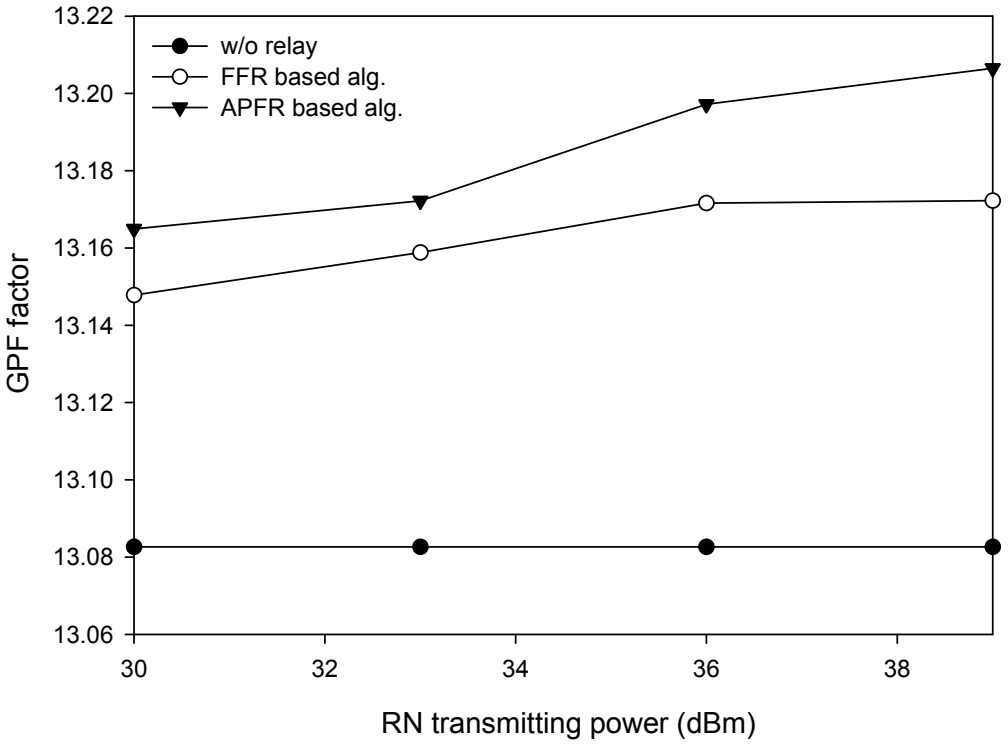

Figure 5.2: GPF factor v.s. RN transmitting power

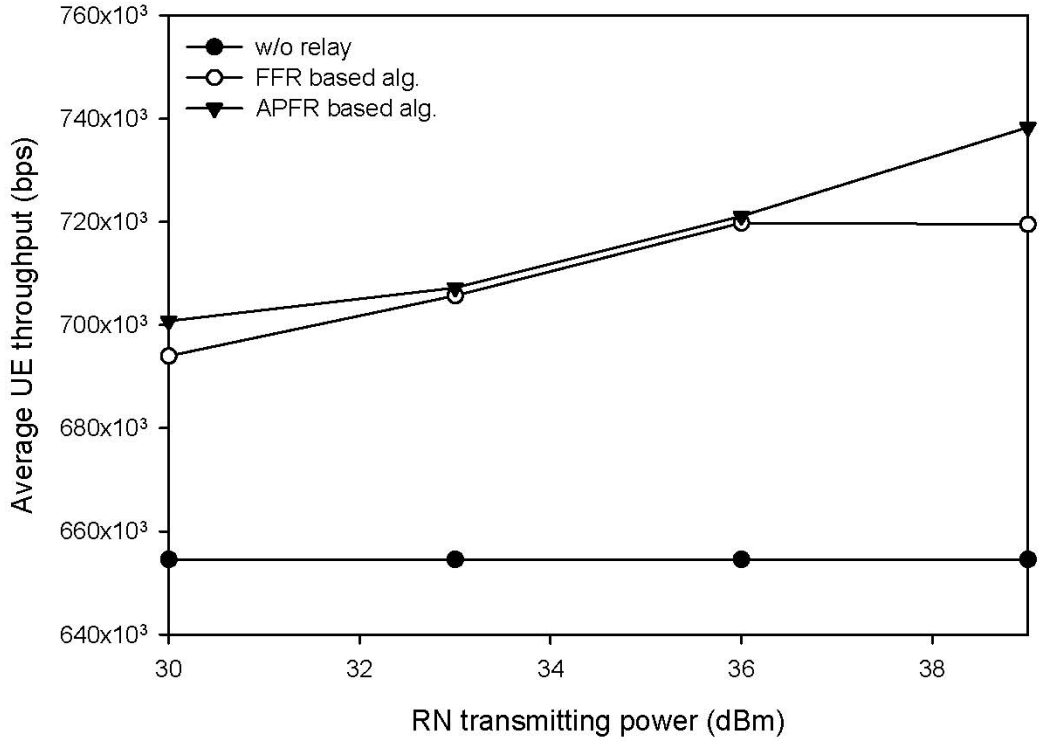

Figure 5.3: Average UE throughput v.s. RN transmitting power

The average throughputs of UEs using different JRSRP algorithms versus different RN transmitting powers are displayed in Fig. 5.3. Deploying RNs, larger throughputs are obtained, compared with the LTE-Advanced networks without relay nodes. Similar with what is shown in Fig. 5.2, the average throughputs using the FFR based algorithm increase insignificantly along with the rising RN transmitting power, and those using the APFR based algorithm are increasing gradually. When the transmitting power of RNs reaches 39 dBm, the gap of average throughputs using the two JRSRP algorithms is much larger than those with other RN transmitting powers.

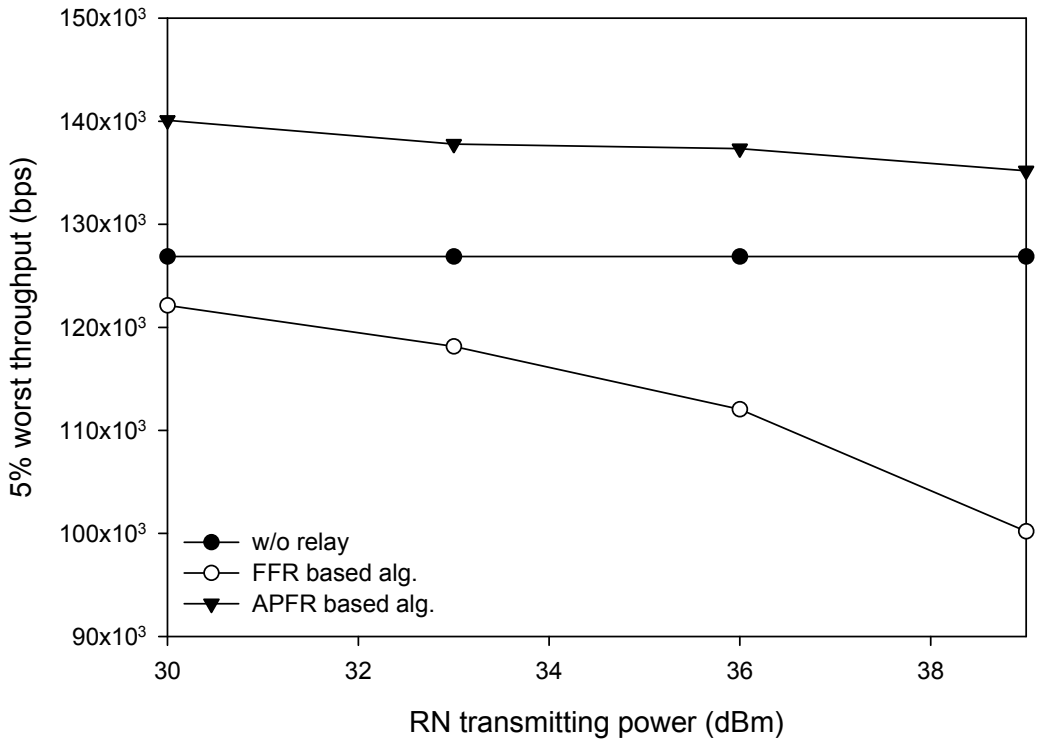

Figure 5.4: 5% worst UE throughput v.s. RN transmitting power

The Fig. 5.4 illustrates the 5% worst UE throughputs with different JRSRP algorithms in terms of RN transmitting power. Due to the interference between access links and direct links, larger RN transmitting powers may be the reason of reducing 5% worst UE throughputs. Compared with the marked drop using the FFR based algorithm, there is a slow decline of the 5% worst UE throughput observed by the APFR based algorithm. What is more, the FFR based algorithm cannot provide larger throughputs for the 5% worst UEs, however the APFR based algorithm can achieve it by considering the interference between access links and direct links. When the RN transmitting power goes up from 30 dBm to 39 dBm, the performance gains of the proposed APFR based algorithm over the benchmark

FFR based algorithm are increase from 15% to 34%.

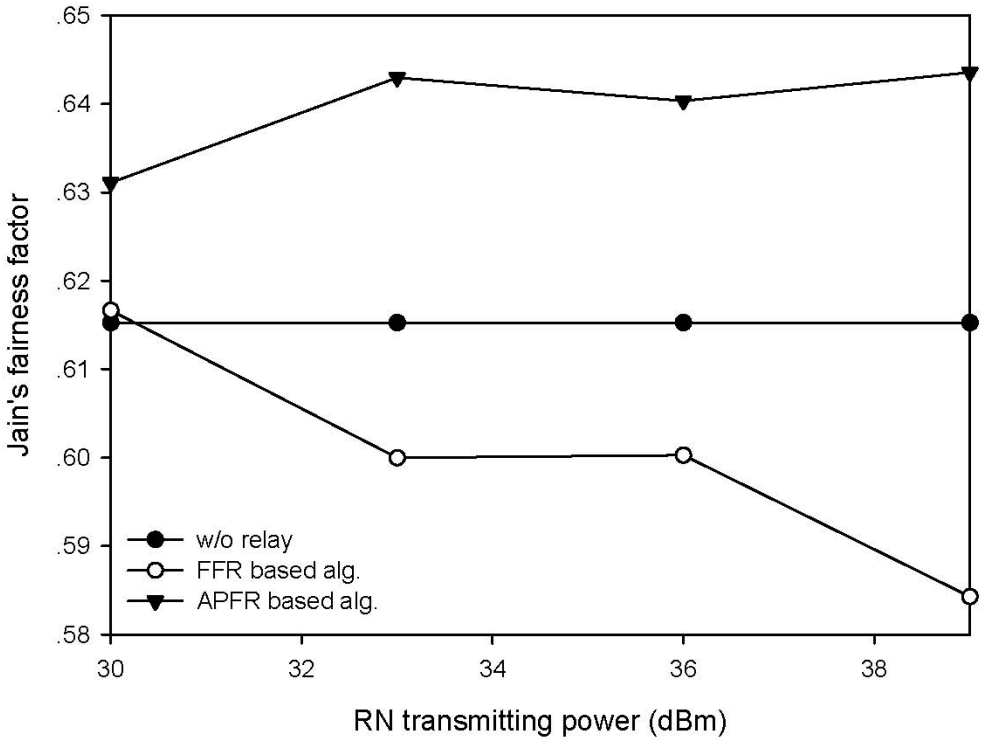

Figure 5.5: Jain's fairness index v.s. RN transmitting power

In Fig. 5.5, the Jain's fairness factors verses the RN transmitting power using different JRSRP algorithms are presented. Along with the increasing RN transmitting power, the Jain's fairness factors show two different trends using the APFR based algorithm and the FFR based algorithm. The Jain's fairness factors fall significantly using the FFR based algorithm and increase slightly using the APFR based algorithm. The higher the transmitting power the RNs have, the more improvement in terms of Jain's fairness factor can be obtained by the APFR based algorithm. Additionally, the FFR based algorithm will achieve lower Jain's fairness factors than those in the LTE-Advanced networks without relays, when the RN transmitting power is no less than 33 dBm. Therefore, a high transmitting power for the RN is not recommended, unless the proposed APFR based JRSRP algorithm is applied.

Table 5.2 depicts the improvement of the proposed APFR based algorithm compared with the benchmarking FFR based algorithm with different RN transmitting power. The maximum value of 34.92% indicates the significant increase of the 5% worst throughput in LTE-Advance networks.

Besides the transmitting power, the position of RNs may also affect the performance of LTE-Advanced networks with relays. When a RN is located closer to the

Table 5.2: The improvement of the proposed algorithm against the benchmarking algorithm in different RN transmitting power

	RN transmitting power (dBM)			
	30	33	36	39
GPF factor	0.0171	0.0134	0.0256	0.0342
Average UE Throughput	0.97%	0.22%	0.19%	2.61%
5% worst UE Throughput	14.70%	16.62%	22.59%	34.92%
Jain's fairness factor	0.0144	0.043	0.0401	0.0593

eNB, the channel condition of its access links will get worse because of the increasing interference from the direct links, but the backhaul link condition will be better thanks to shorter path between the RN and the eNB. Note that the position of RN is at the bore sight towards the adjacent eNB and the distance between the eNBs and their RNs is 0.3, 0.35, 0.4, 0.45 and 0.5 of the distance between two adjacent eNBs, i.e. inter-site distance (ISD).

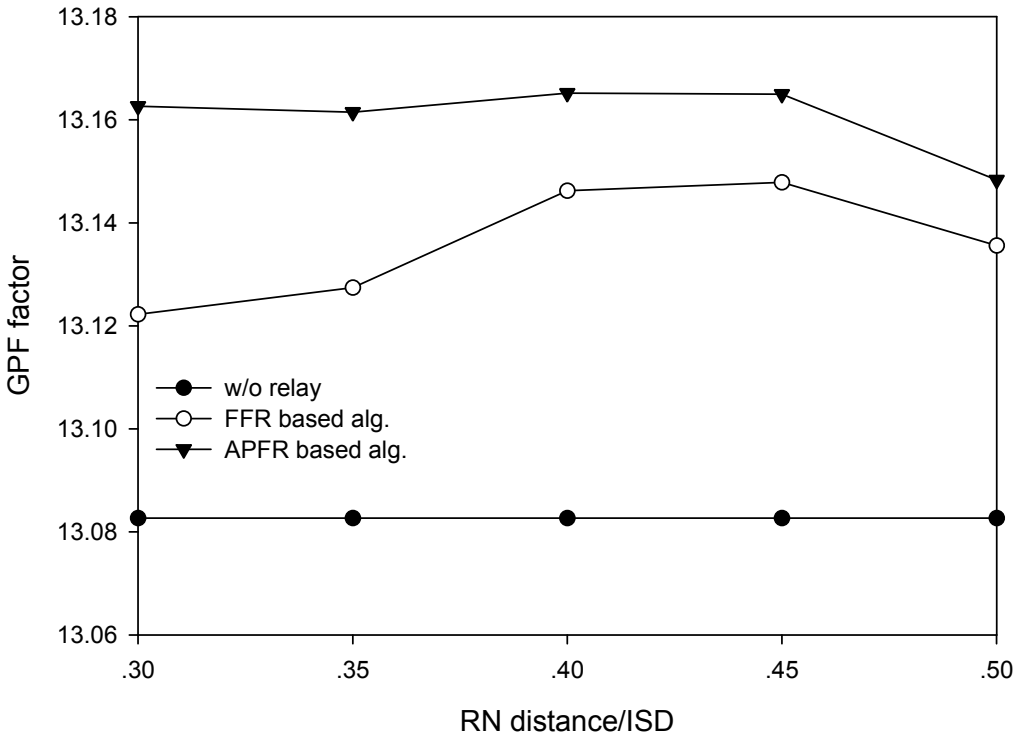

Figure 5.6: GPF factor v.s. RN position

In Fig. 5.6, the GPF factors with different RN positions are shown. When the RNs move beyond 0.3 of the ISD to 0.5 of the ISD, both the proposed JRSRP algorithm based on APFR and the benchmark algorithm based on FFR can obtain

the GPF factor gains, and the proposed APFR based algorithm can always achieve better GPF factors than the benchmarking FFR based algorithm. When the RNs get closer to the eNBs, the downlink performance of access links is worse, while the backhaul link performance improves. It can be observed that the GPF factors using the FFR based JRSRP algorithm decrease gradually when the RNs move towards their donor eNBs from 225 meters (0.45 of the ISD) away from them to 150 meters (0.3 of the ISD). However, the GPF factors using the APFR based algorithm have insignificant differences except when the distance of RN is half of the ISD. Therefore, the APFR based algorithm allows closer RN locations in the LTE-Advanced networks.

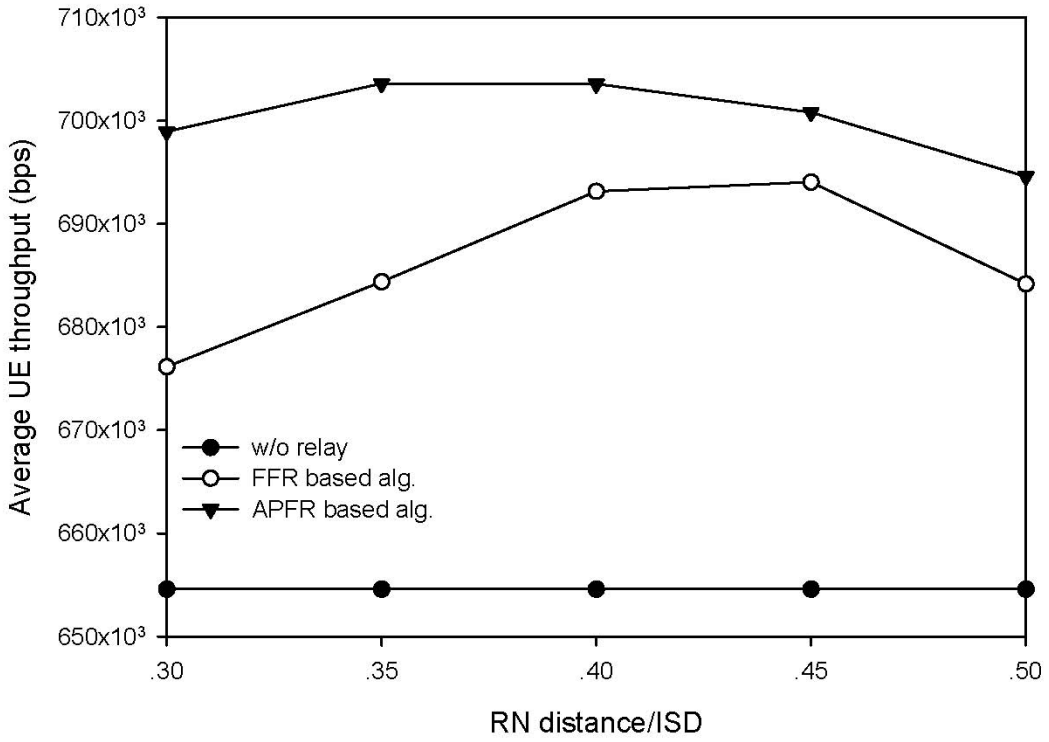

Figure 5.7: Average UE throughput v.s. RN position

The average throughputs of UEs using different JRSRP algorithms versus different RN distances are displayed in Fig. 5.7. Deploying RNs, larger throughputs are obtained, compared with the LTE-Advanced networks without relay node. Similar with what is shown in Fig. 5.6, the average throughput using the FFR based algorithm increases gradually along with larger RN distance away from the eNB before the RN distance reaches 0.35 of the ISD. The average UE throughput using the APFR based algorithm reaches the peak when the RNs are located at 0.35 of the ISD away from their eNBs. The difference of the average UE throughput using these two algorithms is the largest when the distance between the RNs and their

eNBs is only 150 meters (0.3 of the ISD), and the smallest when the RN distance is 0.45 of the ISD.

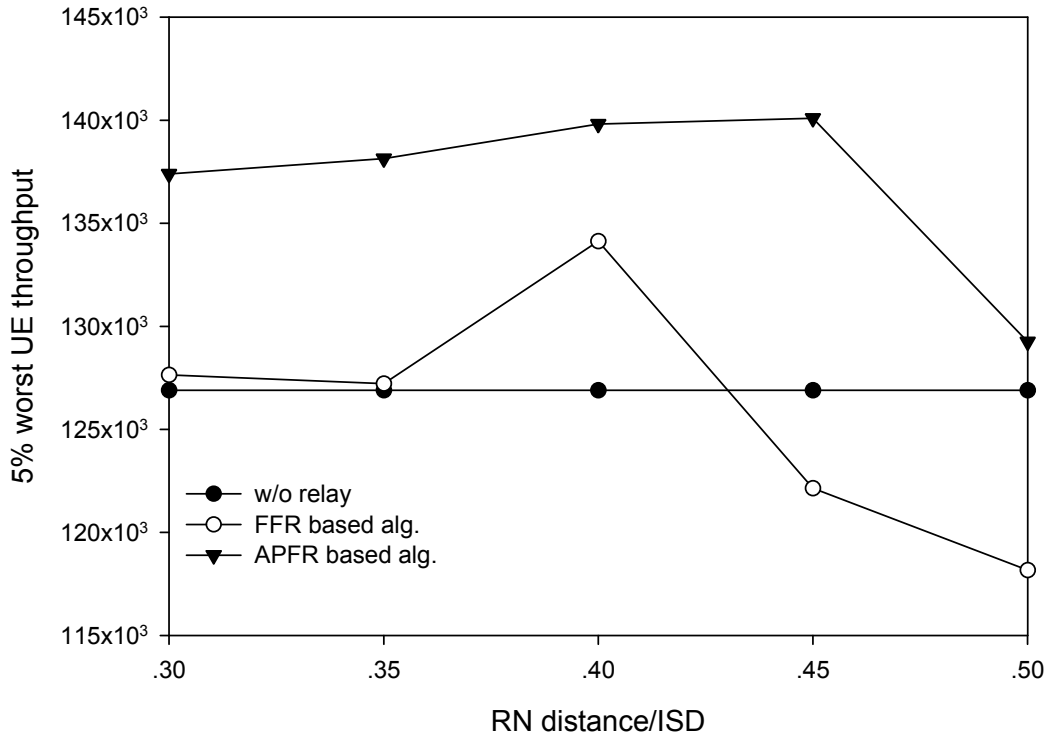

Figure 5.8: 5% worst UE throughput v.s. RN position

The Fig. 5.8 demonstrates the 5% worst UE throughputs using different JRSRP algorithms at different RN positions. Although the interference between access links and direct links gets larger with a shorter distance between access links and direct links, better performance of the backhaul links may compensate the loss of 5% worst UE throughputs in some cases. When the RNs are more than 200 meters (0.4 of the ISD) using the FFR based algorithm or 225 meters away from their eNBs (0.45 of the ISD) using the APFR based algorithm, the 5% worst UE throughputs decrease sharply. Particularly, when the RN distance is between 0.45 and 0.5 of the ISD and the FFR based algorithm is utilised, the 5% worst UE cannot obtain larger throughputs than those in the LTE-Advanced networks without relays. When the RN transmitting power goes up from 30 dBm to 39 dBm, the performance gain of the proposed APFR based algorithm over the FFR based algorithm is between 8% (0.3 of the ISD) and 15% (0.45 of the ISD).

In Fig. 5.9, the Jain's fairness factors verses the RN distance to the ISD using different JRSRP algorithms are depicted. At different locations of RN, the Jain's fairness factors show two different trends using the APFR based algorithm and the

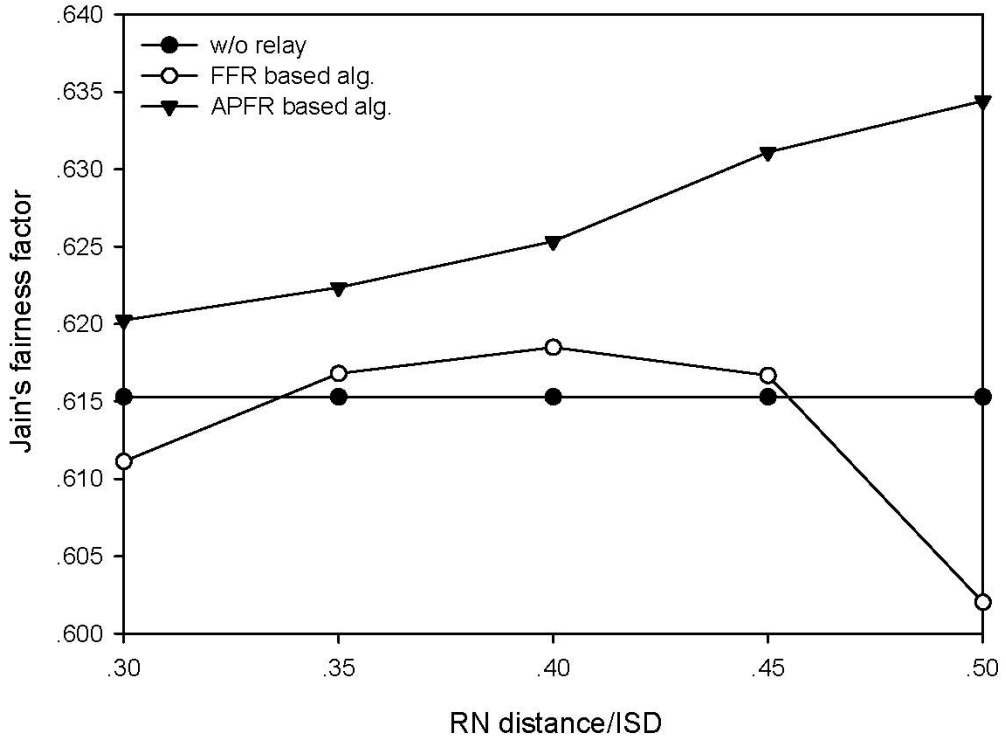

Figure 5.9: Jain's fairness index v.s. RN position

FFR based algorithm respectively. The Jain's fairness factors using the FFR based algorithm increase steadily with RN distances of from 0.3 of the ISD to 0.4 of the ISD, and then fall below the value without relays with the largest RN distance. In contrast, the Jain's fairness factors using the APFR based algorithm increase gradually along with greater RN distances. This is because when the RNs are further away from their eNB, more cell-edge UEs can choose the RNs in order to improve their performance. Hence, the difference between cell-center UEs and cell-edge UEs will be narrowed and better fairness will be achieved.

Table 5.3: The improvement of the proposed algorithm against the benchmarking algorithm with different RN distances from the donor eNBs

	RN positions (/ISD)				
	0.3	0.35	0.4	0.45	0.5
GPF factor	0.0403	0.034	0.0189	0.0171	0.0128
Average UE Throughput	3.37%	2.81%	1.50%	0.97%	1.52%
5% worst UE Throughput	7.64%	8.59%	4.23%	14.70%	9.38%
Jain's fairness factor	0.0092	0.0056	0.0069	0.0144	0.0324

Table 5.3 describes the performance gains of the proposed APFR based algorithm compared with the benchmarking FFR based algorithm with different RN distances from the donor eNBs.

5.7 Conclusion

This chapter presents a preliminary study on adaptive partial frequency reusing (APFR) in LTE-Advanced networks with RNs. Proportional fairness is considered as the performance metric in order to make an effective compromise between throughput and fairness. This study starts with the scenario of one RN in each cell. The generalised proportional fairness (GPF) problem is utilised to formulate the APFR problem for maximising proportional fairness. Thereafter, the GPF problem for APFR is decomposed into two sub-problems, proportional fair based route selection and resource partitioning. This chapter proposes the APFR based joint route selection and resource partitioning (JRSRP) algorithm as a near-optimal solution. Through an experimental performance evaluation, it can be confirmed that the proposed APFR based JRSRP algorithm achieves better proportional fairness than the FFR based JRSRP algorithm. Both throughput and fairness are improved. In addition, because of the better APFR solutions, the increase of interference caused by higher transmitting power and less RN distance can be alleviated. The proposed algorithm will increase the computation complexity of the eNBs and the RNs, however it will not require more signalling channels between the RNs and the donor eNBs.

Chapter 6

Conclusions and Future Work

6.1 Introduction

In this chapter, the research work described in this thesis is summarised. The significance of my contributions to distributed RRM techniques in relay enhanced LTE-Advanced networks is highlighted. Three RRM techniques proposed in this thesis include service-aware adaptive bidirectional optimisation route selection, distributed two-hop proportional fair resource scheduling and adaptive two-hop partial frequency reusing. Some potential topics for future work are also given in this chapter.

6.2 Contributions

Overview of Solutions

The purpose of my research is to rise to the challenges of RRM in the LTE-Advanced networks with in-band half-duplex RNs associated with the introduction of two-hop in-band transmission and low-power RNs. Since the RRM techniques in the single-hop networks may lead to imbalances in two-hop networks, the aim of my research is to achieve a rebalance by designing new techniques in addition to RRM procedures. In order to avoid the imbalance between uplink optimisation and downlink optimisation as the result of a large difference between transmitting power of an eNB and an RN, a service-aware adaptive bidirectional optimisation (ABO) route selection

algorithm was proposed. Since fixed resource partitioning is utilised in the ABO algorithm, load balancing is also considered. Based on different adaptive resource partitioning schemes, distributed two-hop proportional fair resource scheduling algorithms were proposed. Because the resource scheduling of access links and backhaul links should be re-balanced in order to satisfy the matching of data rates in the two hops and the resource numbers in each of the two hops. In order to rebalance the benefits of frequency reusing with the performance loss caused by co-channel interference at the reusing frequency, adaptive two-hop partial frequency reusing is studied in this thesis. A proportional fair joint route selection and resource partitioning algorithm is proposed to obtain a near-optimal solution.

Service-Aware Adaptive Bidirectional Optimisation Route Selection

A service-aware adaptive bidirectional optimisation (ABO) route selection strategy with load balancing is proposed in order to rebalance uplink optimisation and downlink optimisation. The main target of this strategy is to maximise the bidirectional throughput which is the sum of the uplink throughput and the downlink throughput. A traffic model is assumed in the formulation of maximising the bidirectional throughput using route selection, in which there are different types of services with different uplink and downlink requirements. Load balancing is considered by its integration in the ABO strategy in order to improve system performance in heavy-loaded scenarios.

Through a static system-level simulation, the ABO strategy is compared with two benchmark strategies: the Received Signal Power (RSP) based strategy and the Range Expansion (RE) based strategy, with different frame configurations. Both a Round-Robin resource scheduling algorithm and a proportional fair resource scheduling algorithm are deployed. Both 20 MHz and 10 MHz frequency bandwidths are considered. Simulation results show that the ABO strategy is superior to the other two strategies in two points: 1) achieving higher average bidirectional throughput for different frame configurations because of the inherent load balancing feature, and 2) providing better performance for uplink-biased UEs, for example up to 14% gain is achieved in the mean user uplink throughput. Besides, the performance gain of the proposed ABO strategy is larger when 10 MHz frequency bandwidth is applied because the integrated load balancing mechanism can avoid early overloading.

Distributed Two-hop Proportional Fair Resource Allocation

The distributed two-hop proportional fair (DTHPF) resource allocation scheme includes the proposed proportional fair resource scheduling algorithms and adaptive resource partitioning algorithms. The individual resource scheduling processes in the access links and the backhaul links are rebalanced by considering two-hop data rate matching and the resource number constraints between access links and backhaul links. The purpose of the proposed DTHPF resource allocation algorithms is to maximise two-hop end-to-end proportional fairness in the LTE-Advanced networks with RNs. Two different two-hop transmission protocols are considered, which are orthogonal two-hop (OTH) transmission protocol and simultaneous two-hop (STH) transmission protocol. The generalised proportional fairness (GPF) problem using two protocols is formulated and decomposed into two related sub-problems, i.e., a resource partitioning problem and a resource scheduling problem. By adopting the existing resource partitioning solutions, the resource scheduling problem constrained by the two-hop resource partitioning is given and solved using the Lagrangian multiplier method.

Semi-static system level simulation results show that the proposed DTHPF resource allocation scheme achieves a better compromise between throughput and fairness. The orthogonal reuse (OR) pattern in the OTH protocol and the full reuse (FR), 2/3 partial reuse (PR) and 1/3 PR patterns in the STH protocol are considered as the scenarios for the performance evaluations. Through simulations, the following facts can be observed:

1. The proposed DTHPF resource allocation scheme has better GPF factors and better 5% worst UE throughputs, with different RN numbers for all the reuse patterns.

2. The performance of macro UEs in the OR pattern is better than that in the FR pattern, because extra intra-cell interference is generated by reusing the same PRB in direct links and access links in the FR pattern. However, the performance of relay UEs in the FR pattern is better than that in the OR pattern.

3. With less intra-cell interference and less resources for the access links, the performance in the 1/3 PR pattern is better than that in the FR pattern using the proposed scheme and the benchmark scheme. Meanwhile, the performance gains achieved by the proposed scheme compared with the benchmark scheme

is smaller in the 1/3 PR pattern than in the FR and 2/3 PR patterns.

4. As a compromise between the FR pattern and the 1/3 PR pattern, the 2/3 PR pattern can achieve better performance, and significant performance gain can be obtained using the proposed scheme.

Adaptive Two-Hop Partial Frequency Reusing

This thesis also proposes a proportional fair joint route selection and resource partitioning algorithm for adaptive partial frequency reusing (APFR) in LTE-Advanced networks with RNs. Proportional fairness is considered as the performance metric in order to make an effective compromise between throughput and fairness. This study starts with the scenario of one RN in each cell. For maximising proportional fairness, the Generalised proportional fairness (GPF) problem is utilised to formulate the APFR problem. Thereafter, the GPF problem for APFR is decomposed into two sub-problems, which are a route selection problem and a resource partitioning problem. A proportional fair joint route selection and resource partitioning (JRSRP) algorithm is proposed as a improved solution for the APFR problem.

In the system-level simulation, the performance using both the proposed APFR based JRSRP algorithm and the benchmarking FFR based JRSRP algorithm is evaluated with different RN transmitting powers and different RN positions. The simulation results show that the proposed APFR based algorithm can achieve larger GPF factors, throughputs and Jain's fairness factors. Especially, the 5% worst UE throughput is improved by at least 8% to up to 34%, and hence cell-edge UEs are dramatically better off. When the RN transmitting power is higher and the RNs are closer to the eNB, the increase in interference is alleviated by the proposed APFR based algorithm, since the balance between frequency reusing and co-channel interference is better solved.

6.3 Future Works

Adaptive Bidirectional Optimisation Route Selection

When service types and load balancing are considered in the ABO route selection strategy, fair-share resource scheduling algorithms, such as Round-Robin scheduling

and proportional fair scheduling, are considered. For some service types, a throughput threshold is required. Thus, throughput aware fair-share scheduling algorithms, such as max-min scheduling, should be considered. The ABO strategy should be extended to include the max-min scheduling algorithm or hybrid scheduling algorithms.

A important issue of route selection in relay enhanced LTE-Advanced networks is energy efficiency. The power consumption of eNB, RN and UE can be considered together with the system performance in order to maximise the performance metrics with regard to power consumption. Since eNBs, RNs and UEs have different sources of power supply, e.g. UEs are supported by batteries and eNBs are supplied by industrial power, a new energy consumption metric is needed.

Distributed Two-Hop Proportional Fair Resource allocation

The DTHPF resource allocation scheme only considers the downlink, which may be extended to the uplink. In the LTE uplink, SC-FDMA is deployed. Therefore, the resource scheduling in the LTE uplink should comply with some different rules. For example, the resources allocated to a UE should be consecutive and one UE should be scheduled just for once.

The resource constraints of access links and backhaul links determine the resource scheduling algorithms. Two special situations are considered in this thesis. In the none frequency reuse case, the sum of the access resource number and the backhaul resource number is proportional to the UE number; in the fixed frequency reuse case, either the access resource number or the backhaul resource number is the constraint. However, a more generalised situation can be considered for the generalisation of DTHPF resource allocation.

Adaptive Two-Hop Partial Frequency Reusing

The research on adaptive partial frequency reusing (APFR) in this thesis is a preliminary study. Only one RN in a sector is considered. Multiple RNs per cell can be considered to improve performance further.

The joint route selection and resource partitioning algorithm for APFR proposed in this thesis has higher complexity than the conventional received signal power based route selection algorithm and the full frequency reusing (FFR) based resource

partitioning algorithm. Thus, a low-complexity algorithm is needed in order to provide a balance between the effectiveness and the complexity of the proposed algorithm.

References

[1] H. Kaaranen, A. Ahtiainen, L. Laitinen, S. Naghian, and V. Niemi, *UMTS Networks: Architecture, Mobility and Services*. Wiley, Apr. 2005. [Online]. Available: http://www.amazon.com/exec/obidos/redirect?tag=citeulike07-20&path=ASIN/0470011033

[2] T. Halonen, J. Romero, and J. Melero, *GSM, GPRS and EDGE Performance: Evolution Towards 3G/UMTS*. John Wiley & Sons, 2003.

[3] A. Furuskar, S. Mazur, F. Muller, and H. Olofsson, "EDGE: enhanced data rates for GSM and TDMA/136 evolution," *Personal Communications, IEEE*, vol. 6, no. 3, pp. 56–66, 1999.

[4] M. Mouly and M.-B. Pautet, *The GSM System for Mobile Communications*. Telecom Publishing, 1992.

[5] E. Dahlman, B. Gudmundson, M. Nilsson, and A. Skold, "UMTS/IMT-2000 based on wideband CDMA," *Communications Magazine, IEEE*, vol. 36, no. 9, pp. 70–80, 1998.

[6] C. Smith, *3G Wireless Networks*. McGraw-Hill Professional, 2001.

[7] H.-H. Chen, C.-X. Fan, and W. Lu, "China's perspectives on 3G mobile commuunications and beyond: TD-SCDMA technology," *Wireless Communications, IEEE*, vol. 9, no. 2, pp. 48–59, 2002.

[8] J. Zhang, J. Huai, R. Xiao, and B. Li, "Resource management in the next-generation DS-CDMA cellular networks," *Wireless Communications, IEEE*, vol. 11, no. 4, pp. 52–58, 2004.

[9] D. Astely, E. Dahlman, A. Furuskar, Y. Jading, M. Lindstrom, and S. Parkvall, "LTE: the evolution of mobile broadband," *Communications Magazine, IEEE*, vol. 47, no. 4, pp. 44–51, 2009.

[10] K. Pedersen, T. Kolding, F. Frederiksen, I. Kovacs, D. Laselva, and P. Mogensen, "An overview of downlink radio resource management for UTRAN long-term evolution," *Communications Magazine, IEEE*, vol. 47, no. 7, pp. 86–93, 2009.

[11] R. Kwan, C. Leung, and J. Zhang, "Proportional Fair Multiuser Scheduling in LTE," *Signal Processing Letters, IEEE*, vol. 16, no. 6, pp. 461–464, 2009.

[12] C. Wijting, K. Doppler, K. Kalliojarvi, T. Svensson, M. Sternad, G. Auer, N. Johansson, J. Nystrom, M. Olsson, A. Osseiran, M. Dottling, J. Luo, T. Lestable, and S. Pfletschinger, "Key technologies for IMT-advanced mobile communication systems," *Wireless Communications, IEEE*, vol. 16, no. 3, pp. 76–85, 2009.

[13] I. F. Akyildiz, D. M. Gutierrez-Estevez, and E. C. Reyes, "The Evolution to 4G Cellular Systems: LTE-Advanced," *Phys. Commun.*, vol. 3, no. 4, pp. 217–244, Dec. 2010. [Online]. Available: http://dx.doi.org/10.1016/j.phycom.2010.08.001

[14] 3GPP, *Evolved Universal Terrestrial Radio Access (E-UTRA); Further advancements for E-UTRA physical layer aspects*, 3GPP TR 36.814. [Online]. Available: http://www.3gpp.org/ftp/Specs/html-info/36814.htm

[15] S. Parkvall, E. Dahlman, A. Furuskar, Y. Jading, M. Olsson, S. Wanstedt, and K. Zangi, "LTE-Advanced - Evolving LTE towards IMT-Advanced," in *Vehicular Technology Conference, 2008. VTC 2008-Fall. IEEE 68th*, 2008, pp. 1–5.

[16] 3GPP, *Requirements for further advancements for E-UTRA (LTE-Advanced)*, 3rd Generation Partnership Project (3GPP) TR 36.913, Jun. 2008. [Online]. Available: http://www.3gpp.org/ftp/Specs/html-info/36913.htm

[17] F. P. Kelly, "Charging and rate control for elastic traffic," *European Transactions on Telecommunications*, vol. volume 8, pp. 33–37, 1997.

[18] 3GPP, *Requirements for Evolved UTRA (E-UTRA) and Evolved UTRAN (E-UTRAN)*, 3rd Generation Partnership Project (3GPP) TR 25.913, Mar. 2006. [Online]. Available: http://www.3gpp.org/ftp/Specs/html-info/25913.htm

[19] R. v. Nee and R. Prasad, *OFDM for Wireless Multimedia Communications*, 1st ed. Norwood, MA, USA: Artech House, Inc., 2000.

[20] R. Prasad, *OFDM for Wireless Communications Systems*. Norwood, MA, USA: Artech House, Inc., 2004.

[21] H. Myung, J. Lim, and D. Goodman, "Single carrier FDMA for uplink wireless transmission," *Vehicular Technology Magazine, IEEE*, vol. 1, no. 3, pp. 30–38, 2006.

[22] 3GPP, *Evolved Universal Terrestrial Radio Access (E-UTRA) physical channels and modulation (Release 8)*, 3GPP TS 36.211. [Online]. Available: http://www.3gpp.org/ftp/Specs/html-info/36221.htm

[23] 3GPP, *Evolved Universal Terrestrial Radio Access (E-UTRA) and Evolved Universal Terrestrial Radio Access (E-UTRAN); Overall description; Stage 2*, 3rd Generation Partnership Project (3GPP) TS 36.300, Sep. 2008. [Online]. Available: http://www.3gpp.org/ftp/Specs/html-info/36300.htm

[24] 3GPP, *Feasibility study for evolved Universal Terrestrial Radio Access (UTRA) and Universal Terrestrial Radio Access Network (UTRAN)*, 3rd Generation Partnership Project (3GPP) TR 25.912, Aug. 2007. [Online]. Available: http://www.3gpp.org/ftp/Specs/html-info/25912.htm

[25] 3GPP, *Evolved Universal Terrestrial Radio Access (E-UTRA); Radio Resource Control (RRC); Protocol specification*, 3rd Generation Partnership Project (3GPP) TS 36.331, Sep. 2008. [Online]. Available: http://www.3gpp.org/ftp/Specs/html-info/36331.htm

[26] 3GPP, *Evolved Universal Terrestrial Radio Access (E-UTRA); Packet Data Convergence Protocol (PDCP) specification*, 3rd Generation Partnership Project (3GPP) TS 36.323, Sep. 2008. [Online]. Available: http://www.3gpp.org/ftp/Specs/html-info/36323.htm

[27] 3GPP, *Evolved Universal Terrestrial Radio Access (E-UTRA); Radio Link Control (RLC) protocol specification*, 3rd Generation Partnership Project (3GPP) TS 36.322, Sep. 2008. [Online]. Available: http://www.3gpp.org/ftp/Specs/html-info/36322.htm

[28] 3GPP, *Evolved Universal Terrestrial Radio Access (E-UTRA); Medium Access Control (MAC) protocol specification*, 3rd Generation Partnership Project (3GPP) TS 36.321, Sep. 2008. [Online]. Available: http://www.3gpp.org/ftp/Specs/html-info/36321.htm

[29] D. H. Holma and D. A. Toskala, *LTE for UMTS - OFDMA and SC-FDMA Based Radio Access*. Wiley Publishing, 2009.

[30] M. Katevenis, S. Sidiropoulos, and C. Courcoubetis, "Weighted round-robin cell multiplexing in a general-purpose ATM switch chip," *Selected Areas in Communications, IEEE Journal on*, vol. 9, no. 8, pp. 1265–1279, Oct 1991.

[31] S. Borst, "User-level performance of channel-aware scheduling algorithms in wireless data networks," *Networking, IEEE/ACM Transactions on*, vol. 13, no. 3, pp. 636–647, 2005.

[32] 3GPP, *Evolved Universal Terrestrial Radio Access (E-UTRA); Physical layer procedures*, 3rd Generation Partnership Project (3GPP) TS 36.213, Sep. 2008. [Online]. Available: http://www.3gpp.org/ftp/Specs/html-info/36213.htm

[33] G. Boudreau, J. Panicker, N. Guo, R. Chang, N. Wang, and S. Vrzic, "Interference coordination and cancellation for 4G networks," *Communications Magazine, IEEE*, vol. 47, no. 4, pp. 74–81, April 2009.

[34] "R1-082397, Discussion on the various types of Relays," Panasonic, Tech. Rep., July 2008.

[35] F. Jiang and B. Wang, "A Load Balancing Relay Selection Algorithm for Relay Based Cellular Networks," in *Wireless Communications, Networking and Mobile Computing (WiCOM), 2011 7th International Conference on*, 2011, pp. 1–5.

[36] Y. Hu and L. Qiu, "A Novel Multiple Relay Selection Strategy for LTE-Advanced Relay Systems," in *Vehicular Technology Conference (VTC Spring), 2011 IEEE 73rd*, 2011, pp. 1–5.

[37] I. Ben Chaabane, S. Hamouda, and S. Tabbane, "A novel relay selection scheme for LTE-advanced system under delay and load constraints," in *Wireless Communications and Networking Conference Workshops (WCNCW), 2012 IEEE*, 2012, pp. 263–267.

[38] F. Vitiello, S. Redana, and J. Hamalainen, "Admission control for LTE-Advanced relay systems," in *European Wireless, 2012. EW. 18th European Wireless Conference*, 2012, pp. 1–8.

[39] A. A. Rasheed and S. Wager, "Cell range extension in LTE in-band relays: Analysis of radio link, subframe allocation and protocol perfornance of FTP

traffic model," in *European Wireless, 2012. EW. 18th European Wireless Conference*, 2012, pp. 1–6.

[40] A. Saleh, O. Bulakci, S. Redana, B. Raaf, and J. Hamalainen, "Enhancing LTE-Advanced relay deployments via Biasing in cell selection and handover decision," in *Personal Indoor and Mobile Radio Communications (PIMRC), 2010 IEEE 21st International Symposium on*, 2010, pp. 2277–2281.

[41] "3GPP R1-083813, Range expansion for efficient support of heterogeneous networks," Qualcomm Europe, Tech. Rep., October 2008.

[42] "3GPP R1-103264, Performance of eICIC with Control Channel Coverage Limitation," NTT DOCOMO, Tech. Rep., May 2010.

[43] I. Guvenc, M.-R. Jeong, I. Demirdogen, B. Kecicioglu, and F. Watanabe, "Range Expansion and Inter-Cell Interference Coordination (ICIC) for Picocell Networks," in *Vehicular Technology Conference (VTC Fall), 2011 IEEE*, 2011, pp. 1–6.

[44] C.-S. Chiu and C.-C. Huang, "An Interference Coordination Scheme for Picocell Range Expansion in Heterogeneous Networks," in *Vehicular Technology Conference (VTC Spring), 2012 IEEE 75th*, 2012, pp. 1–6.

[45] W. Yang, L. Li, G. Wu, H. Wang, and Y. Wang, "Joint Uplink and Downlink Relay Selection in Cooperative Cellular Networks," in *Vehicular Technology Conference Fall (VTC 2010-Fall), 2010 IEEE 72nd*, 2010, pp. 1–5.

[46] Z. Ma, Y. Zhang, K. Zheng, W. Wang, and M. Wu, "Performance of 3GPP LTE-Advanced networks with Type I relay nodes," in *Communications and Networking in China (CHINACOM), 2010 5th International ICST Conference on*, 2010, pp. 1–5.

[47] L. Xiao and L. Cuthbert, "Load Based Relay Selection Algorithm for Fairness in Relay Based OFDMA Cellular Systems," in *Wireless Communications and Networking Conference, 2009. WCNC 2009. IEEE*, 2009, pp. 1–6.

[48] A. Saleh, S. Redana, B. Raaf, T. Riihonen, J. Hamalainen, and R. Wichman, "Performance of Amplify-and-Forward and Decode-and-Forward Relays in LTE-Advanced," in *Vehicular Technology Conference Fall (VTC 2009-Fall), 2009 IEEE 70th*, 2009, pp. 1–5.

[49] H. Hu, H. Yanikomeroglu, D. Falconer, and S. Periyalwar, "Range extension without capacity penalty in cellular networks with digital fixed relays," in *Global Telecommunications Conference, 2004. GLOBECOM '04. IEEE*, vol. 5, 2004, pp. 3053–3057 Vol.5.

[50] M. Liang, H. Fan, Y. F. Wang, and D. C. Yang, "Power-Based Routing for Two-Hop OFDMA Cellular Networks with Fixed Relay Stations," in *Wireless Communications, Networking and Mobile Computing, 2008. WiCOM '08. 4th International Conference on*, 2008, pp. 1–4.

[51] V. Sreng, H. Yanikomeroglu, and D. D. Falconer, "Relayer selection strategies in cellular networks with peer-to-peer relaying," in *Vehicular Technology Conference, 2003. VTC 2003-Fall. 2003 IEEE 58th*, vol. 3, 2003, pp. 1949–1953 Vol.3.

[52] Z. Ma, K. Zheng, W. Wang, and Y. Liu, "Route Selection Strategies in Cellular Networks with Two-Hop Relaying," in *Wireless Communications, Networking and Mobile Computing, 2009. WiCom '09. 5th International Conference on*, 2009, pp. 1–4.

[53] W.-H. Park and S. Bahk, "Resource management policies for fixed relays in cellular networks," *Computer Communications*, vol. 32, no. 4, pp. 703–711, 3/4 2009.

[54] Z. Ma, W. Xiang, H. Long, and W. Wang, "Proportional fair-based in-cell routing for relay-enhanced cellular networks," in *Wireless Communications and Networking Conference (WCNC), 2011 IEEE*, 2011, pp. 381–385.

[55] J. Lee, H. Wang, W. Seo, and D. Hong, "QoS-guaranteed transmission mode selection for efficient resource utilization in multi-hop cellular networks," *Wireless Communications, IEEE Transactions on*, vol. 7, no. 10, pp. 3697–3701, 2008.

[56] T. Liu and M. Rong, "Utility-based joint routing and spectrum partitioning in relay LTE-Advanced networks," in *Personal Indoor and Mobile Radio Communications (PIMRC), 2011 IEEE 22nd International Symposium on*, 2011, pp. 1914–1918.

[57] H. Ekstrom, "QoS control in the 3GPP evolved packet system," *Communications Magazine, IEEE*, vol. 47, no. 2, pp. 76–83, 2009.

[58] L. Lei, C. Lin, J. Cai, and X. Shen, "Flow-level performance of opportunistic OFDM-TDMA and OFDMA networks," *Wireless Communications, IEEE Transactions on*, vol. 7, no. 12, pp. 5461–5472, 2008.

[59] J. Ikuno, M. Wrulich, and M. Rupp, "System Level Simulation of LTE Networks," in *Vehicular Technology Conference (VTC 2010-Spring), 2010 IEEE 71st*, 2010, pp. 1–5.

[60] T. S. Rappaport, *Wireless communications: principles and practice*, 2nd ed. Upper Saddle River, N.J: Prentice Hall PTR, 2002.

[61] J. S. Hunter, "The exponentially weighted moving average." *Journal of Quality Technology*, vol. 18, no. 4, pp. 203–210, 1986.

[62] K. Balachandran, S. R. Kadaba, and S. Nanda, "Channel Quality Estimation and Rate Adaptation for Cellular Mobile Radio," *IEEE J.Sel. A. Commun.*, vol. 17, no. 7, pp. 1244–1256, Sep. 2006. [Online]. Available: http://dx.doi.org/10.1109/49.778183

[63] J.-G. Choi and S. Bahk, "Cell-Throughput Analysis of the Proportional Fair Scheduler in the Single-Cell Environment," *Vehicular Technology, IEEE Transactions on*, vol. 56, no. 2, pp. 766–778, 2007.

[64] W. Ying, W. Tong, H. Jing, S. Chao, Y. Xinmin, and Z. Ping, "Adaptive Radio Resource Allocation with Novel Priority Strategy Considering Resource Fairness in OFDM-Relay System," in *Vehicular Technology Conference, 2007. VTC-2007 Fall. 2007 IEEE 66th*, 2007, pp. 1872–1876.

[65] L. Huang, M. Rong, L. Wang, Y. Xue, and E. Schulz, "Resource Scheduling for OFDMA/TDD Based Relay Enhanced Cellular Networks," in *Wireless Communications and Networking Conference, 2007.WCNC 2007. IEEE*, 2007, pp. 1544–1548.

[66] L. Wang, Y. Ji, and F. Liu, "A Novel Centralized Resource Scheduling Scheme in OFDMA-based Two-Hop Relay-Enhanced Cellular Systems," in *Networking and Communications, 2008. WIMOB '08. IEEE International Conference on Wireless and Mobile Computing,*, 2008, pp. 113–118.

[67] M. Salem, A. Adinoyi, H. Yanikomeroglu, D. Falconer, and Y.-D. Kim, "A Fair Radio Resource Allocation Scheme for Ubiquitous High-Data-Rate Coverage in OFDMA-Based Cellular Relay Networks," in *Global Telecommunications Conference, 2009. GLOBECOM 2009. IEEE*, 2009, pp. 1–6.

[68] L. Xiao and L. Cuthbert, "A Two-Hop Proportional Fairness Scheduling Algorithm for Relay Based OFDMA Systems," in *Wireless Communications, Networking and Mobile Computing, 2008. WiCOM '08. 4th International Conference on*, 2008, pp. 1–4.

[69] L. Xiao, T. Zhang, Y. Zhu, and L. Cuthbert, "Two-Hop Subchannel Scheduling and Power Allocation for Fairness in OFDMA Relay Networks," in *Wireless and Mobile Communications, 2009. ICWMC '09. Fifth International Conference on*, 2009, pp. 267–271.

[70] W.-G. Ahn and H.-M. Kim, "Proportional fair scheduling in relay enhanced cellular OFDMA systems," in *Personal, Indoor and Mobile Radio Communications, 2008. PIMRC 2008. IEEE 19th International Symposium on*, 2008, pp. 1–4.

[71] Y. Hua, Q. Zhang, and Z. Niu, "Resource Allocation in Multi-cell OFDMA-based Relay Networks." in *INFOCOM*, 2010, pp. 2133–2141.

[72] C. Liu, X. Qin, S. Zhang, and W. Zhou, "Proportional-fair downlink resource allocation in OFDMA-based relay networks," *Communications and Networks, Journal of*, vol. 13, no. 6, pp. 633–638, 2011.

[73] L. You, M. Song, J. Song, Q. Miao, and Y. Zhang, "Adaptive Resource Allocation in OFDMA Relay-Aided Cooperative Cellular Networks," in *Vehicular Technology Conference, 2008. VTC Spring 2008. IEEE*, 2008, pp. 1925–1929.

[74] W.-P. Chang, J.-S. Lin, and K.-T. Feng, "QoS-based resource allocation for relay-enhanced OFDMA networks." in *WCNC*, 2011, pp. 321–326.

[75] Z. Jin and L. Vandendorpe, "Resource Allocation in Multi-Cellular DF Relayed OFDMA Systems." in *GLOBECOM*, 2011, pp. 1–5.

[76] L. Wang, Y. Ji, and F. Liu, "A Semi-Distributed Resource Allocation Scheme for OFDMA Relay-Enhanced Downlink Systems," in *GLOBECOM Workshops, 2008 IEEE*, 2008, pp. 1–6.

[77] L. Jiang, J. Pang, G. Shen, and D. Wang, "A game theoretic channel allocation scheme for multi-user OFDMA relay system," in *Wireless Communications and Networking Conference (WCNC), 2011 IEEE*, 2011, pp. 298–303.

[78] K. Sundaresan and S. Rangarajan, "Adaptive resource scheduling in wireless OFDMA relay networks," in *INFOCOM, 2012 Proceedings IEEE*, 2012, pp. 1080–1088.

[79] Q. Li, R. Hu, Y. Qian, and G. Wu, "A proportional fair radio resource allocation for heterogeneous cellular networks with relays," in *Global Communications Conference (GLOBECOM), 2012 IEEE*, 2012, pp. 5457–5463.

[80] H. Ju, B. Liang, J. Li, and X. Yang, "Dynamic Joint Resource Optimization for LTE-Advanced Relay Networks," *Wireless Communications, IEEE Transactions on*, vol. 12, no. 11, pp. 5668–5678, 2013.

[81] M. J. Neely, *Stochastic Network Optimization with Application to Communication and Queueing Systems*, ser. Synthesis Lectures on Communication Networks. Morgan & Claypool Publishers, 2010.

[82] M. Kaneko and P. Popovski, "Adaptive Resource Allocation in Cellular OFDMA System with Multiple Relay Stations." in *VTC Spring*, 2007, pp. 3026–3030.

[83] W. Wang, J. Liu, D. Li, and Y. Xu, "Throughput-Based Adaptive Resource-Allocation Algorithm for OFDMA Cellular System with Relay Stations," in *Global Telecommunications Conference (GLOBECOM 2011), 2011 IEEE*, 2011, pp. 1–5.

[84] S. Yi and M. Lei, "Backhaul resource allocation in LTE-Advanced relaying systems." in *WCNC*, 2012, pp. 1207–1211.

[85] Y.-S. Lu, Y.-B. Lin, and Y. T. Su, "Dynamic Resource Allocation for Relay-Based OFDMA Systems with Fairness Considerations." in *WCNC*, 2010, pp. 1–6.

[86] T. M. d. Moraes, G. Bauch, and E. Seidel, "QoS-aware Scheduling for In-Band Relays in LTE-Advanced," in *Systems, Communication and Coding (SCC), Proceedings of 2013 9th International ITG Conference on*, 2013, pp. 1–6.

[87] T. M. de Moraes, M. D. Nisar, A. A. Gonzalez, and E. Seidel, "Resource allocation in relay enhanced LTE-Advanced networks," *EURASIP Journal on Wireless Communications and Networking*, vol. 2012, no. 1, pp. 1–12, 2012.

[88] Z. Zhao, J. Wang, S. Redana, and B. Raaf, "Downlink Resource Allocation for LTE-Advanced Networks with Type1 Relay Nodes," in *Vehicular Technology Conference (VTC Fall), 2012 IEEE*, 2012, pp. 1–5.

[89] M. Pikhletsky, F. Khafizov, J. Zhang, and H. Zhuang, "Dynamic Radio Resource Management for OFDMA-Based Relay Enhanced Cellular Network." in *GLOBECOM*, 2011, pp. 1–5.

[90] O. Bulakci, A. Saleh, Z. Ren, S. Redana, B. Raaf, and J. Hamalainen, "Two-step resource sharing and uplink power control optimization in LTE-Advanced relay networks," in *Multi-Carrier Systems Solutions (MC-SS), 2011 8th International Workshop on*, 2011, pp. 1–6.

[91] A. Bou Saleh, O. Bulakci, Z. Ren, S. Redana, B. Raaf, and J. Haemaelaeinen, "Resource Sharing in Relay-enhanced 4G Networks," in *Wireless Conference 2011 - Sustainable Wireless Technologies (European Wireless), 11th European*, April 2011, pp. 1–8.

[92] mer Bulakci, A. B. Saleh, S. Redana, B. Raaf, and J. Hmlinen, "Flexible Backhaul Resource Sharing and Uplink Power Control Optimization in LTE-Advanced Relay Networks." in *VTC Fall*, 2011, pp. 1–6.

[93] D. W. Kifle, O. Bulakci, A. B. Saleh, S. Redana, and F. Granelli, "Joint backhaul co-scheduling and relay cell extension in LTE-Advanced networks uplink performance evaluation," 2012, pp. 1–8.

[94] m. Bulakci, A. Bou Saleh, S. Redana, B. Raaf, and J. Hmlinen, "Resource sharing in LTE-Advanced relay networks: uplink system performance analysis," *Transactions on Emerging Telecommunications Technologies*, vol. 24, no. 1, pp. 32–48, 2013. [Online]. Available: http://dx.doi.org/10.1002/ett.2569

[95] M. Kaneko and P. Popovski, "Radio Resource Allocation Algorithm for Relay-Aided Cellular OFDMA System," in *Communications, 2007. ICC '07. IEEE International Conference on*, 2007, pp. 4831–4836.

[96] M. Kaneko, P. Popovski, and K. Hayashi, "Throughput-Guaranteed Resource-Allocation Algorithms for Relay-Aided Cellular OFDMA System," *Vehicular Technology, IEEE Transactions on*, vol. 58, no. 4, pp. 1951–1964, 2009.

[97] S. Roth, J. Gan, and D. Danev, "Subframe allocation for relay networks in the LTE advanced standard," in *Personal Indoor and Mobile Radio Communications (PIMRC), 2010 IEEE 21st International Symposium on*, 2010, pp. 1758–1763.

[98] T. Kim, T.-Y. Min, and C. Kang, "Opportunistic packet scheduling algorithm for load balancing in a multi-hop relay-enhanced cellular OFDMA-TDD System," in *Communications, 2008. APCC 2008. 14th Asia-Pacific Conference on*, 2008, pp. 1–5.

[99] P. Arnold, V. Rakocevic, O. Ramos, and J. Habermann, "Algorithms for Adaptive Radio Resource Management in Relay-Assisted LTE-A Networks," in *Vehicular Technology Conference (VTC Spring), 2013 IEEE 77th*, 2013, pp. 1–5.

[100] W. Jeon, J. Han, and D. Jeong, "Distributed Resource Allocation for Multi-Cell Relay-Aided OFDMA Systems," *Mobile Computing, IEEE Transactions on*, vol. PP, no. 99, pp. 1–1, 2013.

[101] Z. Ma, W. Xiang, H. Long, and W. Wang, "Proportional Fair Resource Partition for LTE-Advanced Networks with Type I Relay Nodes," in *Communications (ICC), 2011 IEEE International Conference on*, 2011, pp. 1–5.

[102] J. Wang, Z. Ma, Z. Lv, Y. Sheng, and W. Xiang, "Fairness-aware resource partition and routing in relay-enhanced orthogonal-frequency-divisionmultiple-accessing cellular networks," *Communications, IET*, vol. 6, no. 16, pp. 2613–2620, 2012.

[103] C. Y. Wong, R. Cheng, K. Lataief, and R. Murch, "Multiuser OFDM with adaptive subcarrier, bit, and power allocation," *Selected Areas in Communications, IEEE Journal on*, vol. 17, no. 10, pp. 1747–1758, 1999.

[104] V. Erceg, K. S. Hari, and M. Smith, "Channel Models for Fixed Wireless Applications," IEEE 802.16.3c-01/29r4, Tech. Rep., 2001.

[105] P. Li, M. Rong, Y. Xue, and E. Schulz, "Reuse One Frequency Planning for Two-hop Cellular System with Fixed Relay Nodes," in *Wireless Communications and Networking Conference, 2007.WCNC 2007. IEEE*, March 2007, pp. 2253–2258.

[106] L. Cao, T. Zhang, and C. Feng, "Joint Adaptive Soft Frequency Reuse and Virtual Cell Power Control in Relay Enhanced Cellular System," in *Computer Network and Multimedia Technology, 2009. CNMT 2009. International Symposium on*, Jan 2009, pp. 1–5.

[107] J. Wang, J. Liu, D. Wang, J. Pang, G. Shen, and J. Chen, "Load Balance Based Dynamic Inter-Cell Interference Coordination for Relay Enhanced Cellular Network," in *Vehicular Technology Conference (VTC Spring), 2012 IEEE 75th*, May 2012, pp. 1–5.

[108] O. Oyman, "Opportunistic scheduling and spectrum reuse in relay-based cellular networks," *Wireless Communications, IEEE Transactions on*, vol. 9, no. 3, pp. 1074–1085, 2010.

[109] H. Chen, M. Peng, and J. Jiang, "A resource configuration scheme in OFDMA-based cellular relay networks," in *Communications in China Workshops (ICCC), 2012 1st IEEE International Conference on*, Aug 2012, pp. 102–107.

[110] Y. Kim and M. Sichitiu, "Optimal Max-Min Fair Resource Allocation in Multihop Relay-Enhanced WiMAX Networks," *Vehicular Technology, IEEE Transactions on*, vol. 60, no. 8, pp. 3907–3918, 2011.

[111] L. Liang, G. Feng, and Y. Zhang, "Integrated Interference Coordination for Relay-Aided Cellular OFDMA System," in *Communications (ICC), 2011 IEEE International Conference on*, June 2011, pp. 1–5.

[112] L. Liang, G. Feng, and Y. Zhang, "Resource allocation with interference coordination for relay-aided cellular orthogonal frequency division multiple access systems," *Communications, IET*, vol. 6, no. 3, pp. 300–310, February 2012.

[113] L. Liang and G. Feng, "A Game-Theoretic Framework for Interference Coordination in OFDMA Relay Networks," *Vehicular Technology, IEEE Transactions on*, vol. 61, no. 1, pp. 321–332, Jan 2012.

[114] G. Liebl, T. de Moraes, A. Gonzalez Rodriguez, and M. Nisar, "Centralized interference coordination in relay-enhanced networks," in *Wireless Communications and Networking Conference Workshops (WCNCW), 2012 IEEE*, April 2012, pp. 306–311.

[115] H. Mei, J. Bigham, P. Jiang, and E. Bodanese, "Distributed Dynamic Frequency Allocation in Fractional Frequency Reused Relay Based Cellular Networks," *Communications, IEEE Transactions on*, vol. 61, no. 4, pp. 1327–1336, April 2013.

[116] J. Zhang, H. Tian, P. Tian, Y. Huang, and L. Gao, "Dynamic Frequency Reservation Scheme for Interference Coordination in LTE-Advanced Heterogeneous Networks," in *Vehicular Technology Conference (VTC Spring), 2012 IEEE 75th*, May 2012, pp. 1–5.

[117] Y. Pei, H. Tian, T. Wu, and Y. Wang, "Frequency Planning Scheme Based on Interference Coordination for OFDM-Relay Systems," *Communications Letters, IEEE*, vol. 15, no. 1, pp. 13–15, January 2011.

[118] Y. Zhao, X. Fang, R. Huang, and Y. Fang, "Joint Interference Coordination and Load Balancing for OFDMA Multihop Cellular Networks," *Mobile Computing, IEEE Transactions on*, vol. 13, no. 1, pp. 89–101, Jan 2014.

[119] Q. Li, R. Hu, Y. Qian, and G. Wu, "Intracell Cooperation and Resource Allocation in a Heterogeneous Network With Relays," *Vehicular Technology, IEEE Transactions on*, vol. 62, no. 4, pp. 1770–1784, 2013.

[120] R. Jain, D.-M. Chiu, and W. R. Hawe, *A quantitative measure of fairness and discrimination for resource allocation in shared computer system.* Eastern Research Laboratory, Digital Equipment Corporation, 1984.